Revised model for the DNA replication fork in *Bacillus subtilis*: polymerase asymmetry

Vasileios A. Paschalis BSc Hons, MSc

Thesis submitted to the University of Nottingham
for the degree of Doctor of Philosophy

October 2016

Dedicated to everyone who believed in me

Follow your dreams!

Abstract

Replication of DNA is a vital process for growth and cell division in all domains of life. The mechanisms of helicase loading as well as hand-off of nascent RNA primers from the primase to the replicative polymerases during DNA synthesis are of fundamental importance. The prototype structural/functional model provided by the widely studied Gram-negative *Escherichia coli* DNA replication system is not universally applicable. The current model for the Gram-positive *Bacillus subtilis* DNA replication suggests that PolC is the main processive replicative polymerase with DnaE playing an essential but minor role during DNA synthesis. Our results suggest that DnaE is a major polymerase important for DNA replication and DNA repair. DnaE polymerase activity is stimulated in the presence of SSB, the clamp DnaN and PolC polymerase, its error-prone synthesis is modulated by the aforementioned proteins and its errors are corrected *in trans* by the PolC exonuclease domain, in a template specific ternary DNA-DnaE-PolC complex. Hereby, we propose a new revised model for DNA replication in *Bacillus subtilis*, where DnaE is the major replicative polymerase on the lagging strand and PolC, which is the major polymerase on the leading strand, provides the crucial proof-reading activity *in trans*. These findings revise the current model in *Bacillus subtilis* and suggest a division of labour between DnaE and PolC polymerases.

Acknowledgements

I would like to thank all those whose suggestions, assistance and support have been very valuable for the smooth and successful outcome of this work.

Firstly, I would like to thank Professor Panos Soultanas, Professor of Biological Chemistry of the School of Chemistry in The University of Nottingham for the scientific guidance and the moral support. In addition, I thank the University of Nottingham for funding my PhD *via* a Vice Chancellor's Scholarship for Research Excellence award.

This thesis would not have been possible without the help, support and patience of numerous people in The University of Nottingham. I thank Dr Geoff Briggs, Dr Richard Rymer and especially Dr Matthew Green, postdoctoral fellows in the School of Chemistry, The University of Nottingham for the important contributions to this work. I also thank all members of Panos Soultanas Group (Sarah Northall, Eleyna Martin, Scott Easton, Matthaios Pitoulias), Mark Searle Group (Juliet Morgan, Alex Slater, Andy Brennan, Dr Jed Long), Neil Oldaham Group (Dr Jose Afonso, Lucio Manzi, Nkazimulo Tshuma, Jeddidiah Bellamy-Carter), Neil Thomas Group (David Harvey, Victor Tudorica, Ali Al-Ani, Leah Ashley, Tom Coekin, Dr Francesco Zamberlan, Claire Sycamore) and Christoph Loenarz Group (Agata Miezaniec, Teresa Ambrosio) for the flawless cooperation, throughout the duration of our laboratory coexistence.

I am also grateful to my parents and sister for their unequivocal support. Last but not least, I would like to thank my fiancée Dimitra for her personal ongoing support and great patience at all times.

Contents

1 DNA Replication in Bacteria ..... - 1 -

1.1 Initiation of DNA Replication ..... - 1 -

1.2 Helicase Loading Mechanisms and Primosome Assembly ..... - 7 -

1.3 DNA Polymerases and the Elongation Stage of DNA replication ..... - 11 -

1.4 Hand-off Mechanisms ..... - 17 -

1.5 The Replication Model in *Bacillus subtilis* – Aims of this study ..... - 22 -

2 Materials and Methods ..... - 24 -

2.1 Materials ..... - 24 -

2.1.1 Chemical Substances ..... - 24 -

2.1.2 DNA Plasmids ..... - 25 -

2.1.3 Primers and Oligonucleotides ..... - 25 -

2.1.4 *Escherichia coli* strains ..... - 26 -

2.1.5 Commercially available proteins ..... - 27 -

2.2 Methods ..... - 28 -

2.2.1 Electrophoresis ..... - 28 -

2.2.2 Site Directed Mutagenesis ..... - 34 -

2.2.3 Molecular Cloning ..... - 37 -

2.2.4 Cell Techniques ..... - 38 -

2.2.5 Protein Purification – Chromatography ..... - 40 -

2.2.6 Assays ..... - 42 -

3 Protein Cloning, Expression, Purification and Activity Tests ..... - 51 -

3.1 Replicative Helicase DnaC and Helicase-Loader DnaI ..... - 51 -

3.2 Primase DnaG ..... - 59 -

3.2.1 N-terminal Hexahistidine-tagged DnaG primase ..... - 59 -

3.3 DNA Polymerase DnaE ..... - 66 -

3.3.1 C-terminal Intein-tagged DnaE polymerase ..... - 66 -

3.3.2 N-terminal Hexahistidine-tagged Maltose Binding Protein-tagged DnaE polymerase ..... - 71 -

3.4 DNA Polymerase PolC ..... - 80 -

3.4.1 N-terminal Hexahistidine-tagged PolC ..... - 80 -

3.5 Single-strand DNA Binding protein SSB ..... - 91 -

3.5.1 Native SSB ..... - 91 -

3.5.2 N-terminal Hexahistidine-tagged SSBΔ107-172 - 94 -
3.6 Processivity Clamp (DnaN) and Clamp-Loader (DnaX-tau subunit, YqeN-δ subunit, HolB-δ' subunit) - 98 -
4 Ribonucleotides and Deoxyribonucleotides at the fork - 100 -
4.1 RNA primer extension - 100 -
4.2 Impact of deoxyribonucleotides (dNTPs) on polymerase activity - 105 -
4.3 Incorporation of ribonucleotides (rNTPs) during DNA replication - 107 -
5 Functional Interaction Studies - 112 -
5.1 DnaG-DnaE and DnaE-PolC Complexes - 112 -
5.1.1 The DnaG-DnaE Complex - 112 -
5.1.2 The DnaE-PolC Complex - 115 -
5.2 Polymerase cooperation - 128 -
6 Polymerase Processivity and Functional Cooperation - 132 -
6.1 Collaborative functionality during DNA replication - 132 -
6.1.1 DnaE and PolC activity on naked DNA template - 133 -
6.1.2 DnaE and PolC activity on SSB-coated DNA template - 137 -
6.1.3 DnaE dominant activity and displacement from the 3'-OH end of primers - 141 -
6.2 PolC trans-proofreading activity on DnaE - 145 -
7 Conclusory Remarks and Revised Model - 154 -
7.1 Concluding Remarks - 154 -
7.2 Research Outputs - 156 -
7.3 *Bacillus subtilis* DNA replication fork Revised Model - 159 -
Bibliography - 161 -

List of Figures

Figure 1.1 DNA replication fork. - 3 -
Figure 1.3 The architecture of *Bsu*DnaD and *Bsu*DnaB. - 5 -
Figure 1.4 DNA replication initiation in *Bacillus subtilis* at *oriC*. - 6 -
Figure 1.5 Helicase loading mechanisms. - 8 -
Figure 1.6 *Bsu*DnaI-*Bst*DnaB-*Bst*DnaG (HBD) crystal structure - 10 -
Figure 1.7 *Escherichia coli* replication forks - 11 -
Figure 1.8 Clamp-loader architecture in Gram-positive and Gram-negative bacteria - 12 -
Figure 1.9 Structural organisation of C family DNA polymerases - 13 -
Figure 1.10 *Taq*DnaE. *Ec*DnaE and *Gka*PolC domains. - 15 -
Figure 1.11 Hand-off Model in T7 bacteriophage. - 18 -
Figure 1.12 Hand-off Model in T4 bacteriophage. - 19 -
Figure 1.13 Mechanism of RNA primer hand-off in hPolα/primase complex. - 21 -
Figure 1.14 Hand-off Model in low G-C content, Gram (+) bacteria - 23 -
Figure 2.1 Helicase Assay Construct - 43 -
Figure 2.2 Primer Extension Assay Construct - 45 -
Figure 2.3 EMSA substrates - 49 -
Figure 3.1 DnaC and DnaI purification steps - 52 -
Figure 3.2 DnaC and DnaI Hiload 26/60 Superdex 200 prep grade column. - 53 -
Figure 3.3 DnaC and DnaI Hiload 26/60 Superdex 75 prep grade column.. - 54 -
Figure 3.4 DnaC and DnaI Hitrap Q HP column. - 55 -
Figure 3.5 Hiload 26/60 Superdex 200 prep grade column chromatogram of DnaC after the guanidinium chloride treatment - 56 -
Figure 3.6 Purification scheme of DnaC and DnaI. - 56 -
Figure 3.7 DnaC and DnaI time course and concentration titration helicase assays - 57 -
Figure 3.8 p2BT N-terminal His-tagged *Bsu*DnaG plasmid map - 60 -
Figure 3.9 N-terminal His-tagged DnaG expression strain test - 61 -
Figure 3.10 N-terminal His-tagged DnaG Histrap HP column - 62 -
Figure 3.11 DnaG Ortho-Histrap HP column. - 63 -
Figure 3.12 N-terminal Histidine-tagged DnaG purification and scheme. - 64 -
Figure 3.13 DnaG activity assay. - 64 -
Figure 3.14 pTYB3 C-terminal Intein-tagged *Bsu*DnaE plasmid map. - 67 -
Figure 3.15 C-terminal Intein-tagged DnaE expression strain test. - 68 -
Figure 3.16 C-terminal Intein-tagged DnaE purification steps and scheme - 69 -
Figure 3.17 (Intein-tagged) DnaE activity assay. - 70 -
Figure 3.18 p2CT N-terminal Histidine-tagged MBP-tagged *Bsu*DnaE plasmid map - 72 -
Figure 3.19 HMM logo of conserved Aspartic acid (D) residues in DNA polymerases' polymerase catalytic site. - 72 -
Figure 3.20 Alignment of *Ec*DnaE and *Bsu*DnaE. - 73 -

Figure 3.21 N-terminal Histidine-tagged Maltose Binding Protein (MBP)-tagged DnaE expression strain test.....- 75 -
Figure 3.22 N-terminal MBP-tagged His-tagged DnaE Histrap HP column. .....- 76 -
Figure 3.23 N-terminal His-tagged MBP-tagged DnaE Hitrap Q HP column.....- 77 -
Figure 3.24 [N-terminal Hexahistidine-tag Maltose Binding Protein (MBP)-tag cleaved] DnaE purification steps and scheme. .....- 78 -
Figure 3.25 (Histidine-tag MBP-tag cleaved) DnaE/DnaE$_{pol-}$ activity assay. .....- 79 -
Figure 3.26 p2BT N-terminal Histidine-tagged *Bsu*PolC plasmid map. .....- 81 -
F**igure 3.27** Alignment of *Ec*DnaE, *Bsu*DnaE and *Bsu*PolC.....- 82 -
Figure 3.28 HMM logo of conserved acidic (D, E) residues in DNA polymerases' exonuclease catalytic site. .....- 83 -
Figure 3.29 Alignment of *Ec*PolA, *Ec*DnaQ and *Bsu*PolC. .....- 83 -
Figure 3.30 N-terminal Histidine-tagged PolC expression strain test. .....- 85 -
Figure 3.31 N-terminal His-tagged PolC Histrap HP column.....- 86 -
Figure 3.32 N-terminal His-tagged PolC Hitrap Q HP column. .....- 87 -
Figure 3.33 N-terminal Histidine-tagged PolC Hiload 26/60 Superdex 200 prep grade column. .....- 87 -
Figure 3.34 N-terminal Hexahistidine-tagged PolC purification steps and scheme.....- 88 -
Figure 3.35 (Histidine-tag claved) PolC/PolC$_{pol-}$/PolC$_{exo-}$ activity assay. .....- 89 -
Figure 3.36 Native SSB Hitrap Q HP column. .....- 92 -
Figure 3.37 Native SSB Hiload 26/60 Superdex 75 prep grade column.....- 93 -
Figure 3.38 Native SSB purification steps and scheme. .....- 94 -
Figure 3.39 N-terminal Histidine-tagged SSBΔ107-172 Histrap HP column. .....- 95 -
Figure 3.40 N-terminal Histidine-tagged SSBΔ107-172 Hiload 26/60 Superdex 75 prep grade column. .....- 96 -
Figure 3.41 N-terminal Histidine-tagged SSBΔ107-172 purification steps and scheme.....- 97 -
Figure 3.42 Processivity clamp and clamp-loader proteins.....- 99 -
Figure 4.1 DnaE and PolC RNA primer extension assays. .....- 101 -
Figure 4.2 Alignment of *Bsu*PolC with *Bsu*DnaE, *Gka*PolC, *Ec*DnaE and *Taq*DnaE Thumb domains. .....- 103 -
Figure 4.3 *Ec*DnaE and *Gka*PolC DNA binding. .....- 104 -
Figure 4.4 DNA primer extension assays (dNTP concentration titration). .....- 106 -
Figure 4.5 rNTPs incorporation. .....- 108 -
Figure 4.6 Alignment of *Bsu*PolC with *Bsu*DnaE, *Gka*PolC, *Ec*DnaE and *Taq*DnaE "steric gate" .....- 110 -
Figure 5.1 EMSAs DnaG, DnaE, DnaG-DnaG (5 mins).....- 113 -
Figure 5.2 DnaE binds DNA with higher affinity than PolC (15 mins). EMSAs DnaE$_{wt}$, PolC$_{wt}$, PolC$_{exo-}$.....- 116 -
Figure 5.3 dNTPs affect the DnaE-PolC complex formation. EMSAs DnaE-PolC (+dGTP) (15 mins). .....- 118 -
Figure 5.4 PolC does not bind to 3' overhang substrates. EMSAs PolC, PolC$_{exo-}$ (15 mins)..... .....- 120 -

Figure 5.5 DnaE binds DNA with higher affinity than PolC (5 mins). EMSAs $DnaE_{wt}$, $PolC_{wt}$, $PolC_{exo-}$…… - 122 -
Figure 5.6 dNTPs do not affect PolC binding to DNA**.** EMSAs PolC in the presence of 1 mM and 10 mM dGTP - 124 -
Figure 5.7 DNA-DnaE-PolC complex is template specific. EMSAs DnaE-PolC, DnaE-$PolC_{exo-}$ (5 mins) - 126 -
Figure 5.8 Primer hand-off between DnaE and PolC is unlikely to occur in early stages of primer extension. DNA Primer extension assays with small template (time course). - 129 -
Figure 5.9 DnaE and PolC cooperate in DNA primer extension. Data analysis of the DNA primer extension assays using small template - 130 -
Figure 6.1 DnaE can synthesize long nascent DNA. DnaE primer extension assays on a long template. - 133 -
Figure 6.2 DnaE, PolC and DnaE+PolC activities on naked M13mp18 template. - 134 -
Figure 6.3 Control primer extension assays on naked M13mp18 template. - 136 -
Figure 6.4 DnaE, PolC and DnaE+PolC primer extension assays on SSB and SSBΔ107-172-coated M13mp18 template - 139 -
Figure 6.5 DnaN and SSB stimulate polymerase activity. DnaE dominant activity and displacement from the 3'-OH ends - 143 -
Figure 6.6 Control primer extension assays with $DnaE_{pol-}$ and PolC in RNA primed template… - 144 -
Figure 6.7 Evidence for physical recruitment of PolC by DnaE at the 3'-OH ends of nascent DNA Exonuclease Assays - 147 -
Figure 6.8 DnaE error-prone polymerase activity.. - 149 -
Figure 6.9 The effect of PolC on DnaE error-prone polymerase activity. - 150 -
Figure 7.1 A revised speculative model for the *Bacillus subtilis* replisome. - 160 -

List of Tables

Table 2.1 Chemical Substances ..... - 24 -

Table 2.2 Expression Plasmids ..... - 25 -

Table 2.3 DNA Primers ..... - 25 -

Table 2.4 Oligonucleotides ..... - 26 -

Table 2.5 *Escherichia coli* strains ..... - 26 -

Table 2.6 Commercially available proteins ..... - 27 -

Table 2.7 Fragment Size and percentage of agarose ..... - 29 -

Table 2.8 Migration of macromolecules in PAGE ..... - 31 -

Table 2.9 PCR Cycling Conditions ..... - 35 -

Table 2.10 PCR reaction reagents ..... - 35 -

List of Acronyms and Abbreviations

4-(2-hydroxyethyl)-1-piperazineethanesulfonic acid	HEPES
Adenosine Triphosphate	ATP
Ammonium Persulphate	APS
Anion Exchange Chromatography	AEC
ATPases associated with various cellular activities	AAA+ ATPases
Cation Exchange Chromatography	CEC
C-terminal domain	CTD
deoxyribonucleic acid	DNA
deoxyribonucleotide	dNTP
Dithiothreitol	DTT
DNA Unwinding Element	DUE
DnaD – DnaB Homology Domains	DDBH
Ethylenediaminetetraacetic acid	EDTA
Fast Protein Liquid Chromatography	FPLC
Gel Filtration Molecular (Size) Exclusion chromatography	SEC
helicase binding domain	HBD
helix-hairpin-helix	HhH
Helix-Turn-Helix	HTH
Immobilised Metal Affinity Chromatography	IMAC
Intein-Mediated Purification with an Affinity Chitin-binding Tag	IMPACT
ion exchange chromatography	IEC
isoelectric point	pI
Isopropyl β-D-1-thiogalactopyranoside	IPTG
kiloDalton	kDa
Ligation Independent Cloning	LIC
Lysogeny Broth	LB Broth
minutes	mins
nanometer	nm
N-terminal domain	NTD
origin of replication	oriC
Phenylmethanesulfonylfluoride	PMSF
Polyacrylamide Gel Electrophoresis	PAGE
polymerase chain reaction	PCR
Polymerase Histidinol Phosphatase	PHP
polynucleotide	PNK
ribonucleic acid	RNA
ribonucleotide	rNTP
RNA polymerase domain	RPD
single-strand binding protein	SSB
Sodium Dodecyl Sulfate	SDS
Tetramethylethylenediamine	TEMED
volume/volume	v/v
weight/volume	w/v
Zinc-binding domain	ZBD

1 DNA Replication in Bacteria

This chapter comprises the Introduction of DNA replication in Bacteria. Additionally, it provides some examples of primer transfer from one polymerase to an other in different kingdoms of life.

1.1 Initiation of DNA Replication

DNA replication is a preeminent step for growth and cell division of all kingdoms of life (bacteria, archaea and eukaryotes) (Costa et al., 2013). The Gram-negative model organism *Escherichia coli* once thought to be a universal model for the investigation of DNA replication. Although, recent studies suggest that the Gram – positive low G-C content phylum of Firmicutes, consisting of three classes (*Bacilli, Clostridia* and *Mollicutes*) provides a better model (Briggs et al., 2012). *Escherichia coli* and *Bacillus subtilis* have diverged more than 3 billion years ago and the majority of bacteria show greater resemblance in terms of cellular functions and mechanisms to *Bacillus subtilis* than *Escherichia coli* (Battistuzzi et al., 2004). DNA replication proceeds in three steps: initiation, elongation and termination. Initiation of DNA replication implies recognition and unwinding of the origin of replication (*oriC*) and loading of replicative helicases onto single-strand DNA (Soultanas, 2012). Two replication forks are generated moving bidirectionally (**Figure 1.1**) (O'Donnell et al., 2013). This process relies on universally conserved AAA+ ATPases (ATPases

associated with various cellular activities) and ring – shaped hexameric helicases (Costa et al., 2013).

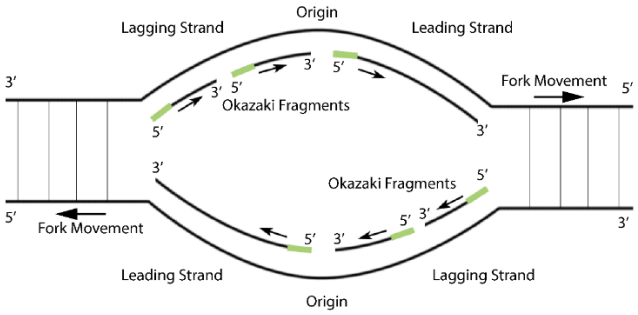


Figure 1.1 DNA replication fork. DNA replication initiates from a single origin, *oriC*. Each origin of replication creates two replication forks progressing at opposite directions. Large multi-protein molecular machines, known as replisomes, are assembled at those specific chromosomal sites and copy the parental genome. Each replication fork consists of a leading and a lagging strand due to the unidirectional 5'->3' polymerase activity of polymerases. Arrows indicate the direction of nascent DNA synthesis and fork progression.

Replication in bacteria initiates from the conserved *oriC*, which is in close proximity to the gene encoding the universally conserved replication initiator protein DnaA (Ogasawara & Yoshikawa, 1992). Initiation encompasses the recruitment and binding of DnaA to a single origin of replication that consists of two sequence elements: conserved repeats essential for the initiator recognition and an AT-rich DNA Unwinding Element (DUE)(Gille & Messer, 1991). Initiation entails DnaA-induced local melting of the DUE and loading of the replicative helicase, resulting in further DNA unwinding (Smits et al., 2010). In *Escherichia coli*, the primosome consists of DnaA (*Ec*DnaA), the helicase-loader DnaC (*Ec*DnaC), the

helicase DnaB (*Ec*DnaB) and the primase DnaG (*Ec*DnaG) (Kaguni, 2011). By comparison, the primosome in low G-C content, Gram-positive *Bacillus subtilis* includes DnaA (*Bsu*DnaA), two unique and essential proteins DnaD (*Bsu*DnaD) and DnaB (*Bsu*DnaB), the helicase-loader DnaI (*Bsu*DnaI), the replicative helicase DnaC (*Bsu*DnaC) and the primase DnaG (*Bsu*DnaG) (Briggs et al., 2012). The proteins of *Bacillus subtilis* primosome are recruited at the origin of replication in a hierarchical order, represented in **Figure 1.2**.

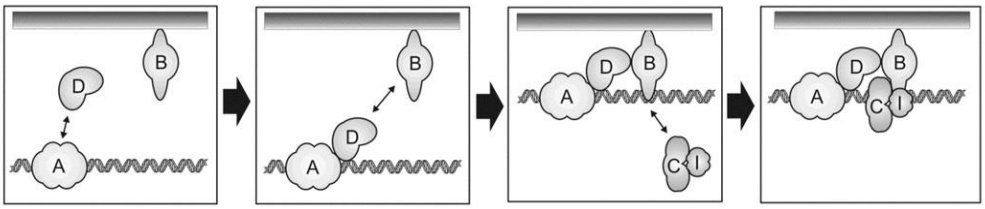


Figure 1.2 *Bacillus subtilis* primosome assembly. *Bacillus subtilis* DNA replication initiation proteins are assembled at *oriC* in hierarchical order. DnaA (A) interacts sequentially with DnaD (D) and DnaB (B), the complex is recruited to the cell membrane and in turn recruits the helicase-loader (I) – helicase (C) complex to the *oriC*. [Adopted from (Smits et al., 2010)].

DnaA (*Ec*DnaA/*Bsu*DnaA) comprises four domains. Domain I is responsible for interaction with regulatory proteins (Kaguni, 2006), domain II is a flexible linker (Ozaki & Katayama, 2009), domain III is a AAA+ ATPase that forms homooligomeric filaments, binds to single-strand DNA and promotes melting of the DUE (hydrogen bonds between nucleotides) (Felczak & Kaguni, 2004; Ozaki et al., 2008), whereas domain IV consists of a Helix-Turn-Helix (HTH) element that

specifically binds to DnaA-box clusters adjacent to the AT-rich DUE (Blaesing et al., 2000). Collectively, these domains confer DnaA the ability to function as an AAA+ ATPase replication initiator and transcription factor, that binds to several chromosomal regions, melts the DUE and facilitates loading of the replicative helicase onto single-strand DNA (Smits et al., 2011).

DnaD (*Bsu*DnaD) and DnaB (*Bsu*DnaB), as well as their homologues, are found in low G-C content, Gram – positive Firmicutes and are essential for DNA replication initiation (I Bruck & O'Donnell, 2000). They are structurally related, with *Bacillus subtilis* DnaD comprising two DnaD – DnaB Homology Domains (DDBH) DDBH1 and DDBH2, and DnaB three domains DDBH1-DDBH2-DDBH2 (**Figure 1.3**)(Marston et al., 2010). DnaD DDBH1 forms dimers which associate into tetramers and then higher-order oligomers generating large scaffolds (Schneider et al., 2008). DDBH2 domain confers single and double-strand DNA binding activities, instigating the formation of high-order oligomers by the native protein (Carneiro et al., 2006). In addition, DnaD and DnaB associate with the same chromosomal regions that DnaA associates with, in the same hierarchical order as that in *oriC*, modulating the activity of DnaA or regulating transcription of genes (Smits et al., 2011). Moreover, they present DNA remodelling activities. DnaB condenses DNA by lateral compaction and regulates the attachment of the replisome to the cell membrane (Rokop et al., 2004; Zhang et al., 2005). DnaD remodels supercoiled DNA by increasing negative twist and changing writhe accordingly keeping the linking number of supercoiled DNA intact (Zhang et al., 2006). DnaB and DnaD-like proteins in many Firmicutes, act as helicase co-loaders in conjugation with the

dedicated proteins for helicase loading (Núñez-Ramírez et al., 2007; Velten et al., 2003).

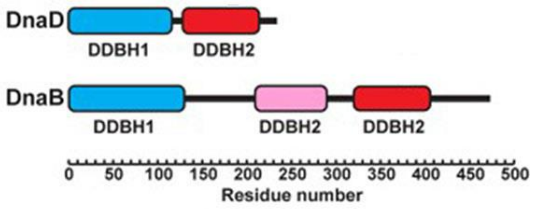


Figure 1.3 The architecture of *Bsu*DnaD and *Bsu*DnaB. A schematic figure showing the DDBH1 and DDBH2 domains in *Bacillus subtilis* DnaD and DnaB proteins [Adopted from (Briggs et al., 2012)].

To summarise, during DNA replication initiation in *Bacillus subtilis*, DnaA binds to DnaA-boxes within the *oriC*, forms nucleoprotein filaments and promotes association of DnaD with chromosomal regions adjacent to DnaA-boxes. DnaD affects the conformation of DnaA filaments, to aid in the untwisting and melting of the DUE in collaboration with DnaA and mediates the recruitment of additional DnaA proteins. The formation of DnaD scaffolds causes the DNA to bend, bridging the dual origin of *Bacillus subtilis* and promoting DnaA filament interaction, which is stabilized by DnaD activity. DnaB is recruited to the DNA-DnaA-DnaD complex and the DNA Unwinding Element (DUE) unwinds, assisted by the negative supercoiling induced by DnaD (**Figure 1.4**).

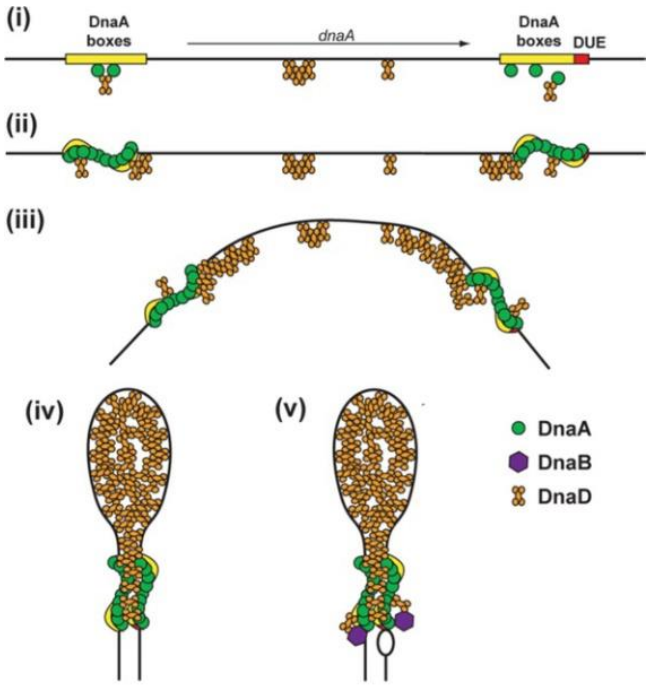


Figure 1.4 DNA replication initiation in *Bacillus subtilis* at *oriC*. DnaA binds to DnaA-boxes (i), DnaD is recruited to the origin of replication (*oriC*) and promotes formation of additional DnaA protein filaments *via* the formation of a DnaD scaffold (ii), DnaD generated scaffold causes the DNA to form a loop (iii) bringing the DnaA filaments of the bipartite *oriC* and promoting their interaction by stabilising the complex (iv), DnaB is then recruited and the DNA Unwinding Element (DUE) fully unwinds [Adopted from (Briggs et al., 2012)].

1.2 Helicase Loading Mechanisms and Primosome Assembly

Biological systems have evolved different helicase loading mechanisms due to differences in *oriC* architectures and in proteins that constitute the replisome, in order to regulate more effectively the DNA replication process (Soultanas, 2012).

In bacteria, a single helicase comprises the front end of the newly emerging replication fork, forming a twin-tiered hexameric ring (DnaB in *Escherichia coli*; DnaC in *Bacillus subtilis*). They encircle the single-strand DNA (lagging strand) and promote DNA unwinding during translocation. The conserved N-terminal domains (NTD) form one tier and are structurally homologous to the helicase interaction domain of the primase (X.-C. Su et al., 2006) and interact with the primase (Bird et al., 2000). The C-terminal domains (CTD) form the second tier and have ATPase activity, serving as the translocation engine (Bailey et al., 2007). DNA unwinding occurs as the helicase translocates 5'->3' with the CTD tier oriented at the front towards the duplex side of the fork, excluding the leading strand from the ring interior (S. Bailey et al., 2007; LeBowitz & McMacken, 1986; Liu et al., 2013).

Helicase loading is accomplished by specialised helicase-loaders. In *Bacillus subtilis*, there are two proteins that cooperate, DnaB and the AAA+ ATPase DnaI helicase-loader (Velten et al., 2003), whereas in *Escherichia coli*, a single protein with AAA+ ATPase activity *Ec*DnaC promotes helicase loading (Koonin, 1992). Helicase-loaders consist of an AAA+ C-terminal domain and an NTD responsible for the interaction with the helicase and regulation of single-strand DNA binding within the CTD (Ioannou et al., 2006). The CTD is homologous to DnaA (Mott et al., 2008).

Helicase-loaders are classified in two classes: the "ring-breakers" and the "ring-makers". "Ring-breakers" act on preassembled hexameric helicase rings and promote the helicase loading onto single-strand DNA by opening the ring to allow threading of the single-strand DNA template through the opening and subsequent closing of the ring trapping the template. By comparison, "ring-makers" assemble the functional hexameric helicase ring around single-strand DNA template (**Figure 1.5**) (Davey & O'Donnell, 2003).

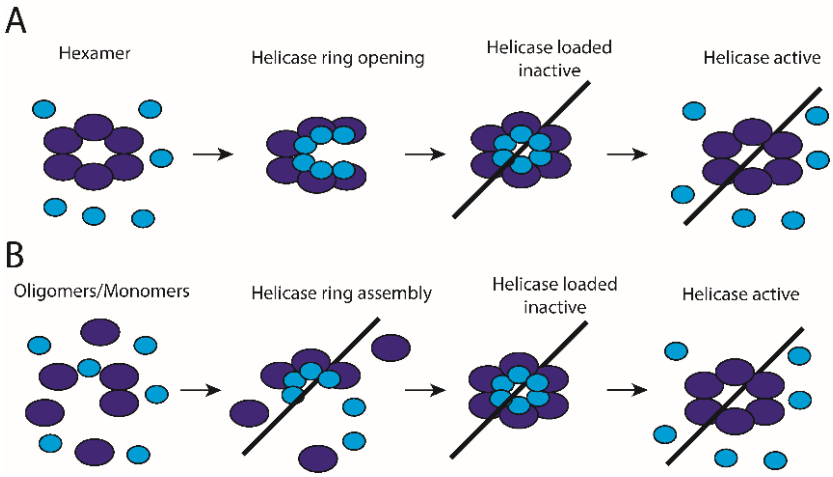


Figure 1.5 Helicase loading mechanisms. Schematic representation of the helicase-loader classes, where helicases are blue, helicase-loaders teal and single-strand DNA is shown as black straight line. (A) "Ring-breakers" open preassembled helicase rings and promote loading onto single-strand DNA, whereas (B) "ring-makers" assemble hexameric rings around single-strand DNA.

In *Escherichia coli*, the helicase-loader *Ec*DnaC cooperates with *Ec*DnaA to load the hexameric helicase at the *oriC*. *Ec*DnaA initially destabilizes and unwinds the DUE and then promotes helicase loading *via* an interaction between its I domain

and the NTD of the helicase (Ozaki & Katayama, 2012). Lack of detectable interaction between the helicase-loader *Ec*DnaC and *Ec*DnaA suggests that *Ec*DnaC binds to the CTD of the helicase *Ec*DnaB, forming a mini helical spiral. This helical spiral modulates the N-terminal configuration as well as the C-terminal region of the helicase *Ec*DnaB. These structural changes are considered important to open the helicase ring, *via* an ATP-dependent mechanism. ATP binding stabilizes the open ring ("ring-breaker" mechanism) (Arias-Palomo et al., 2013; Makowska-Grzyska & Kaguni, 2010; Schaeffer et al., 2005).

In Gram-positive, low G-C content *Bacilli*, the helicase-loader does not form the helical structure observed in *Escherichia coli* (Tsai et al., 2009). Its NTD binds to the CTD of the helicase *via* a Zn^{+2} binding fold (Ioannou et al., 2006; Loscha et al., 2009), forming a six-six dodecameric complex. In *Bacillus subtilis*, the hexameric ring helicase (DnaC) is inactive, even in presence of its helicase-loader (DnaI) and the co-loader DnaB, suggesting a "ring-making" loading mechanism. According to this mechanism, helicase monomers are assembled into functional hexameric rings directly onto the single-strand lagging strand DNA template (Rannou et al., 2013; Velten et al., 2003).

Helicase-loaders constitute a checkpoint in the transition from the initiation to the elongation stage of DNA replication (Kaguni, 2011). The NTD of the helicase interacts with the CTD of the primase to form a functional replisome, that synthesises RNA primers (Tougu & Marians, 1996). Primase DnaG is a DNA-dependent RNA polymerase and comprises three domains: the N-terminal Zn-binding domain, the RNA polymerase domain (RPD) and the C-terminal helicase

binding domain (HBD) (Tougu et al., 1994). It synthesises *de novo* short RNA oligonucleotides, that are required by polymerases in order to initiate the synthesis of both leading and lagging strands (Frick & Richardson, 2001).

The interaction of primase with the helicase loader-helicase complex (**Figure 1.6**), induces a conformational change in the helicase. The helicase-loader hydrolyses ATP and releases the helicase (Makowska-Grzyska & Kaguni, 2010). These changes release and activate the helicase-primase complex to translocate along single-strand DNA and to synthesise *de novo* RNA primers (Liu et al., 2013). The primase stimulates the ATPase and helicase activities of the helicase (Bird et al., 2000), while the helicase modulates and increases the synthesis of RNA primers (Thirlway & Soultanas, 2006).

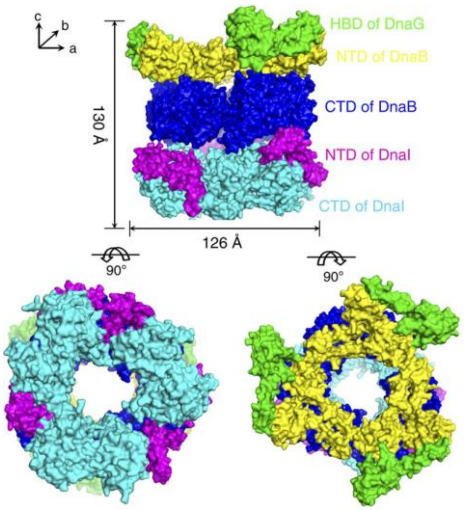


Figure 1.6 *Bsu*DnaI-*Bst*DnaB-*Bst*DnaG (HBD) crystal structure. The crystal structure of *Bacillus subtilis* helicase-loader (*Bsu*DnaI) (cyan, purple), *Bacillus stearothermophilus* helicase (*Bst*DnaB) (blue, yellow) and *Bacillus stearothermophilus* primase (*Bst*DnaG) Helicase Binding Domain (HBD) (green). The dimensions of the complex are 130 Å and 126 Å [Adopted from (Liu et al., 2013)].

1.3 DNA Polymerases and the Elongation Stage of DNA replication

Chromosomal replicases from all life kingdoms are tripartite. The *Escherichia coli* DNA polymerase III holoenzyme encompasses a DNA polymerase III core (α-ε-θ subunits), the multisubunit clamp-loader complex DnaX (τ, γ, δ, δ ', χ and ψ subunits) and the β clamp, a processivity factor (Antony et al., 2013) (**Figure 1.7**). It forms an initiation complex where the sliding clamp β is loaded around DNA by the clamp-loader, forming a ring of two β subunits arranged as a head-to-tail with pseudo-six-fold symmetry (Argiriadi et al., 2006; A. Johnson & O'Donnell, 2003). This process is ATP-dependent. Then, DNA polymerase III associates with the loaded clamp (Kong et al., 1992; Stukenberg et al., 1991).

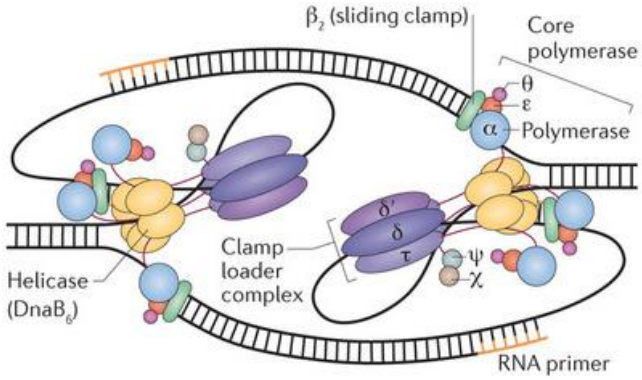


Figure 1.7 *Escherichia coli* replication forks. DNA polymerase III holoenzyme complexes are assembled at the melted *oriC* and proceed bidirectionally around the circular chromosome [Adopted from (Robinson & van Oijen, 2013)].

Escherichia coli clamp-loader consists of seven subunits, encoded by five genes, with the ATP binding subunits (τ and γ) coded by the *dnaX* gene (Kelman & O'Donnell, 1995). Three DnaX proteins with single copies of subunits δ and δ' form a pentameric ring (Jeruzalmi et al., 2001). The χ and ψ subunits stabilize the pentameric ring and bind to SSB (**Figure 1.8**) (Kelman et al., 1998). The *Escherichia coli* clamp-loader core, constists of the compleax $\tau_2\gamma$ and bridges two DNA polymerase III holoenzymes. In Firmicutes, the clamp-loader core comprises three τ proteins, facilitating the association of three polymerases with the replication process (Bruck & O'Donnell, 2000).

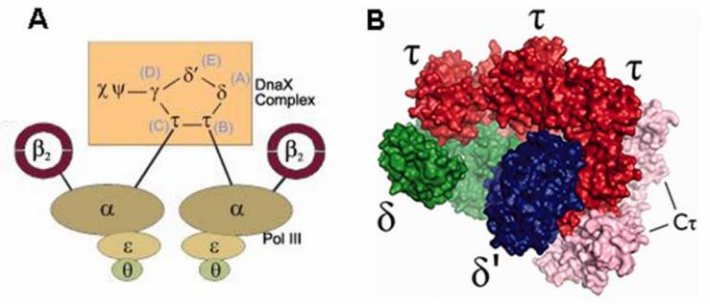


Figure 1.8 Clamp-loader architecture in Gram-positive and Gram-negative bacteria. (**A**) Known subunit interactions within *Escherichia coli* clamp-loader. (**B**) Homology model for *Bacillus subtilis* clamp-loader complex [Adopted from (McHenry, 2011a) and (Afonso et al., 2013)].

The third part of the bacterial DNA polymerase III holoenzyme is the polymerase α, which is classified as a family C polymerase (Ito & Braithwaite, 1991). It comes into two major forms, DnaE and PolC (Evans et al., 2008) and is categorised into four groups namely PolC, DnaE1, DnaE2 and DnaE3 (Timinskas et

al., 2014). DnaE and PolC are homologous, but PolC has some domains rearranged and an endogenous Mg^{+2}-dependent exonuclease (proofreading) activity (**Figure 1.9**). *Escherichia coli* Pol III α subunit forms a heterotrimeric core (with the 3'->5' exonuclease ε subunit and the polypeptide θ) and synthesises nascent DNA in both leading and lagging strands (Hamdan et al., 2002; Mueller et al., 2005). In low G-C content, Gram-positive Firmicutes there are two vital DNA polymerases, essential for chromosomal replication, DnaE and PolC (Dervyn et al., 2001; McInerney et al., 2007). PolC is considered the main replicative polymerase in both strands. On the contrary, DnaE extends RNA primers, synthesised *de novo* by primase DnaG, only by a few nucleotides before handing off to PolC (Sanders et al., 2010), in functional analogy to the eukaryotic Pol α and Pol δ, respectively (Pellegrini, 2012).

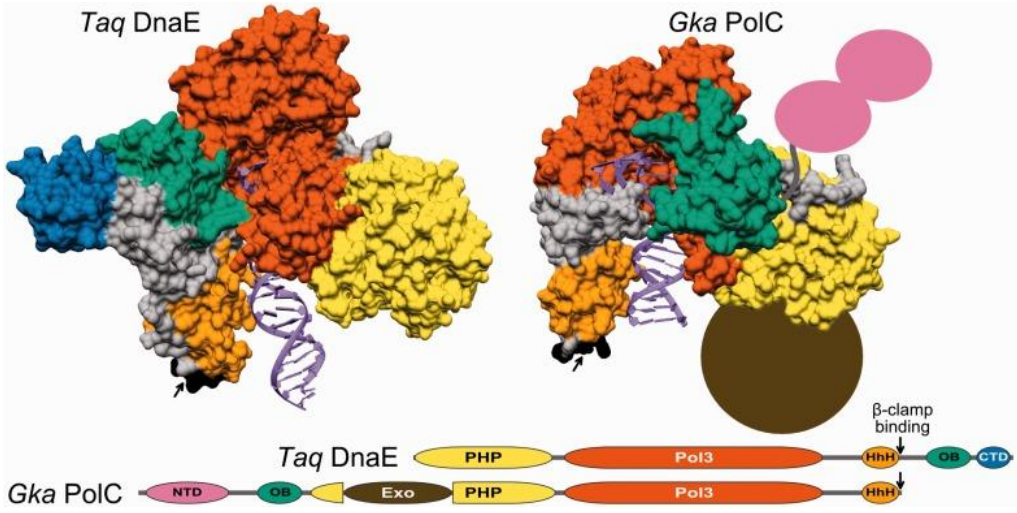


Figure 1.9 Structural organisation of C family DNA polymerases. DnaE and PolC structures of C family DNA polymerases, from the crystal structures of *Thermus aquaticus* DnaE (*Taq*DnaE) and *Geobacillus kaustophilus* PolC (*Gka*PolC), complexed with DNA, with the linear organisation of their domains at the bottom of the figure [Adopted from (Timinskas et al., 2014)].

DNA polymerases contain palm, thumb and fingers domains, in the shape of a cupped right hand (**Figure 1.9** and **Figure 1.10**). Family C of DNA polymerases encompasses a PHP (Polymerase Histidinol Phosphatase) domain that binds to the ε subunit with proofreading activity in DnaE-type polymerases (Wieczorek & McHenry, 2006) and exhibits an Zn^{+2}-dependent exonuclease (proofreading) activity itself (Stano et al., 2006). The palm domain contains a universally conserved Lysine residue and forms a salt bridge with the phosphate moiety of the terminal base of the primer. Last, the fingers domain contains four conserved Arginines in the interface with the palm, forming a nucleotide binding site, that binds deoxyribonucleotides (dNTPs) and transfers them to the catalytic site (Bailey et al., 2006). The catalytic pocket is formed by the thumb, fingers and palm domains upon DNA binding with three acidic residues coordinating two Mg^{+2} ions and facilitating dNTP incorporation (Pritchard & McHenry, 1999). The C-terminal region is responsible for interactions with the clamp-loader τ and the β clamp (Kim & McHenry, 1996). It also contains additional structural elements, homologous to DNA binding proteins, including a helix-hairpin-helix (HhH) motif and an OB fold, that bind single-strand DNA (Doherty et al., 1996; Theobald et al., 2003). The β binding domain exhibits double-strand DNA binding activity due to the HhH motif and its flanking loops (Wing et al., 2008), whereas the τ binding domain interacts weakly with the clamp-loader and is not required for processive replication. Finally, the PolC group of polymerases also contains an intrinsically disordered NTD.

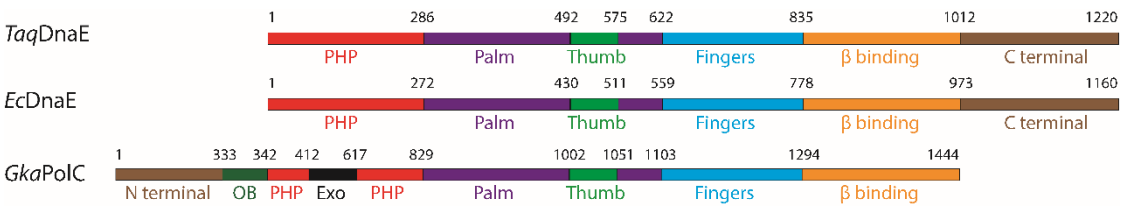


Figure 1.10 *Taq*DnaE. *Ec*DnaE and *Gka*PolC domains. Schematic diagram indicating the structural domains of *Thermus aquaticus* DNA polymerase III (*Taq*DnaE) (Scott Bailey et al., 2006; Wing et al., 2008), *Escherichia coli* DNA polymerase III (*Ec*DnaE) (Lamers et al. 2006) and *Geobacillus kaustophilus* PolC (*Gka*PolC) (Evans et al., 2008).

DNA polymerases are unable to rapidly synthesize long stretches of DNA, due to frequent dissociation from the template strands (McHenry, 2011c). The lifetime of a polymerase on template DNA during synthesis (known as processivity) is increased by binding to a sliding clamp (DnaN) and stabilisation within the replication fork (Hedglin et al., 2013). In *Escherichia coli*, the DnaE-type DNA polymerase III is attached to the replisome *via* direct interaction with the CTD of the clamp-loader τ subunit (DnaX) (X.-C. Su et al., 2007). By comparison, the *Bacillus subtilis* τ subunit interacts weakly only with PolC and not with the error - prone DnaE (I Bruck & O'Donnell, 2000; I Bruck et al., 2005). DnaE is localised at the replication fork *via* a ternary complex (DnaC-DnaG-DnaE) assembled on the lagging strand. (Rannou et al., 2013). The τ containing clamp-loader complex chaperones the associated polymerase onto the β clamp (DnaN), increasing the rate of initiation complex formation (Downey & McHenry, 2010). Additionally, in *Escherichia coli*, the χ subunit of the clamp-loader complex interacts with SSB. This

interaction stimulates the processivity of DNA replication (Antony et al., 2013), by allowing the polymerase to replicate SSB-coated DNA and by stabilising the polymerase on DNA in strand displacement reactions (Glover & McHenry, 1998). On the contrary, in *Bacillus subtilis* this type of stimulation is absent due to lack of χ and ψ subunits from the cognate clamp-loader complex (Afonso et al., 2013). Moreover, DnaE polymerase interacts with YqeN (HolA), the delta (δ) subunit of the clamp-loader complex and SSB (Costes et al., 2010; Rannou et al., 2013).

1.4 Hand-off Mechanisms

Mechanisms for hand-off of newly synthesized RNA primers to polymerases differ amongst different organisms. In some organisms this mechanism has been revealed, whereas in others is still unidentified. Hereby, there are known mechanisms of primer transfer in four different organisms.

In *Escherichia coli*, a three-point switch model has been suggested for the hand-off of newly synthesised RNA primer from the primase *Ec*DnaG to the replicative polymerase. According to this model, the SSB interaction with the primase comprises a crucial step. Disruption of the SSB-primase interaction by the clamp-loader, causes the primase to halt RNA primer synthesis and to dissociate from the primosome. The clamp-loader interacts with SSB and assembles the β clamp onto the primed single-strand DNA. Then, the β clamp recruits the DNA polymerase III core (α subunit) (Yuzhakov et al., 1999). In other words, the polymerase does not have access to the RNA primer, unless the χ subunit of the clamp-loader binds first the SSB, to which the primase is bound, permitting the displacement of the primase *Ec*DnaG from the *de novo* synthesised RNA primer. Recent studies delineated the crucial role of SSB-χ clamp-loader subunit interaction in replisomal stability and in productive leading strand DNA synthesis, suggesting that this interaction is not supported in lagging strand primer utilisation (Marceau et al., 2011). Consequently, the mechanism of RNA primer hand-off is still unknown.

In T7 bacteriophage, the primase comprises two domains, a Zinc-binding domain (ZBD) and a RNA polymerase domain (RPD). These domains do not interact in the absence of the substrate. However, during primer synthesis, both bind DNA, triggering a close conformation of the primase. After the primer is synthesised, only the ZBD remains bound to the primed template and delivers the primer to T7 DNA polymerase (**Figure 1.11**) (Kato et al., 2004).

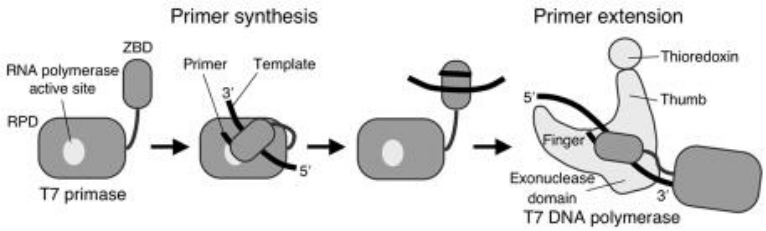


Figure 1.11 Hand-off Model in T7 bacteriophage. The T7 RNA polymerase domain (RPD) interacts with the Zinc-binding domain (ZBD) only in the presence of single-strand DNA, resulting in the synthesis of RNA primers. Then the RPD dissociates from the substrate and the ZBD, that is still bound, transfers the primed template to the T7 DNA polymerase [Adopted from (Kato et al., 2004)].

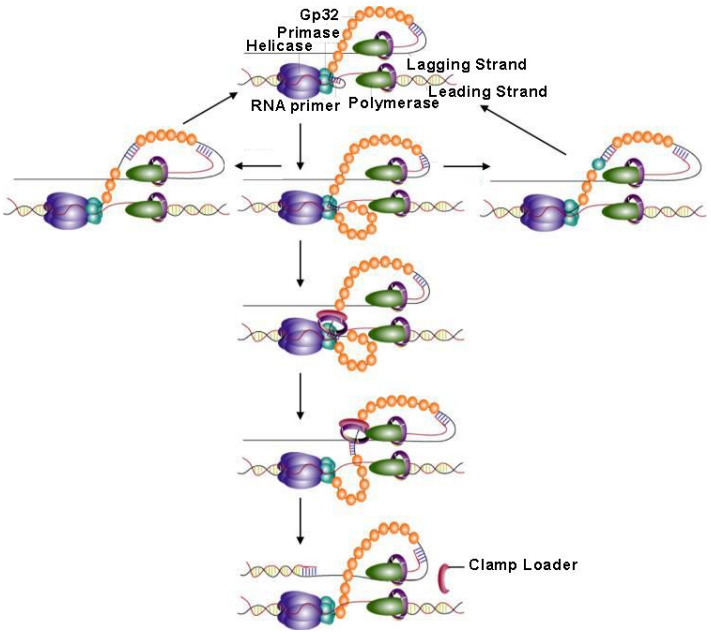


Figure 1.12 Hand-off Model in T4 bacteriophage. The replicative helicase is purple, the primase cyan, single-strand DNA binding proteins (Gp32) are yellow, the replicative polymerase is green and the processivity clamp is red. The successful loading of the clamp is pivotal for the primer to be transferred to the DNA polymerase, since it comprises the intermediate between the primase the replicative polymerase [Adopted from (Nelson, Kumar, & Benkovic, 2008)].

In T4 bacteriophage replisome, lagging strand DNA replication initiates with the synthesis of an RNA primer by the primase. In the meantime, the lagging strand DNA polymerase synthesises an Okazaki fragment, causing the lagging strand loop to increase in size while the helicase unwinds the DNA helix, generating a second loop. If the clamp isn't loaded in time, the primase either releases the primer and remains with the replisome, or releases the replisome and dissociates, in which case a new primase has to be recruited. If the clamp is loaded, the RNA primer is transferred to the clamp, promoting the release of the lagging strand template from

the polymerase and recycle to the new clamp loaded RNA primer (**Figure 1.12**) (Nelson et al., 2008).

DNA replication in eukaryotes requires the coordinated actions of three DNA polymerases: Pol α, Pol δ and Pol ε (Hübscher et al., 2003). The Pol α/primase complex synthesises *de novo* short RNA primers by its primase domain and extends them by its polymerase domain. Then, the hybrid RNA/DNA primers are transferred to the main replicative polymerases Pol δ and Pol ε in the lagging and leading strands respectively (Johansson & MacNeill, 2010; Lujan et al., 2016). Although recently, the polymerase asymmetry in eukaryotic system has been challenged. Data indicate that Pol δ constitutes the major polymerase in both strands and Pol ε provides the proofreading activity (R. E. Johnson et al., 2015). Despite the fact that the mechanism of the primer synthesis (Coloma et al., 2016; Perera et al., 2013) and the sequential order of polymerases have been identified, it wasn't until recently when the mechanism of RNA primer hand-off from the primase to the polymerase domain of Pol α/primase complex was revealed (Baranovskiy et al., 2016); described in **Figure 1.13**. This primer transfer constitutes a functional analogy to *Bacillus subtilis* primase DnaG and error-prone DnaE polymerase. Similarly, the primer transfer from eukaryotic Pol α to either Pol ε or Pol δ is a functional analogy to *Bacillus subtilis* DnaE and PolC polymerases respectively.

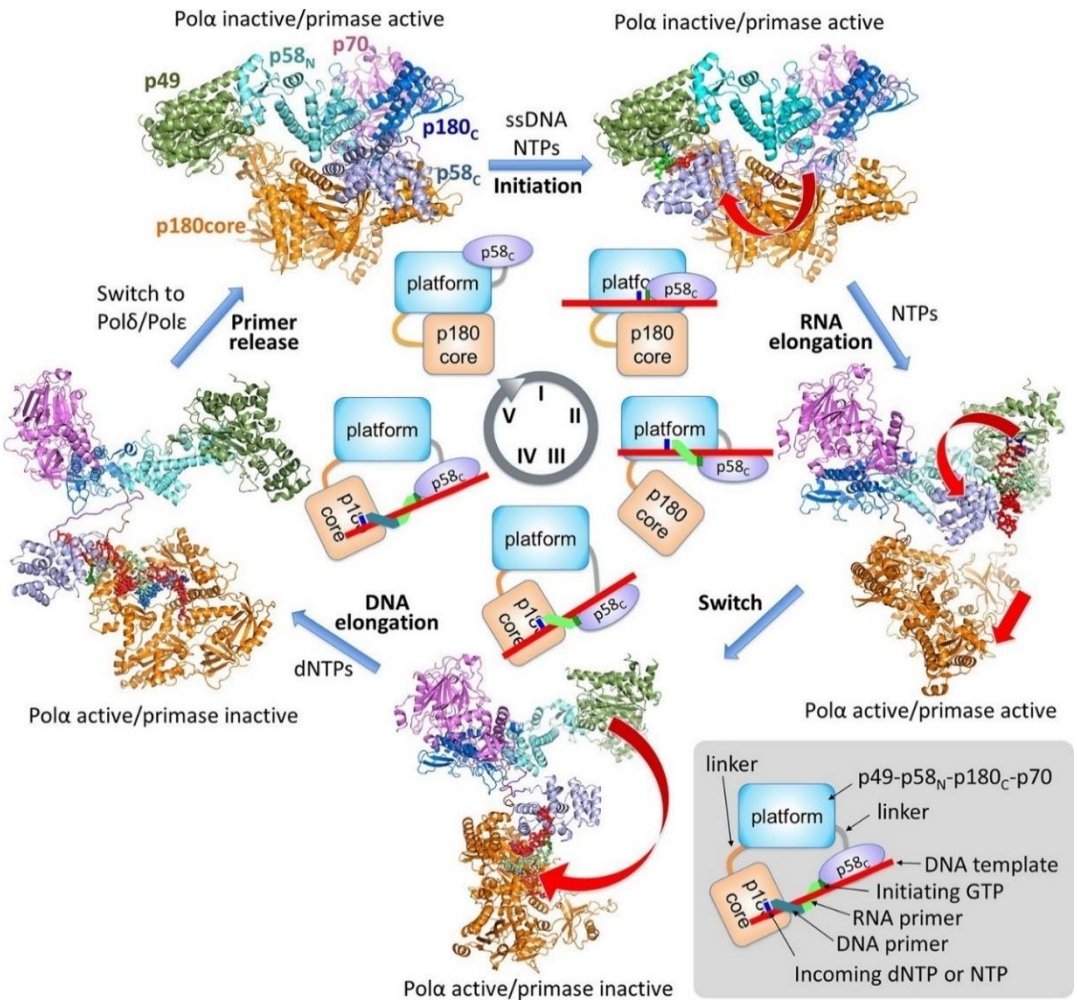


Figure 1.13 Mechanism of RNA primer hand-off in hPolα/primase complex. hPol α/primase comprises two domains constituting the primase (p58 and p49) and two domains comprising the polymerase (p180 and p70). The hand-off steps are labelled by roman numerals in the centre and are shown with blue arrows, whereas red arrows indicate the changes in domain orientation. The primase catalytic subunit (p58c) recognises the poly-C sequence and synthesises *de novo* short RNA primers (I) and translocates towards the catalytic polymerase subunit (p180core) causing its dissociation from the platform subunits (II). Then, the RNA-primed template is loaded to the polymerase activity subunit (III), Pol α extends the primer using dNTPs, whilst the primase remains bound to the 5' of the primer (IV), followed by the replacement of Pol α with either Pol δ (in the lagging strand) or Pol ε (in the leading strand) [Adopted from (Baranovskiy et al., 2016)].

1.5 The Replication Model in *Bacillus subtilis* – Aims of this study

The current model for the elongation stage of *Bacillus subtilis* DNA replication suggests that the elongation starts with the recruitment of the primase DnaG in the replication fork, *via* an interaction with the replicative helicase DnaC. Primase DnaG synthesises *de novo* short RNA primers in both leading and lagging strands that are transferred to DnaE polymerase with the assistance of the clamp-loader and the clamp (McHenry, 2011b) or without the requirement of other auxiliary proteins (Rannou et al., 2013). Subsequently, the RNA primer is extended only by a few nucleotides and then transferred to PolC, the main replicative polymerase (Sanders et al., 2010). Thus, DnaE plays a minor role in briefly extending RNA primers, in the leading strand at least once, and during Okazaki fragment synthesis in the lagging strand. On the contrary, PolC is the main processive replicative polymerase that synthesises the bulk of the nascent DNA. The elongation stage of DNA replication in the lagging strand of DNA is represented in **Figure 1.14**. The molecular interactions that underlie the hand-off of the RNA primer to DnaE polymerase and then the extended RNA-DNA hybrid primer to PolC polymerase are unknown.

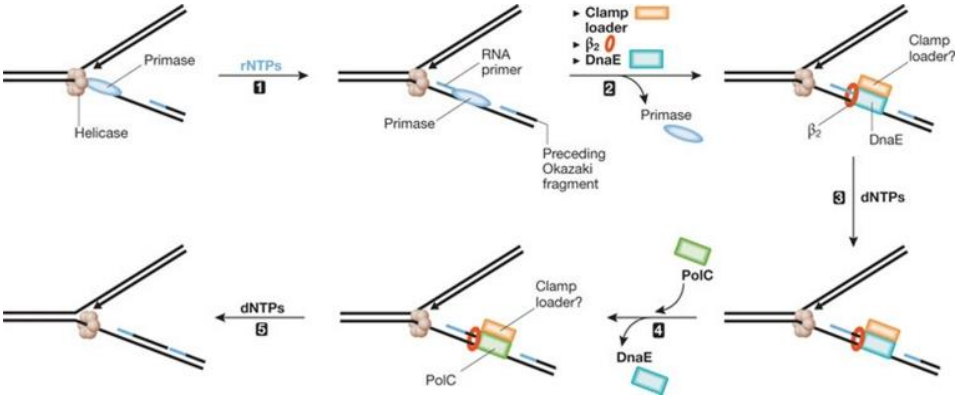


Figure 1.14 Hand-off Model in low G-C content, Gram (+) bacteria. This model represents the hand-off mechanism during the lagging strand DNA synthesis in low G-C content, Gram-positive bacteria. DnaG primase synthesises *de novo* short RNA primers that are transferred to DnaE. DnaE extends those RNA primers only by a few nucleotides before handing-off to the main replicative polymerase PolC [Adopted from (McHenry, 2011b)].

The aim of this study is the reconstruction of *Bacillus subtilis* replisome *in vitro*, in order to investigate the poorly defined roles and interactions amongst DnaG primase, DnaE and PolC polymerases. Initially, we examined the DnaG-DnaE and DnaE-PolC complexes formation. Furthermore, we explored the processivities of DnaE and PolC, scrutinising the effects of the β clamp (DnaN), the clamp-loader complex and single-strand DNA Binding proteins (SSB). Then, we studied the processivity of the error-prone DnaE polymerase in the absence of dNTPs. Finally, we re-evaluated the current replication model *in Bacillus subtilis* regarding the polymerase asymmetry between DnaE and PolC polymerases.

2 Materials and Methods

2.1 Materials

2.1.1 Chemical Substances

Table 2.1 Chemical Substances

Substances	Supplier
4-(2-hydroxyethyl)-1-piperazineethanesulfonic acid (HEPES)	Sigma
2xYT Broth	Melford
Accugel 19:1	Fisher Scientific
Adenosine Triphosphate (ATP)	Melford
Agarose	Melford
Ammonium persulphate	Melford
Ammonium sulphate	Sigma
Antifoam 204	Sigma
Boric acid	Fisher Scientific
Bromophenol blue	Fisher Scientific
Carbenicillin	Melford
Dithiothreitol (DTT)	Sigma
Ethylenediaminetetraacetic acid(EDTA)	Sigma
Gelcode blue safe protein stain	Thermo Scientific
Glucose	Fisher Scientific
Glycerol	Sigma
Glycine	Fisher Scientific
Guanidinium chloride	VWR Chemicals
Isopropyl β-D-1-thiogalactopyranoside (IPTG)	VWR Chemicals
Lysogeny Broth (LB Broth)	Melford
Lysogeny Broth with agar	Sigma
Magnesium chloride	VWR Chemicals
PageRuler Plus Unstained Protein Ladder	Fisher Scientific
Phenylmethanesulfonylfluoride (PMSF)	Sigma
Precision Plus Protein standard	Bio-Rad
Protease Inhibitor Cocktail	Fisher Scientific
Protogel	Fisher Scientific
Sequagel - Ureagel system	Fisher Scientific
Sodium Chloride	Fisher Scientific
Sodium Dodecyl Sulfate (SDS)	Fisher Scientific
Tetramethylethylenediamine (TEMED)	Sigma
Tris(hydroxymethyl)aminomethane	Fisher Scientific
Tryptone	Fluka
Urea	Melford
Yeast Extract	Becton, Dickinson

2.1.2 DNA Plasmids

Table 2.2 Expression Plasmids

Plasmid name	Resistance	Use
pSMG33	Ampicillin	Expression of *Bsu*DnaC-*Bsu*DnaI
pSMG11	Ampicillin	Expression of C-term Intein-tagged *Bsu*DnaG
p2BT-BsuDnaG	Ampicillin	Expression of N-term His-tagged *Bsu*DnaG
pTYB3-DnaE	Ampicillin	Expression of C-term Intein-tagged *Bsu*DnaE
p2CT-BsuDnaE	Ampicillin	Expression of N-term MBP His-tagged *Bsu*DnaE
pA1-BsuPolC	Ampicillin	Expression of *Bsu*PolC
p2BT-BsuPolC	Ampicillin	Expression of N-term His-tagged *Bsu*PolC
pET22b-SSB	Ampicillin	Expression of *Bsu*SSB
pET28b-His SSBΔ107-172	Kanamycin	Expression of *Bsu*SSBΔ107-172

2.1.3 Primers and Oligonucleotides

Table 2.3 DNA Primers

Primer	Sequence (5' to 3')	Use
DnaEpoldF	TGCTATTGACTTTCCCGATACTAGA AGGGATG (32)	*Bsu*DnaE D382A/D384A (polymerase-deficient)
DnaEpoldR	ATAGCCGGCATGCTGACGCGTT (22)	*Bsu*DnaE D382A/D384A (polymerase-deficient)
PolCpoldF	CGCTTTGAACTTCTCAGGGGAATAT C (26)	*Bsu*PolC D966A/D968A (polymerase-deficient)
PolCpoldR	ATAGCAGGTACTTTGTCCCCTTTAA ATC (28)	*Bsu*PolC D966A/D968A (polymerase-deficient)
PolCexodF	TGCGACGACAGGATTGTCTGCTG (23)	*Bsu*PolC D425A/E427A (exonuclease-deficient)
PolCexodR	ACAGCAAAAACAACATATGTTTCTT CTTCG (30)	*Bsu*PolC D425A/E427A (exonuclease-deficient)
NTHTDnaGF	TACTTCCAATCCAATGCAATGGGAA ATCGGATACCAGATG (40)	*Bsu*DnaG LIC
NTHTDnaGR	TTATCCACTTCCAATGTTATTATTT TAAAGATCGGTTCAATGTAAC (46)	*Bsu*DnaG LIC
NTHTDnaEF	TACTTCCAATCCAATGCAATGTCTT TTGTTCACCTGCAAG (40)	*Bsu*DnaE LIC
NTHTDnaER	TTATCCACTTCCAATGTTATTACCA CTGTTTTAAAACGACGTTTTTTTG (49)	*Bsu*DnaE LIC
NTHTPolCF	TACTTCCAATCCAATGCAATGGAAC AGCTGTCCGTAAAC (39)	*Bsu*PolC LIC
NTHTPolCR	TTATCCACTTCCAATGTTATTAGAA CAGTGACAATTGGTTTTGATC (46)	*Bsu*PolC LIC

Table 2.4 Oligonucleotides

Oligo	Sequence (5' to 3')	Length (nt)
CA65TTTA15M13	CACACACACACACACACACACACACACACACACACACACACACACACACACACACACACACACACCCCCTTTAAAAAAAAAAAAAAAAAGCCAAAAG**CAGTGCCAAGCTTGCATGCC**	110
PTT5C4(TG)	AAGGGGGTGTGTGTG	15
PTT5C4(UG)	AAGGGGGUGUGUGUG	15
PTT5C3(TG)TA	AAGGGGGTGTGTGTA	15
DNAM13	CAGTGCCAAGCTTGCATGCC	20
DNAM13c→a	CAGTGCCAAGCTTGCATGCA	20
RNAM13	CAGUGCCAAGCUUGCAUGCC	20
11(AC)A5CTT	ACACACACACACACACACACACACCCCCTT	30
19(CA)5CTT	CACACACACACACACACACACACACACACACACACACACACCCCCTT	45
4(CA)5CTT7(AC)A	CACACACACCCCCTTACACACACACACACA	30

2.1.4 *Escherichia coli* strains

Table 2.5 *Escherichia coli* strains

Strain	Use
XL-1 Blue	Plasmid storage
DH5a	Plasmid storage
MCC142	Expression of *Bsu*DnaC-*Bsu*DnaI
MC1061	Expression of C terminal Intein-tagged *Bsu*DnaG
DMSO 1504 Ap1.L1	Expression of *Bsu*PolC
BL21(DE3) Rosetta	Expression of T7 promoter
Rosetta(DE3)pLysS	Expression of T7 promoter
C41(DE3)	Expression of T7 promoter
BLR(DE3)	Expression of T7 promoter
BB810(DE3)	Expression of T7 promoter
B834(DE3)	Expression of T7 promoter
Lemo21 (DE3)	Expression of T7 promoter

2.1.5 Commercially available proteins

Table 2.6 Commercially available proteins

Protein	Use
Q5 polymerase	PCR reaction
DpnI	Digestion of methylated DNA
T4 Polynucleotide kinase	Phosphorylation, Radiolabeling of oligonucleotides
T4 ligase	Ligation reaction
DNase I	DNA digestion
Benzonase	DNA digestion
SspI-HF	LIC cloning
T4 DNA polymerase LIC-qualified	LIC cloning

2.2 Methods

2.2.1 Electrophoresis

2.2.1.1 Agarose Gel Electrophoresis

Agarose gel electrophoresis is widely used to separate nucleic acid fragments according to their size and conformation. Agarose consists of repeated L - and D - galactose subunits that associate non – covalently during gelation, forming a matrix, conferring molecular sieving abilities. The samples are loaded on precast wells in the gel and the applied electric field causes the fragments to migrate to the positively charged anode, due to the negative charge of the phosphate backbone of nucleic acids. The rate of migration through an agarose gel is regulated by: a. the size of the nucleic acid, b. the nucleic acid conformation, c. the agarose concentration, d. the agarose type, e. the applied voltage and f. the electrophoresis buffer. The distance of migration is inversely proportional to the log of the molecular weight (Lee et al., 2012).

2.2.1.1.1 Non Denaturing Agarose Gel Electrophoresis

Agarose gels were prepared by weighing the appropriate agarose mass (**Table 2.7)** into an Erlenmeyer flask. The flask was filled with 1x running buffer (1x TAE: 40 mM Tris, 1.1% (v/v) Acetic acid and 1 mM EDTA) and the mixture was melted

by heating in a microwave. The agarose solution was left to cool down to 50ºC, ethidium bromide was added (0.5 μg/ml) and the solution was poured into the gel tray and allowed to set at room temperature for 30 minutes. The samples were mixed with the appropriate volume of 6x Purple Gel Loading Dye (New England Biolabs), loaded into the gel wells alongside with Quick-load Purple 2-Log DNA Ladder (New England Biolabs) and electric field was applied between the electrodes of the gel running apparatus (5 Volts/cm). Electrophoresis was carried out in Mini-Sub Cell GT and Wide Mini-Sub Cell GT Systems from Bio-Rad. When electrophoresis was completed, nucleic acids were visualised using a molecular imager.

Table 2.7 Fragment Size and percentage of agarose

Fragment Size (bp)	Agarose % (w/v)
<400	1.2
<1000	1
>5000	0.7

2.2.1.1.2 Alkaline Agarose Gel Electrophoresis

Alkaline agarose gels were prepared by weighing the amount of agarose into an Erlenmeyer flask, filling the flask up to the desired volume with deionised water and heating the mixture in a microwave. The agarose solution was left to cool down to 50ºC before adding the appropriate volume of 10x Alkaline Agarose Gel Electrophoresis Buffer (500 mM NaOH and 10 mM EDTA) and pouring the solution into the casting tray, where it was left to set at room temperature for 30

minutes (Southern, 2002). Samples were mixed with the appropriate volume of 6x Alkaline Agarose Gel Loading Buffer [300 mM NaOH, 6 mM EDTA, 18% (v/v) glycerol, 0.15% (w/v) bromophenol blue and 0.25% (w/v) xylene cyanol] and incubated at 95°C for five minutes. Subsequently, they were loaded into the gel wells and electric field was applied between the electrodes of the gel running apparatus (3 Volts/cm). Alkaline agarose gels were resolved using the Bethesda Research Laboratories Model H5 system. After the completion of electrophoresis, the alkaline agarose gel was immersed in 7% (w/v) trichloroacetic acid for 30 minutes, dried overnight and analysed using a molecular imager and associated software (Bio-Rad).

2.2.1.2 Polyacrylamide Gel Electrophoresis

Polyacrylamide Gels are widely used to separate and analyse proteins and relatively small nucleic acid molecules. Gels are formed from polymerisation of acrylamide and N, N'-methylene –bis-acrylamide, that acts as the acrylamide strand cross-linker. The polymerisation reaction is catalysed by a free radical donor (Ammonium Persulphate-APS) along with the reaction initiator (N,N,N,N'-tetramethylethylenediamin-TEMED), that promotes free radical production. The ratio of N,N'-methylene –bis-acrylamide to acrylamide and the total concentration of both components define the pore size of the formed porous gel matrix (**Table 2.8**). Samples are loaded on the precast wells and electric field is applied. The mobility of a macromolecule in the applied electric field is inversely proportional to

its size and shape and directly proportional to the applied voltage between the electrodes and the charge of the macromolecule (BIO-RAD, n.d.).

Table 2.8 Migration of macromolecules in PAGE

	Native PAGE	Denaturing PAGE	
Acrylamide % (v/v)	Fragment Size (bp)	Fragment Size (bases)	Molecular Mass (kDa)
5	>500	80-200	60-400
8	60-500	40-100	40-350
10	50-300	20-80	30-200
12	40-200	10-50	20-150
15	25-150	5-40	10-100
20	5-100	<20	5-50

2.2.1.2.1 Non Denaturing Polyacrylamide Gel Electrophoresis

Non Denaturing (native) Polyacrylamide Gels are widely used to detect any process that affects the charge and/or the conformation of macromolecules. In this study, this type of polyacrylamide gels was used to resolve binding events between proteins and DNA molecules. The native polyacrylamide gels were prepared by mixing the appropriate volume of acrylamide:bis-acrylamide and 10x running buffer (10x TBE: 0.9 M Tris base, 0.9 M Boric acid and 20 mM EDTA) with 10% (w/v) Ammonium Persulphate (APS) and N,N,N,N'-tetramethylethylenediamin (TEMED), as indicated (BIO-RAD, n.d.). The solution was poured into Gel Cassette Assembly (Bio-Rad Mini Protean Tetra Cell) and allowed to set at room temperature

for 30 minutes (Harwood, 2000). Then, gels were placed into the Bio-Rad Mini Trans Blot Cell vertical electrophoresis system. The samples were mixed with loading dye [50% (v/v) glycerol, 0.15% (w/v) bromophenol blue and 0.25% (w/v) xylene cyanol] and loaded into the gel wells and electric field was applied (5 Volts/cm). When electrophoresis was completed, gels were dried using a pump-heater-vacuum system and exposed to phosphor screens (Bio-Rad) overnight. Analysis of gels was performed using molecular imager and associated software (Bio-Rad).

2.2.1.2.2 SDS Polyacrylamide Gel Electrophoresis

SDS PAGE is the most common technique to separate and estimate the molecular mass of a protein. It utilises the ability of Sodium Dodecyl Sulphate (SDS), an anionic detergent, to disrupt all non-covalent inter and intramolecular interactions and in combination with reducing agents (DTT) to linearise all proteins, conferring negative charge. Thus, all SDS-treated proteins are being solely separated according to their size, which is a linear function of molecular mass, when migrating towards the positively charged anode. The discontinuous Laemmli Buffer System is used for the electrophoresis of SDS Polyacrylamide Gels (Laemmli, 1970). It comprises a stacking gel [4% (v/v) acrylamide buffered in Tris-HCl pH 6.8], a resolving-separating gel [8-20% (v/v) acrylamide buffered in Tris-HCl pH 8.8] and SDS PAGE running buffer (30 g/L Tris base, 144 g/L Glycine and 10 g/L SDS). Gels were prepared in a similar manner to native polyacrylamide gels, by mixing the

appropriate volumes of acrylamide:bis-acrylamide with the resolving and the stacking buffers, pouring them into the Gel Cassette Assembly (Bio-Rad Mini Protean Tetra Cell) and allowed to set at room temperature for 30 minutes seriatim (BIO-RAD, n.d.). Then, gels were placed into the Bio-Rad Mini Trans Blot Cell vertical electrophoresis system. Samples were mixed with SDS-PAGE Loading Buffer [6x Loading Buffer: 180 mM Tris-HCl pH 6.8, 12% (w/v) SDS, 30% (v/v) glycerol, 0.15% (w/v) bromophenol blue and 200 mM DTT] and incubated at 95ºC for five minutes. Subsequently, they were loaded into the gel wells alongside with PageRuler Unstained Protein Ladder (ThermoFisher Scientific) and electric field was applied (10 Volts/cm). After the completion of the electrophoresis, the SDS polyacrylamide gels were stained using GelCode Blue Safe Protein Stain (ThermoFisher Scientific) (Coomassie stain) and visualised using molecular imager.

2.2.1.2.3 Ureagel Denaturing Gel Electrophoresis

Urea Denaturing Gels were used to separate and analyse single-strand nucleic acids. These gels were prepared using the Sequagel Ureagel System (National Diagnostics), by mixing the appropriate volumes of UreaGel Concentrate (237.5 g/L acrylamide, 12.5 g/L methylene bis-acrylamide and 7.5 M urea), UreaGel Diluent (7.5 M urea) and UreaGel Buffer (0.89 M Tris base, 0.89 M Boric acid, 20 mM EDTA and 7.5 M urea) with suitable volumes of 10% (w/v) APS and TEMED, as indicated (National Diagnostics, n.d.). The solution was poured into Gel Cassette Assembly (Bio-Rad Mini Protean Tetra Cell) and allowed to set at room temperature for 30

minutes. Then, the gels were placed into the Bio-Rad Mini Trans Blot Cell vertical electrophoresis system filled with TBE as running buffer (10x TBE: 0.9 M Tris base, 0.9 M Boric acid and 20 mM EDTA). Subsequently, the samples were mixed with loading dye [95% (v/v) formamide, 0.15% (w/v) bromophenol blue and 0.25% (w/v) xylene cyanol], loaded into the gel wells and electric field was applied (10 Volts/cm) (Summer et al., 2009). When the electrophoresis was completed, the gels were dried using a pump-heater-vacuum system and exposed to phosphor screens (Bio-Rad) overnight. Analysis of the gels was performed using molecular imager and associated software (Bio-Rad).

2.2.2 Site Directed Mutagenesis

2.2.2.1 Plasmid Isolation

Plasmids were isolated using the GeneJet Plasmid Miniprep kit by Thermo Scientific altering slightly the protocol. Cells were harvested using centrifugation at 14000 g for 90 seconds, suspended, lysed and neutralised using the provided buffers. Cell debris and chromosomal DNA were removed by centrifugation at 14000 g for five minutes. Then, the lysate was applied on the silica column to selectively bind DNA at high-salt concentration. This is achieved by loading the lysate to the spin column, centrifuging at 14000 g for 90 seconds, transferring the flow-through to the same column and centrifuging at 14000 g for 90 seconds. The silica membrane was washed to remove contaminants and dried by centrifugation at 14000 g for two

minutes to ensure ethanol removal. Last, silica membrane was incubated for two minutes with the provided elution buffer before elution by centrifugation at 14000 g for two minutes. The purified plasmids were stored at 4°C.

2.2.2.2 Polymerase Chain Reaction (PCR)

A series of PCR reactions were conducted in order to subclone genes into plasmids and create the desired mutations. Cycling conditions and reaction components are shown in **Table 2.9** and **Table 2.10,** respectively.

Table 2.9 PCR Cycling Conditions

Step	Temperature	Time
Initial Denaturation	98°C	5 minutes
	98°C	1 minute
25 Cycles	annealing temperature	30 seconds
	72°C	30 seconds/kb
Final Elongation	72°C	5 minutes
Hold	4°C - 10°C	

Table 2.10 PCR reaction reagents

	Reaction Concentration
Sterile water	-
Q5 polymerase buffer	1x
dNTPs	0.25 mM
Primer A	0.5 µM
Primer B	0.5 µM
DNA template	1 ng - 20 ng
Q5 polymerase	1 Unit

2.2.2.3 Gel Extraction – PCR Clean up

The GeneJet Gel extraction and DNA clean up kit by Thermo Scientific was used in order to remove primers, primer dimers, dNTPs, enzymes and salts that may inhibit future reactions. DNA fragments were excised from agarose gels, solubilised and adjusted using the provided buffers. Then, the sample was applied on the provided silica columns to selectively bind DNA. The silica membrane was washed to remove contaminants and dried by centrifugation at 14000 g for two minutes to ensure ethanol removal. Last, silica membrane was incubated for two minutes with the provided buffer before eluted by centrifugation at 14000 g for two minutes. The purified DNA was stored at 4°C.

2.2.2.4 DpnI, kinase and ligase treatment

All PCR products were treated with DpnI to remove template DNA, since DpnI digests methylated and hemi-methylated DNA. The DpnI enzyme was used with NEB4 restriction digestion buffer (New England Biolabs). Additionally, PCR derived plasmids were treated with kinase and ligase in order to phosphorylate the ends and ligate them. T4 PNK kinase and T4 ligase were used with their suitable buffers (New England Biolabs), plasmids were incubated at 37°C for 20 minutes for the phosphorylation and afterwards left overnight at room temperature to promote the ligation of the phosphorylated ends.

2.2.3 Molecular Cloning

2.2.3.1 Ligation Independent Cloning (LIC)

We used Ligation Independent Cloning (LIC) (Zanders, 2005) in order to subclone genes from *Bacillus subtilis* into the vectors p2BT and p2CT (a kind gift from James Berger). Initially we carried out colony PCR (**Section 2.2.2.2**) from a single *Bacillus subtilis* colony, using the corresponding primers (**Table 2.3**) and recommended annealing temperatures ("New England Biolabs Tm Calculator,"). The destination vectors were digested with SspI-HF (New England Biolabs) restriction endonuclease (3 μg of vector and 20 Units of SspI in 50 μl reaction volume) at 37°C for two hours to linearise them. Both PCR and digestion reaction products were analysed on 1% (w/v) agarose gels (**Section 2.2.1.1.1**), purified performing agarose gel extraction (**Section 2.2.2.3**) and treated with T4 DNA polymerase LIC-qualified (Novagen). The T4 DNA polymerase reaction consisted of 0.1 pmol of vector or 0.2 pmol of insert, 5 mM DTT, 2.5 mM dGTP or 2.5 mM dCTP, respectively, and 1 Unit of T4 DNA polymerase LIC-qualified in 20 μl reaction volume and incubated at room temperature for 40 minutes prior to heat deactivation of T4 DNA polymerase at 75°C for 20 minutes. Thereafter, 2 μl of both T4 DNA polymerase treated vectors and inserts were combined and incubated at room temperature for 10 minutes before the annealing reaction was terminated by the addition of 1.3 μl 25 mM EDTA (incubation at room temperature for 10 more

minutes). Lastly, the annealing product was used to transform electrocompetent XL-1 Blue cells (**Section 2.2.4.2**).

2.2.4 Cell Techniques

2.2.4.1 Production of *Escherichia coli* electrocompetent cells

Electroporation was selected as the method to transform *Escherichia coli* cells. The desired cell strain was streaked onto an agar plate with the appropriate selection and incubated overnight. Using a single colony from this plate an overnight pre-culture was prepared along with the preparation (autoclave) of the growth media (LB Broth), centrifuge tubes and deionised water. Growth media were inoculated with the pre-culture (1:100 dilution) and incubated at 37°C with shaking until the optical density at 595 nm reached 0.7. The culture was then incubated at 4°C for 30 minutes to drastically slow down cellular growth. Cells were harvested in pre-chilled sterile centrifuge tubes at 3500 g for ten minutes at 4°C, suspended in sterile deionised water by swirling at 4°C and harvested at 5000 g for seven minutes at 4°C. The process of harvest, suspension in sterile deionised water and again harvest was repeated four times before cells were suspended in 1:100 volume of sterile 30% (v/v) glycerol, aliquoted, snap – frozen in liquid nitrogen and stored at -80°C.

2.2.4.2 Electroporation

Electrocompetent cells were transformed as follows: an aliquot was mixed with 1.5 µl – 5 µl of plasmid and incubated on ice for two minutes before being transferred into the electroporation cuvette and electroporated. Fresh LB Broth was added straight after the electroporation, the medium was transferred into a sterile tube and incubated at 37°C for one to two hours. Lastly, the cells were streaked on Luria agar plates with the appropriate antibiotic and incubated at 37°C overnight.

2.2.4.3 Glycerol Stock strain preparation

All cell strains created were stored at -80°C. The desired cell strain was streaked onto an agar plate with the appropriate antibiotic and incubated overnight, followed by the initiation of a small scale overnight culture. One ml of the overnight culture was harvested using centrifugation at 1000 g for five minutes, the growth medium was discarded, the cells were suspended in 200 µl of glycerol storage buffer [LB Broth and 10% (v/v) glycerol], snap – frozen in liquid nitrogen and stored at -80°C.

2.2.5 Protein Purification – Chromatography

2.2.5.1 Ammonium Sulphate Precipitation

Solubility of proteins in aqueous buffers is affected by their charge, ionic strength and the pH of their environment. Taking into consideration these parameters, selective precipitation of proteins can be achieved, by changing the ionic strength of the solution, in pH that ensures that the protein of interest is charged. The commonly used salt for protein precipitation is ammonium sulphate, due to itshigh solubility in water and no adverse effects on the enzymatic activity (Duong-Ly & Gabelli, 2014; Wingfield, 2016). In this study, Ammonium Sulphate Precipitation was used as a purification step and a way to change the buffer and/or to concentrate a protein solution. Mass of ammonium sulphate was added up to a specific concentration so as to selectively precipitate and collect the protein of interest by centrifugation at 4000 g, for 20 minutes at 4^{o}C.

2.2.5.2 Fast Protein Liquid Chromatography (FPLC) system and Chromatography Columns

Fast Protein Liquid Chromatography (AKTA system) in conjugation with a variety of chromatography columns were used for the purification of the desired proteins. Its basic principles rely on the fact that different components of a mixture have differences in size and shape, as well as their affinities for materials vary

depending on the ionic strength and the pH of the solution (Madadlou et al., 2011). In this study, we used affinity chromatography, ion exchange chromatography and molecular exclusion chromatography.

The Affinity Chromatography makes use of highly specific interactions between molecules. A particular binding ligand is immobilised to the stationary phase (commonly agarose). When a protein solution is passed over the phase, the protein molecules bind to the ligand with the specific binding affinity. For the purposes of this study, we used three types of affinity chromatography systems: **a.** Intein-Mediated Purification with an Affinity Chitin-binding Tag (IMPACT) system, that utilises the affinity of intein-tagged proteins to chitin beads (Mitchell & Lorsch, 2015), **b**. Immobilised Metal Affinity Chromatography (IMAC) system, that uses the affinity of hexahistidine-tagged proteins to transition metals (Ni^{+2}) (Block et al., 2009) and **c.** Heparin, that has two modes of interaction with proteins, as an affinity ligand with DNA binding molecules and as a cationic exchanger, resulting from its sulphate groups (Farooqui, 1980; Xiong et al., 2008).

The ion exchange chromatography (IEC) separation relies on the fact that proteins have different net surface charges, due to their amino acid sequence, in a solution with specific ionic strength and pH. The columns are made of synthetic polymers that contain charged functional groups. Proteins in a buffer with low ionic strength and in pH above their isoelectric point (pI) (pI is defined as the pH at which a protein has no net charge) bind to positively charged anionic stationary phases (Anion Exchange Chromatography – AEC). On the contrary, in pH below their pI,

proteins bind to negatively charged cationic matrices (Cation Exchange Chromatography – CEC) (A. Williams et al., 1999).

The Gel Filtration Molecular (Size) Exclusion chromatography (SEC) separates the components according to their size and shape. It can also be used to change the buffer of a solution, instead of dialysis or ammonium sulphate precipitation and suspension in the desired buffer. The chromatography columns are made of dextran and agarose beads with pores, in which the smaller proteins are trapped (included) and retarded from eluting, in contrast to the bigger proteins that elute first (excluded proteins) (Lathe & Ruthven, 1956; Mori & Barth, 1999).

2.2.6 Assays

2.2.6.1 Oligonucleotide Radiolabelling Construct Preparation

Oligonucleotides were radiolabelled at 5'-P ends using γ-^{32}P ATP (Perkin Elmer) and T4 Polynucleotide Kinase (T4 PNK) (New England Biolabs). The radiolabelling reaction consisted of 0.1 μM oligonucleotide (**Table 2.4**), 0.167 μM γ-^{32}P ATP and 10 Units of T4 PNK in 20 μl reaction volume and was incubated at 37°C for two hours. Then, T4 PNK was deactivated by incubation at 75°C for 30 minutes. Subsequently, the oligonucleotide was annealed onto the template (oligonucleotide or single-strand M13mp18 template). The annealing reaction comprised of the whole radiolabelling reaction, 12.5 μg of the template and 3.68 μl 20x SSC buffer (3 M NaCl and 300 mM Na_3Citrate) and was incubated at 95°C for two minutes before

allowing to slow cool to 35°C. Lastly, the annealed product was purified using Micro Bio-Spin columns with Bio-gel P-6 (Bio-Rad), the concentration was adjusted at 10 nM and stored at -20°C.

2.2.6.2 Helicase Unwinding Assays

Helicase activity was detected by monitoring the displacement of radiolabelled oligonucleotide (110 bases) (CA65TTTA15M13) (**Table 2.4**) annealed to single-strand M13mp18 template (Affymetrix) (**Figure 2.1**).

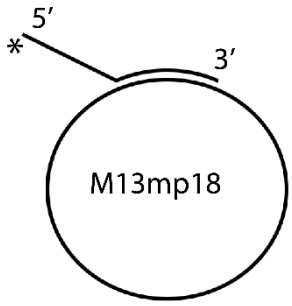


Figure 2.1 Helicase Assay Construct

The helicase assays were carried out in 20 mM HEPES-NaOH pH 7.5, 50 mM NaCl, 10 mM $MgCl_2$ and 1 mM DTT. The helicase DnaC in the reaction buffer was pre-incubated at 37°C for five minutes. Then the helicase-loader DnaI with the radiolabelled construct (0.66 nM) were added and the mixture was incubated at 37°C for five more minutes. The reaction was initiated with 2.5 mM ATP and incubated at 37°C. Assays were terminated with the addition of 1/5th 5x SDS-STOP buffer [100 mM Tris-HCl pH 8.0, 200 mM EDTA, 2.5% (w/v) SDS and 50 % (v/v) glycerol] and

samples were analysed through 10% (v/v) native polyacrylamide TBE gels (**Section 2.2.1.2.1**). Gels were dried using a pump-heater-vacuum system and exposed to phosphor screens (Bio-Rad) overnight. Analysis of gels was done using molecular imager and associated software (Bio-Rad) and the percentage of displacement was plotted using Graphpad-Prism 6.

2.2.6.3 Primase Activity Assay

Primase activity was detected by monitoring *de novo* formation of RNA primers using single-strand M13mp18 template (Affymetrix). RNA primers were extended by DnaE polymerase and the reaction product was used as template to perform conventional PCR using Q5 DNA polymerase (NEB). Q5 DNA polymerase can only recognise and extend DNA primers. Assays were carried out in 15 µl reaction volume in buffer consisting of 20 mM HEPES-NaOH pH 7.5, 50 mM NaCl, 10 mM $MgCl_2$, 1 mM DTT, 500 µM dNTPs, 500 µM rNTPs, 2.5 mM ATP and 2 nM substrate (ssM13mp18). They contained all possible combinations of helicase DnaC (240 nM), helicase-loader DnaI (240 nM), primase DnaG (120 nM) and DnaE polymerase (40 nM) (all concetrations are referring to the monomeric state of proteins). The reaction mixtures containing everything (except rNTPs, ATP and the substrate) were pre-incubated at 37°C for five minutes and then the reaction was initiated by the addition of a mixture of the remaining components (rNTPs, ATP, substrate), followed by incubation at 37°C for 60 minutes. Reactions were terminated by incubation at 95°C for five minutes. Thereafter, PCRs were carried out with Q5

DNA polymerase, using 1 μl of the previous reaction along with 250 μM dNTPs and 1 Unit of Q5 DNA polymerase in 20 μl total volume reactions. PCR cycling conditions are described in **Table 2.9**. The annealing temperature was selected at 62°C and the extension time for 5 minutes at 72°C.It was impossible to calculate the actual annealing temperatures of DnaE polymerase products, due to their random sizes. Lastly, PCR products were analysed through 1% (w/v) agarose gel (**Section 2.2.1.1.1**).

2.2.6.4 Primer Extension Assay with small template

The polymerase activity was detected by monitoring the extension of radiolabelled oligonucleotide DNA (PTT5C4(TG) 15 bases 5'-AAGGGGGTGTGTGTG-3') or RNA (PTT5C4(UG) 15 bases 5'-AAGGGGGUGUGUGUG-3') annealed to 110 bases nucleotide CA65TTTA15M13 (**Table 2.4**) (**Figure 2.2**).

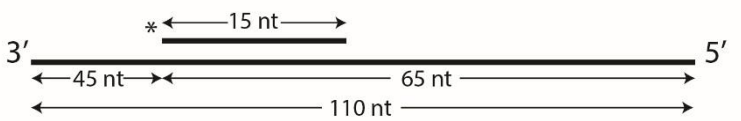


Figure 2.2 Primer Extension Assay Construct

Primer extension assays were carried out in 15 μl volume reactions containing 20 mM HEPES-NaOH pH 7.5, 50 mM NaCl, 10 mM $MgCl_2$, 1 mM DTT

and 20-200 μM dNTPs. The reaction mixture containing the buffer, dNTPs and the polymerase was pre-incubated at 37°C for five minutes before the initiation of the reaction by the addition of the radiolabelled construct (2 nM) and further incubation at 37°C. Assays were terminated with the addition of 1/5th 5x Urea-Stop buffer (5 mM Tris-HCl pH 7.5, 20 mM EDTA and 7.5 M urea). Samples were then boiled at 95°C for two minutes and analysed through 15% (v/v) ureagel denaturing PAG (**Section 2.2.1.2.3**). Gels were dried using a pump-heater-vacuum system and exposed to phosphor screens (Bio-Rad) overnight. Analysis of gels was performed using molecular imager and associated software (Bio-Rad) and the percentage of products was plotted using Graphpad – Prism 6.

2.2.6.5 Primer Extension Assays with M13mp18 template – Processivity Assay

We carried out Primer extension assays using single-strand M13mp18 template (7249 bases) by annealing single-strand radiolabelled oligonucleotide RNA (5'- CAGUGCCAAGCUUGCAUGCC-3') or DNA (5'-CAGTGCCAAGCTTGCATGCC-3') primer onto M13mp18. We monitored the primer extension at 37°C with or without the processivity clamp DnaN (β) plus the clamp-loader [DnaX (τ), HolB (δ') and YqeN (δ)], in the absence or presence of SSB or SSBΔ107-172 using alkaline agarose electrophoresis (**Section 2.2.1.1.2**). The RNA primer was used in all reactions with DnaE or DnaE plus PolC and the DNA primer was used in reactions containing only PolC.

Assays were carried out in a total volume of 105 µl in reaction buffer comprised of 20 mM HEPES-NaOH pH 7.5, 50 mM NaCl, 10 mM $MgCl_2$, 1 mM DTT, 500 µM dNTPs, 2.5 mM ATP and 2 nM radioactively labelled naked primed single-strand M13mp18 template. In all reactions with SSB or SSBΔ107-172 and the clamp DnaN, the reaction buffer was pre-incubated at 37°C with SSB (1 µM) or SSBΔ107-172 (1 µM), DnaN (80 nM), DnaX (120 nM) HolB (40 nM) and YqeN (40 nM) at 37°C for five minutes. Then, reactions were initiated by the addition of the appropriate polymerase DnaE (80 nM), PolC (80 nM) or the mixture of DnaE and PolC (80 nM each). 15 µl samples were taken at time intervals, inactivated by the addition of 50 mM EDTA and 1/6th alkaline agarose loading dye [300 mM NaOH, 6 mM EDTA, 18 % (v/v) glycerol, 0.15% (w/v) bromophenol blue and 0.25% (w/v) xylene cyanol]. Subsequently, they were heated to 95°C for 2 minutes and analysed through 1.5% (w/v) alkaline agarose gels. Alkaline agarose gels were fixed for 30 minutes in 7% (w/v) trichloroacetic acid, dried overnight and data analysis was conducted using a molecular imager and associated software (Bio-Rad).

2.2.6.6 Electrophoretic Mobility Shift Assay (EMSA)

DNA binding properties of proteins were detected by performing Electrophoretic Mobility Shift Assays. Nine constructs were used:

A. radiolabelled oligonucleotide RNA 5'- AAGGGGGUGUGUGUG -3' (15 bases) annealed to oligonucleotide 5' - ACACACACACACACACACACACACCCCCTT - 3' (30 bases),

B. radiolabelled oligonucleotide DNA 5'- AAGGGGGTGTGTGTG -3' (15 bases) annealed to oligonucleotide 5'- ACACACACACACACACACACACCCCCTT -3' (30 bases),

C. radiolabelled oligonucleotide DNA 5'- AAGGGGGTGTGTGTA -3' (15 bases) annealed to oligonucleotide 5'- ACACACACACACACACACACACCCCCTT -3' (30 bases),

D. radiolabelled oligonucleotide 5'- ACACACACACACACACACACCCCCCTT -3' (30 bases),

E. radiolabelled oligonucleotide RNA 5'- AAGGGGGUGUGUGUG -3' (15 bases) annealed to oligonucleotide 5'- CACACACACACACACACACACACACACACA CACACACACCCC CTT -3' (45 bases),

F. radiolabelled oligonucleotide 5'- CACACACACACACACACACACACACA CACACACACACCCCCTT -3' (45 bases),

G. radiolabelled oligonucleotide RNA 5'- AAGGGGGUGUGUGUG-3' (15 bases),

H. radiolabelled oligonucleotide RNA 5'- AAGGGGGUGUGUGUG-3' (15 bases) annealed to oligonucleotide 5' - CACACACACCCCCTTACACACACACACACA -3' (30 bases) and

I. radiolabelled oligonucleotide DNA 5'- AAGGGGGTGTGTGTG -3' (15 bases) annealed to oligonucleotide 5'- CACACACACCCCCTTACACACACACACACA -3' (30 bases).

All EMSA constructs are represented in **Figure 2.3.** The constructs were created as described in **Section 2.2.6.1**.

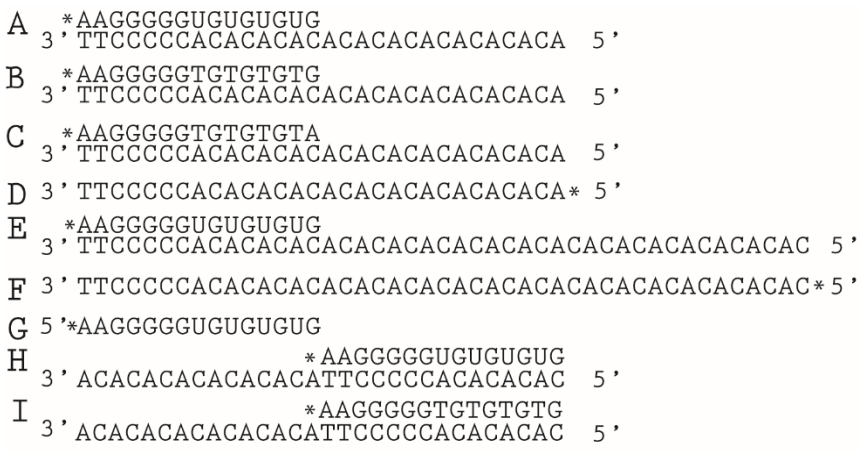


Figure 2.3 EMSA substrates

Assays were carried out in 15 µl volume reactions in buffer containing 20 mM HEPES-NaOH pH 7.5, 50 mM NaCl, 10 mM $MgCl_2$ and 1 mM DTT. The reaction mixture of buffer and substrate (0.66 nM) was pre-incubated at 37°C for five minutes before the addition of the protein at different concentrations, as indicated, and further incubation at 37°C for five or 15 minutes, as indicated in each assay. In EMSAs where two proteins were used, the second protein was added after the incubation of the reaction mixture with the first protein for five minutes, followed by further incubation at 37°C for five minutes or 15 minutes, as indicated in each assay. Samples were mixed with 1/5th of 5x loading buffer [50% (v/v) glycerol, 0.15% (w/v) bromophenol blue and 0.25% (w/v) xylene cyanol] and analysed through 5% (v/v) native polyacrylamide gels (**Section 2.2.1.2.1**). Gels were dried using a pump-heater-vacuum system and exposed to phosphor screens (Bio-Rad) overnight. Analysis of gels was done using molecular imager and associated software (Bio-Rad).

2.2.6.7 Exonuclease Activity Assays

PolC exonuclease activity assays were carried out using DNA (5'-CAGTGCCAAGC TTGCATGCC-3') oligonucleotide (20 bases) annealed onto single-strand M13mp18 template (7249 bases) monitoring primer degradation. Assays were carried out with or without the processivity clamp DnaN (β) plus the clamp-loader [DnaX (τ), HolB (δ') and YqeN (δ)], in the absence or presence of SSB or SSBΔ107-172, using DnaE, PolC, $PolC_{pol-}$, $PolC_{exo-}$ and the combinations of DnaE with either the wild type PolC or one of the deficient proteins.

Assays were carried out in 50 µl volume reactions containing 20 mM HEPES-NaOH pH 7.5, 50 mM NaCl, 10 mM $MgCl_2$, 1 mM DTT, 2.5 mM ATP and 2 nM radioactively labelled DNA primed single-strand M13mp18 template. In all reactions with SSB or SSBΔ107-172 and clamp DnaN, the reaction buffer was pre-incubated with SSB (1 µM) or SSBΔ107-172 (1 µM), DnaN (80 nM), DnaX (120 nM) HolB (40 nM) and YqeN (40 nM) at 37°C for five minutes before the addition of the appropriate polymerase. In assays where two polymerases were used, the reaction mixture was incubated with DnaE polymerase (80 nM) prior to addition of PolC polymerase wild type or deficient mutants (80 nM) and further incubation at 37°C for 15 minutes. Each reaction was terminated with boiling at 95°C for five minutes and samples were resolved through 15% (v/v) denaturing ureagels (**Section 2.2.1.2.3**). Gels were dried using a pump-heater-vacuum system and exposed to phosphor screens (Bio-Rad) overnight. Analysis of gels was done using molecular imager and associated software (Bio-Rad).

3 Protein Cloning, Expression, Purification and Activity Tests

This chapter constists the first chapter of results and describes the cloning, expression, purification and activity assays for the replisomal proteins used in this project.

3.1 Replicative Helicase DnaC and Helicase-Loader DnaI

3.1.1.1 Helicase DnaC and Helicase-loader DnaI Expression

Bacillus subtilis helicase DnaC (50.6 kDa) and helicase-loader DnaI (36.1 kDa) were co-expressed using the pSMG33 plasmid in the MCC142 *Escherichia coli* expression strain in order to achive soluble DnaC protein (Velten et al., 2003). Cells were grown in 2xYT Broth with 50 µg/ml carbenicillin at 37°C, 180 rpm until mid-log phase (OD_{595} = 0.5), prior to induction with 1 mM IPTG and further incubation at 37°C, 180 rpm for three hours. The cell pellet was harvested by centrifugation at 3000 g, for 15 minutes at 4°C, suspended in 25 mM Tris - HCl pH 8.0, 2 mM EDTA, 10 mM DTT, 200 mM NaCl, 2.5 mM ATP, 5 mM $MgCl_2$ and 0.5 mg/ml lysozyme, incubated at 4°C for 30 minutes and stored at -80°C.

3.1.1.2 Helicase DnaC and Helicase-loader DnaI Purification

The cell pellet was thawed, sonicated and the lysate was clarified by centrifugation at 40000 g, 30 minutes, 4ºC and filtered (0.22 µm diameter filters). Thereafter, solid ammonium sulphate was added to the eluate at 4ºC to final concentration of 30% (w/v) and the precipitated protein was collected by centrifugation at 20000 g, 15 minutes, 4ºC. It was then suspended in 50 mM Tris - HCl pH 7.5, 1 mM DTT, 50 mM NaCl, 1 mM ATP and 2 mM $MgCl_2$, filtered (0.22 µm diameter filters) and loaded on Hiload 26/60 Superdex 200 prep grade gel filtration column (GE Healthcare), equilibrated in 50 mM Tris - HCl pH 7.5, 1 mM DTT, 50 mM NaCl, 1 mM ATP and 2 mM $MgCl_2$. All the purification steps before chromatography are presented in **Figure 3.1** and the result of the Hiload 26/60 Superdex 200 prep grade column in **Figure 3.2**.

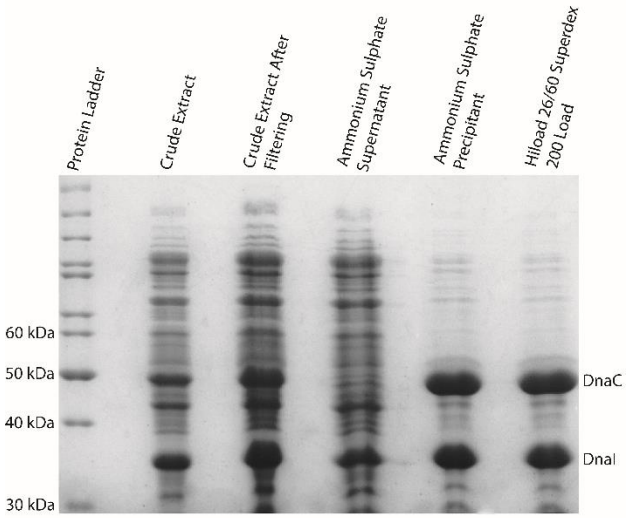


Figure 3.1 DnaC and DnaI purification steps. 15% (v/v) SDS PAGE monitoring the purification of DnaC and DnaI before loading on the Hiload 26/60 Superdex 200 prep grade gel filtration column.

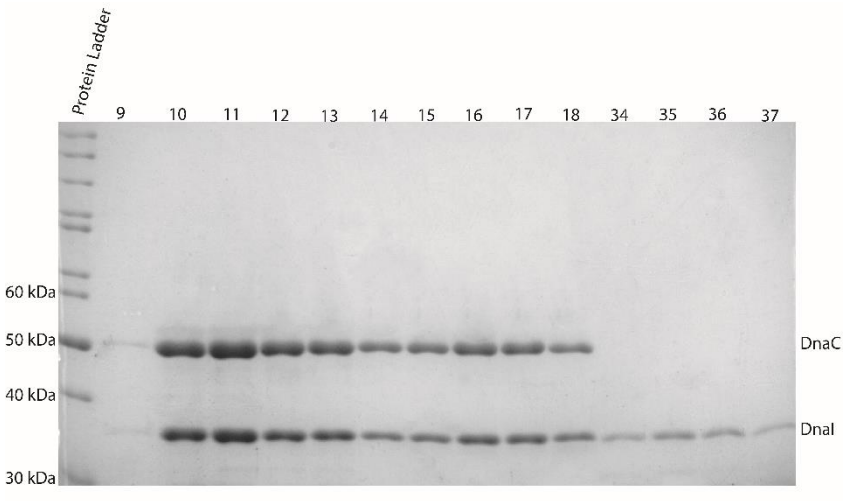


Figure 3.2 DnaC and DnaI Hiload 26/60 Superdex 200 prep grade column. 15% (v/v) SDS PAGE monitoring the purification of DnaC and DnaI from the gel filtration column. Fractions 10-18 were pooled for the next purification step.

The next step comprised the addition of solid ammonium sulphate to pooled fractions at 4ºC to final concentration of 30% (w/v) and the collection of the precipitated proteins by centrifugation at 20000 g, 15 minutes, 4ºC. Subsequently, the proteins were suspended in 50 mM Tris - HCl pH 8.0, 1 mM DTT, 50 mM NaCl and 2 M urea, filtered (0.22 μm diameter filters) and loaded on Hiload 26/60 Superdex 75 prep grade gel filtration column (GE Healthcare), equilibrated in 50 mM Tris - HCl pH 8.0, 1 mM DTT, 50 mM NaCl and 2 M urea (**Figure 3.3**). This step aimed the separation of the homohexameric helicase DnaC from the homohexameric helicase-loader DnaI.

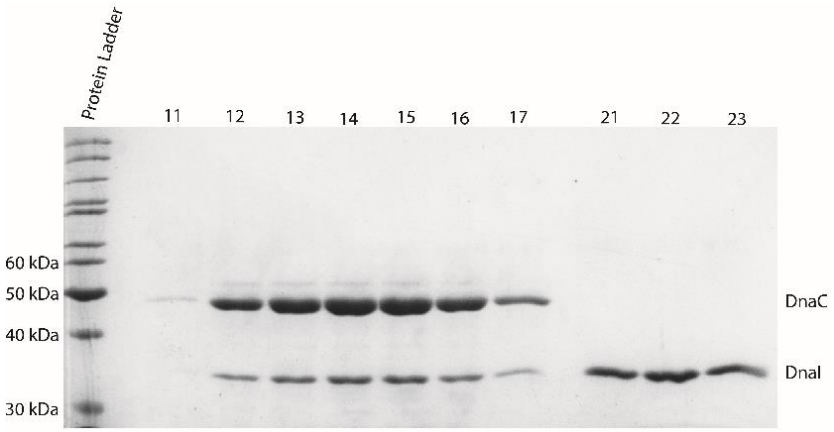


Figure 3.3 DnaC and DnaI Hiload 26/60 Superdex 75 prep grade column. 15% (v/v) SDS PAGE monitoring the purification of DnaC and DnaI from the gel filtration column. Fractions 12 - 17 and 21 -23 were pooled separately for the next purification step.

The next purification step included the use of Hitrap Q HP columns (GE Healthcare), one for each protein. The pooled fractions were loaded on 5 ml Hitrap Q HP column (GE Healthcare), equilibrated in 50 mM Tris-HCl pH 8.0 and 1 mM DTT and the proteins were eluted with a 15 column volume gradient to 1 M NaCl (**Figure 3.4**).

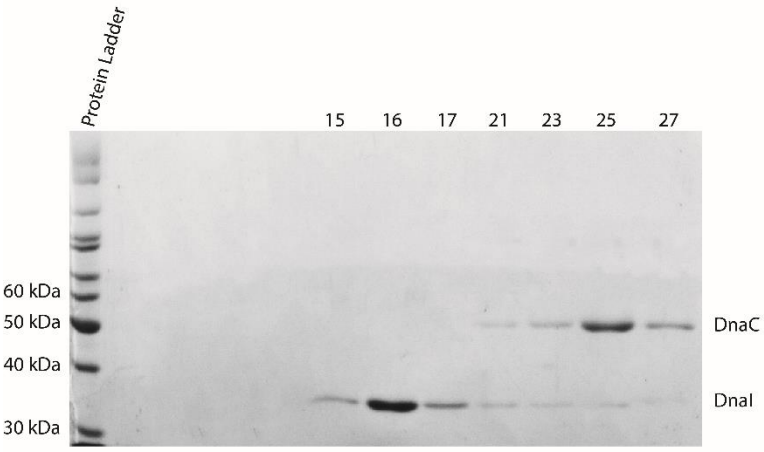


Figure 3.4 DnaC and DnaI Hitrap Q HP column. 15% (v/v) SDS PAGE monitoring the purification of DnaC and DnaI from 5 ml Hitrap Q HP column. Fractions 15 - 17 and 25 - 27 were pooled separately for the next purification step.

Both proteins were pure after the use of Hitrap Q HP columns and DnaI was ready for extensive dialysis against storage buffer [20 mM HEPES- NaOH pH 8.0, 1 mM DTT, 50 mM NaCl and 50% (v/v) glycerol], quantification spectrophotometrically (extinction coefficient 26610 M^{-1} cm^{-1}) and storage at -80ºC. Rannou et. al (Rannou et al., 2013) has shown that the purified hexameric form of DnaC helicase is not active and it requires treatment with guanidinium chloride in order to obtain the active monomeric form (ring-maker mechanism for the helicase loading). Thus, helicase DnaC was treated with 1.5 M guanidinium chloride (final concentration) in order to obtain the monomeric active form. Then, the treated sample of DnaC was loaded on Hiload 26/60 Superdex 200 prep grade gel filtration column (GE Healthcare), equilibrated in 50 mM Tris - HCl pH 8.0, 1 mM DTT, 50 mM NaCl and 1.5 M guanidinium chloride, resulting in separation of the monomeric DnaC from oligomeric fractions. The chromatogram of the purification column is presented in **Figure 3.5**, with the first peak to be the oligomeric form of

the helicase and the second peak the active monomeric form. Fractions were pooled separately, dialysed overnight against 20 mM HEPES – NaOH pH 8.0, 1 mM DTT, 50 mM NaCl and 50% (v/v) glycerol, quantified spectrophotometrically (extinction coefficient 26485 M^{-1} cm^{-1}) and stored at -80ºC.

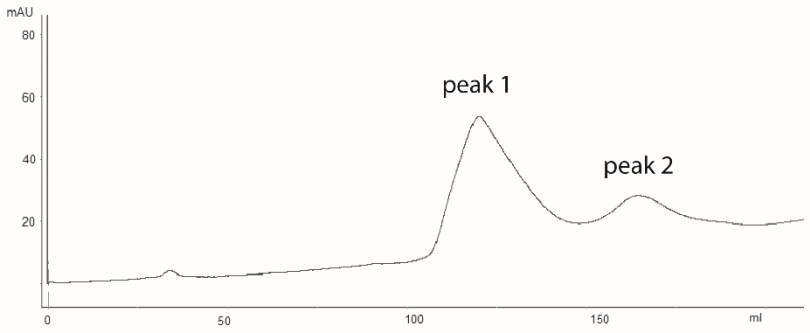


Figure 3.5 Hiload 26/60 Superdex 200 prep grade column chromatogram (A_{280}) of DnaC after the guanidinium chloride treatment showing oligomeric (peak 1) and monomeric (peak 2) fractions.

The purification scheme of helicase DnaC and helicase-loader DnaI is presented in **Figure 3.6.**

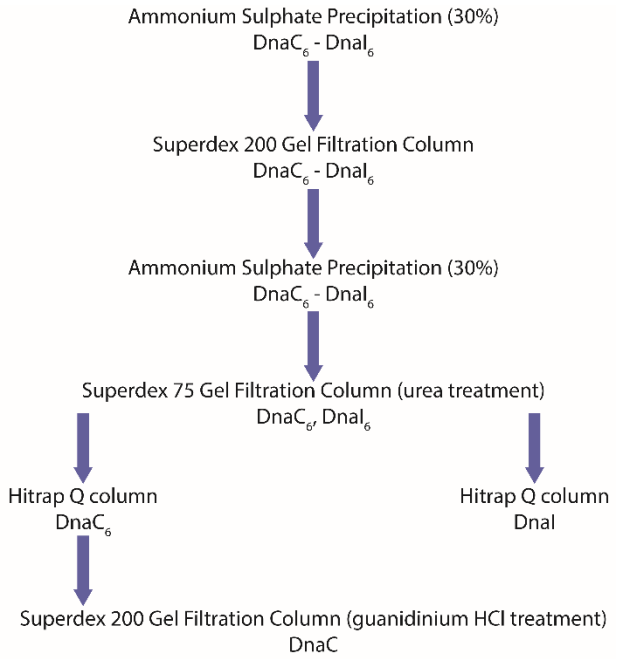


Figure 3.6 Purification scheme of DnaC and DnaI.

3.1.1.3 Helicase DnaC and Helicase-loader DnaI Activity Test

Helicase DnaC and helicase-loader DnaI activities were assayed as described in **Section 2.2.6.2** and samples were analysed by electrophoresis through non-denaturing polyacrylamide gels, as described in **Section 2.2.1.2.1**.

Single-point helicase assays were carried out (data not shown) and when the presence of the helicase activity was established, further time course reactions and concentration titration helicase assays were carried out (**Figure 3.7**).

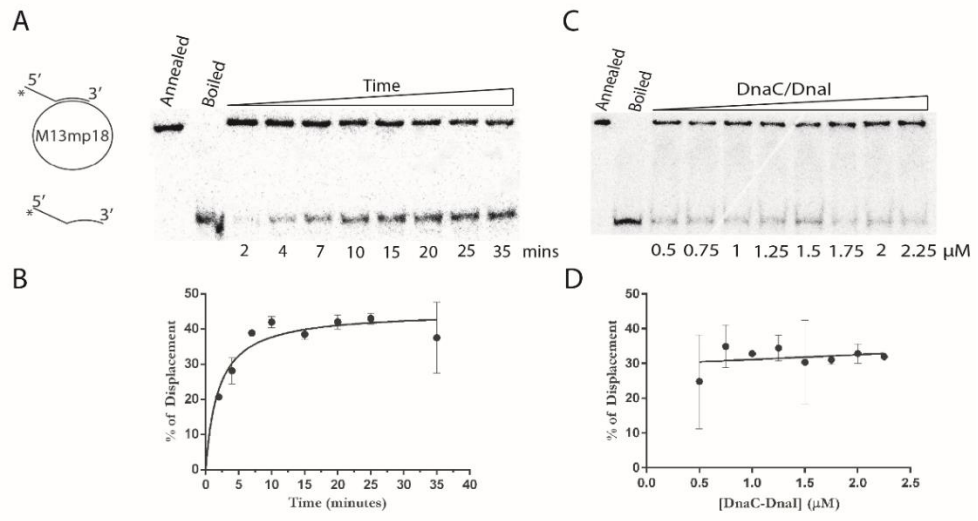


Figure 3.7 DnaC and DnaI time course (**A, B**) and concentration titration (**C, D**) helicase assays. Helicase assays and the plot of percentage of displacement of radiolabelled oligonucleotide from an annealed radiolabelled oligonucleotide – M13mp18 template. In time course assays (**A**) the concentration of both helicase and helicase-loader were 0.5 µM, whereas in the concentration titration reactions (**C**) the incubation time (25 minutes), the probe concentration (0.66 nM) and the DnaC/DnaI ratio were constant. Samples were analysed through 10% (v/v) non-denaturing TBE PAG and data analysis was done using GraphPad – Prism 6. Assays were carried out in triplicates and error bars show standard deviations.

Our data show that maximum percentage displacement was achieved after 20 minutes (**Figure 3.7 A, B**), although, in our single-point helicase assays, the incubation time was 25 minutes to further ensure maximum displacement. Additionally, from our data with the concentration titration assays, where the incubation time (25 minutes), the concentration of the construct (0.66 nM) and the ratio of the DnaC/DnaI were constant, it can be deduced that the percentage displacement is independent of the concentration of the proteins involved in that particular system (**Figure 3.7 C, D)**.

Our data correlate well with the suggested model that *Bacillus subtilis* helicase follows a ring assembly mechanism (Velten et al., 2003), since helicase assays using purified hexameric DnaC (verified using analytical gel filtration) didn't show any unwinding activity (data not shown). Interestingly, in *Escherichia coli*, the primase enhances the helicase activity, by releasing the helicase from the cognate loader (Makowska-Grzyska & Kaguni, 2010). Similar observations were made in *Clostridium difficile* (Paper in Preparation). The helicase-loader promotes the loading of the helicase onto DNA templates, but the helicase activity is limited, until the primase releases the helicase from its loader. This observation could explain the apparent absence of helicase activity in our system.

3.2 Primase DnaG

The *dnag* gene was subcloned from the pSMG11 plasmid (kind gift from Laurent Jannière) into a pET derived vector (p2BT) and DnaG primase was expressed with N-terminal hexahistidine tag. The methods followed for cloning, expression and purification of hexahistidine-tagged DnaG primase are described below.

3.2.1 N-terminal Hexahistidine-tagged DnaG primase

3.2.1.1 Primase DnaG Cloning

N-terminal Histidine-tagged DnaG construct was created using Ligation Independent Cloning (LIC), as described in **Section 2.2.3.1**, with the host plasmid p2BT (kind gift from James Berger) generating the final p2BT-BsuDnaG expression plasmid (**Figure 3.8**).

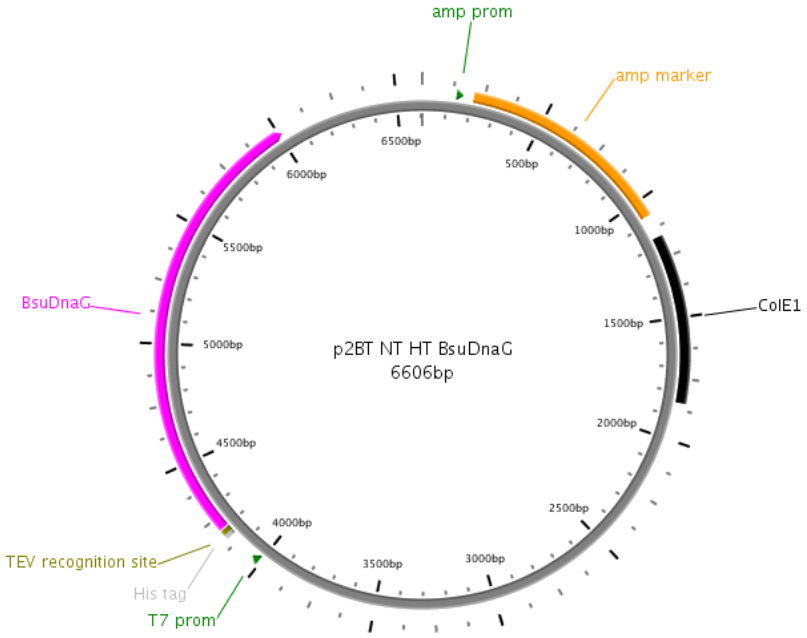


Figure 3.8 p2BT N-terminal His-tagged *Bsu*DnaG plasmid map.

3.2.1.2 Primase DnaG Expression

Upon completion of successful subcloning, a series of expression strain tests were carried out in order to optimise expression of soluble protein as shown in **Figure 3.9**.

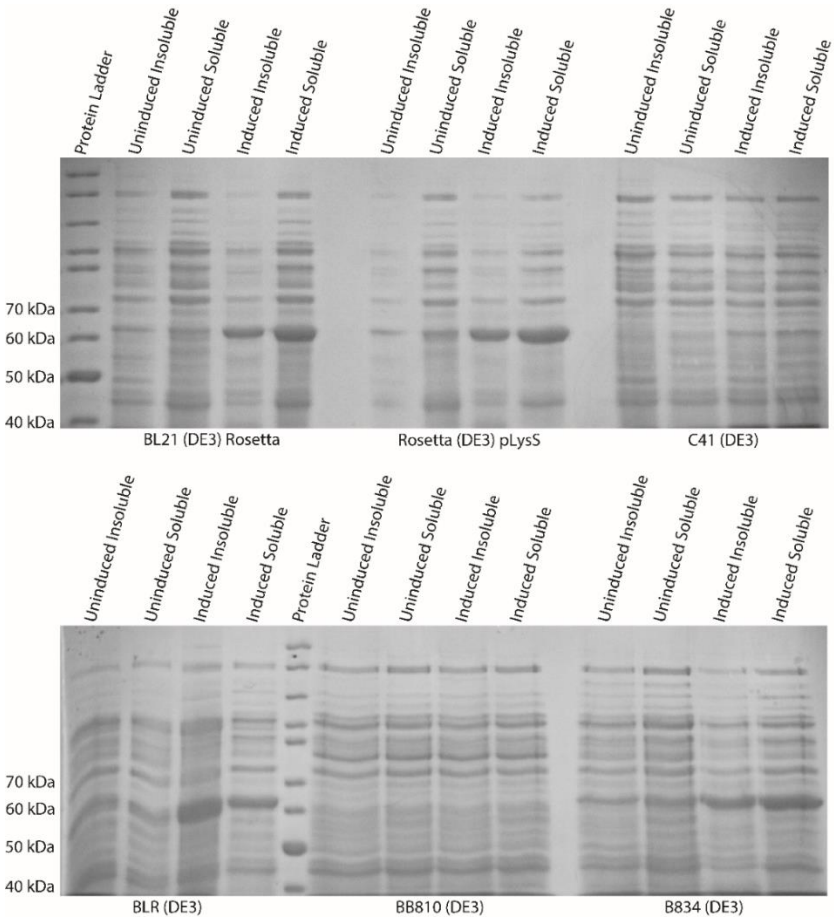


Figure 3.9 N-terminal His-tagged DnaG expression strain test. 12% (v/v) SDS PAGE monitoring the expression of N-terminal Histidine-tagged DnaG in several of our lab expression strains for T7 promoters.

Thus, *Bacillus subtilis* N-terminal His-tagged DnaG primase (68.8 kDa) was expressed in BL21 (DE3) Rosetta or Rosetta (DE3) pLysS *Escherichia coli* strain using the p2BT plasmid. Cells were grown in 2xYT broth with 50 µg /ml carbenicillin and 1% (w/v) filter sterile glucose at 37ºC, 180 rpm until late stage of mid log phase (OD_{595} = 0.8). Afterwards, cells were incubated at 4ºC for ten minutes, prior to induction with 1 mM IPTG, followed by further incubation at 25ºC, 180 rpm for three hours. The cell pellet was harvested by centrifugation at 3000 g, for 15 minutes at 4ºC and stored at -80ºC.

3.2.1.3 Primase DnaG Purification

The cell pellet was suspended in 30 ml/l cell growth sonication buffer [50 mM Tris-HCl pH 8.0, 0.5 M NaCl, 20 mM imidazole, 10% (v/v) glycerol, 1 mM PMSF and protease inhibitor cocktail mix (Fisher)] and sonicated. The lysate was clarified by centrifugation at 40000 g, 30 minutes, 4ºC, followed by filtering (0.22 µm diameter filters). It was then loaded on 5 ml Histrap HP column (GE Healthcare), equilibrated in 50 mM Tris-HCl pH 8.0, 0.5 M NaCl, 20 mM imidazole and 10% (v/v) glycerol. The column was washed extensively with the equilibration buffer and N-terminal hexahistidine-tagged DnaG primase was eluted performing a 15 column volume gradient from 0.02 to 0.5 M imidazole (**Figure 3.10**).

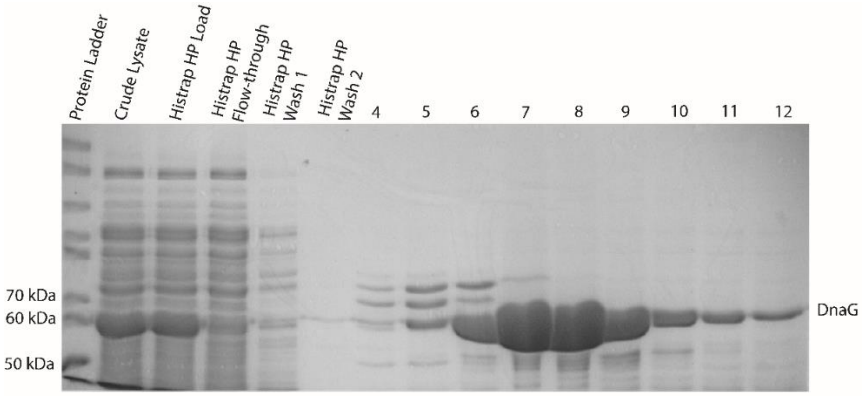


Figure 3.10 N-terminal His-tagged DnaG Histrap HP column. 12% (v/v) SDS PAGE monitoring the purification of DnaG from 5 ml Histrap HP column. Fractions 6 - 12 were pooled for the next purification step.

Fractions containing hexahistidine-tagged DnaG primase were pooled and dialysed against two litres of 50 mM Tris-HCl pH 8.0, 20 mM imidazole, 0.5 M NaCl and 10% (v/v) glycerol at 4ºC. Subsequently, the protein concentration was

quantified spectrophotometrically using NanoDrop and TEV protease was added at 1:5 (TEV:DnaG) mass ratio, followed by overnight incubation at 4ºC. Then, the sample was loaded on 5 ml Histrap HP column (GE Healthcare), equilibrated in 50 mM Tris-HCl pH 8.0, 0.5 M NaCl, 20 mM imidazole and 10% (v/v) glycerol and the flow-through was collected (**Figure 3.11**). Lastly, purified DnaG primase was dialysed overnight against 20 mM HEPES pH 7.5, 100 mM NaCl, 1 mM DTT and 10% (v/v) glycerol, quantified spectrophotometrically (extinction coefficient 45520 M^{-1} cm^{-1}) and stored at -80ºC.

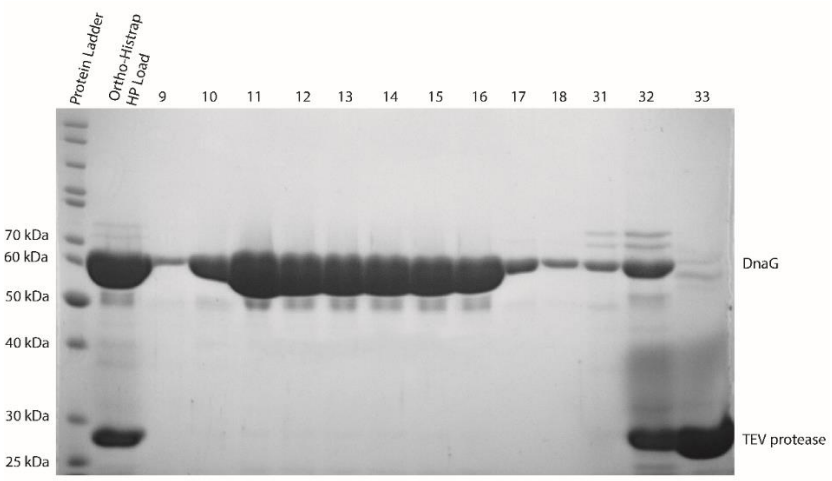


Figure 3.11 DnaG Ortho-Histrap HP column. 12% (v/v) SDS PAGE monitoring the purification of DnaG from 5 ml Histrap HP column after overnight cleavage of the Histidine-tag using TEV protease. Fractions 10 - 16 were pooled for dialysis into storage buffer. Fractions 31-33 show the uncleaved N-terminal Histidine-tagged DnaG and the TEV protease (28 kDa).

To summarise, the purification of N-terminal Histidine-tagged DnaG primase is shown in **Figure 3.12**.

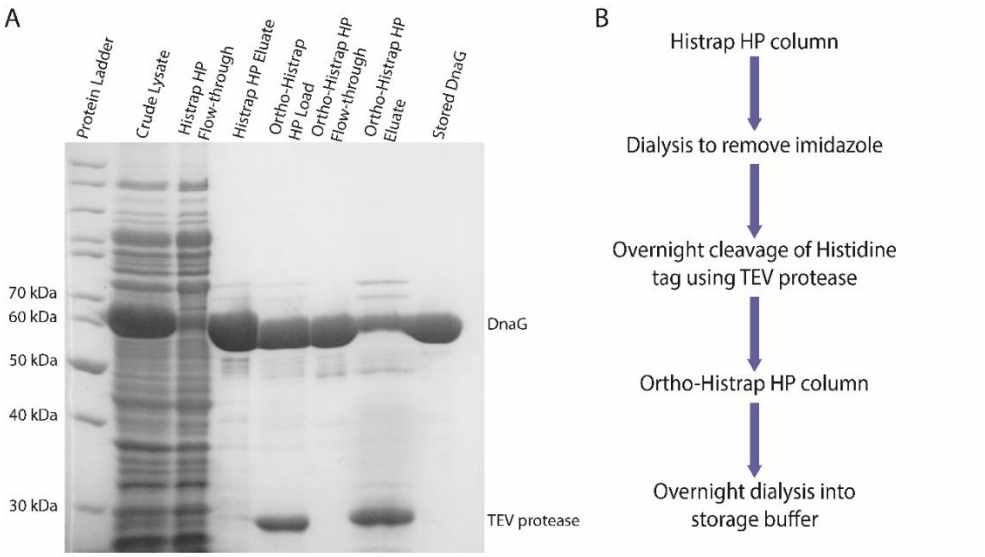


Figure 3.12 N-terminal Histidine-tagged DnaG purification (**A**) and scheme (**B**).

3.2.1.4 Primase DnaG Activity Test

The activity of DnaG primase was investigated by detection of *de novo* synthesised RNA primers, described elsewhere (**Section 2.2.6.3**). The conventional PCR products were analysed through 1% (w/v) agarose gels (**Figure 3.13**).

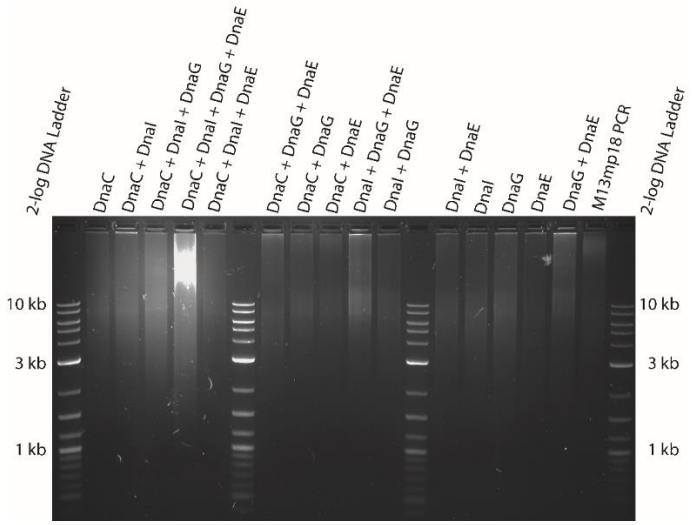


Figure 3.13 DnaG activity assay. Samples of the performed PCR using Q5 DNA polymerase analysed through a 1% (w/v) agarose gel showing *de novo* synthesis of RNA primers by the primase DnaG.

Our data indicate that *de novo* synthesis of RNA primers occurred optimally only in the presence of all proteins of the primosome (DnaC, DnaI, DnaG). According to the existing model for the DNA replication in *Bacillus* subtilis, the helicase-loader DnaI loads and assembles the helicase DnaC into the active hexameric ring. Then, the helicase recruits DnaG primase *via* a direct protein-protein interaction, the primase DnaG recognises poly-thymidine sequences along the M13mp18 single-strand template and synthesises *de novo* RNA primers. Subsequently, DnaE polymerase, which is recruited by primase DnaG *via* a direct protein-protein interaction (Rannou et al., 2013), extends RNA primers, synthesising nascent DNA fragments. We speculate that these RNA-DNA hybrid fragments with 3'-OH ends were specifically utilised by the commercially available Q5 DNA polymerase (New England Biolabs) in order to synthesise long DNA fragments. Q5 DNA polymerase recognises and extends only DNA primers.

3.3 DNA Polymerase DnaE

Bacillus subtilis error-prone DnaE polymerase (125.3 kDa) was initially expressed and purified according to already published method with slight alternations (Rannou et al., 2013). Additionally, the *dnaE* gene was subcloned from the pTYB3-Intein BsuDnaE plasmid (kind gift from Laurent Jannière) into a pET derived vector (p2CT) and the protein was expressed with N-terminal hexahistidine tag, in order to aid the purification process. Expression and purification of C-terminal Intein-tagged DnaE, cloning, expression and purification of N-terminal Maltose Binding protein (MBP)-tagged Hexahistidine- tagged DnaE polymerase, as well as the activity assays are presented in this section. Additionally, this section describes site-directed mutagenesis carried out in order to obtain a polymerase deficient mutant of DnaE.

3.3.1 C-terminal Intein-tagged DnaE polymerase

3.3.1.1 DnaE polymerase Expression

Bacillus subtilis DnaE polymerase (125.3 kDa) was expressed as intein fused protein using the pTYB3 plasmid (kind gift from Laurent Jannière) (**Figure 3.14**). In order to optimise the expression of soluble protein, a series of expression strains expression tests were done (**Figure 3.15**), indicating that *Escherichia coli* Rosetta (DE3) pLysS strain is the most suitable for soluble DnaE expression. Cells were

grown in 2xYT broth with 50 μg/ml carbenicillin and 1% (w/v) filter sterile glucose at 37°C, 180 rpm until late stage of mid log phase (OD_{595} = 0.8), followed by incubation at 4°C for ten minutes. Then protein production was induced with 1 mM IPTG and cells were incubated at 25°C, 180 rpm for three hours. The cell pellet was harvested by centrifugation at 3000 g, for 15 minutes at 4°C and stored at -80°C.

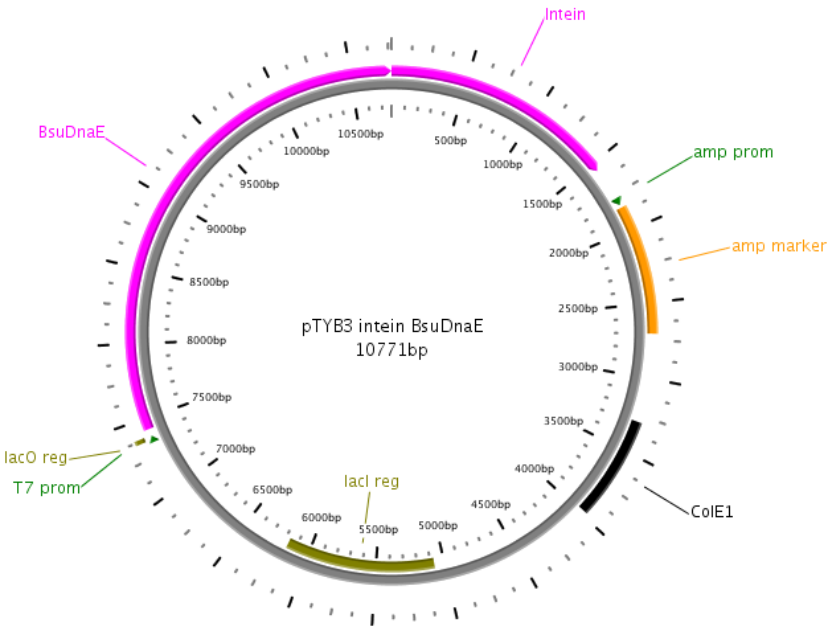


Figure 3.14 pTYB3 C-terminal Intein-tagged *Bsu*DnaE plasmid map.

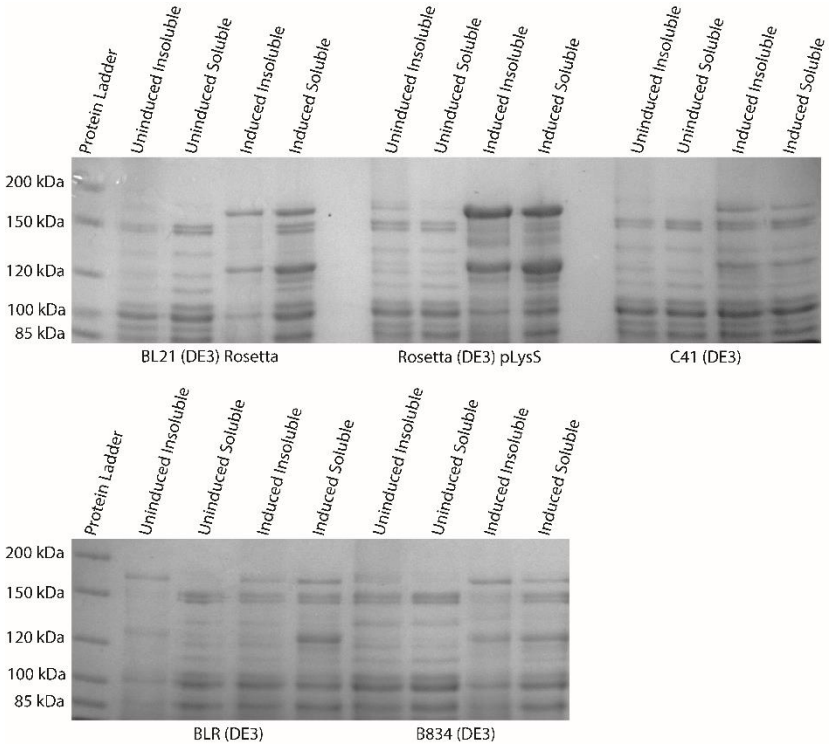


Figure 3.15 C-terminal Intein-tagged DnaE expression strain test. 10% (v/v) SDS PAGE monitoring the expression of C-terminal Intein-tagged DnaE in several of our lab expression strains for T7 promoters.

3.3.1.2 DnaE polymerase Purification

The cell pellet was suspended in 30 ml/l cell growth sonication buffer [50 mM Tris-HCl pH 7.5, 1 mM EDTA, 1 M NaCl, 1 mM PMSF and protease inhibitor cocktail mix (Fisher)] and sonicated. The insoluble fraction was separated and discarded by centrifugation at 30000 g, 30 minutes, 4°C. Soluble lysate was loaded overnight at 4°C onto chitin beads (~15 ml/l cell growth), using a super loop at <1 ml/min flow rate, followed by slow washing with 1 L of 50 mM Tris-HCl pH 7.5 and 1 M NaCl. After further washing with 50 mM Tris-HCl pH 7.5 and 2 M NaCl and again 50 mM Tris-HCl pH 7.5 and 1 M NaCl, DTT was added to the column up to a

final concentration of 100 mM and mixed with the beads. The column was sealed and left overnight at 4ºC with the DTT, followed by elution with three to four column volumes of 50 mM Tris-HCl pH 7.5. Thereafter, solid ammonium sulphate was added to the eluate at 4ºC to final concentration of 50% (w/v). Precipitated protein was collected by centrifugation at 20000 g, 15 minutes, 4ºC and suspended in 50 mM Tris-HCl pH 8.0. Then, DnaE was loaded onto a 5 ml Hitrap Q HP column (GE healthcare), equilibrated in 50 mM Tris-HCl pH 8.0, keeping the conductivity below 4 mS which is essential for column binding, and eluted with a ten column volume gradient from 0-1 M NaCl. The respective peak was pooled, dialysed overnight into 20 mM HEPES-NaOH pH 7.5, 300 mM NaCl and 20% (v/v) glycerol, DnaE polymerase concentration was quantified spectrophotometrically (extinction coefficient 87030 M^{-1} cm^{-1}) and stored at -80ºC. The purification of (C-terminal Intein-tagged) DnaE polymerase is shown in **Figure 3.16**.

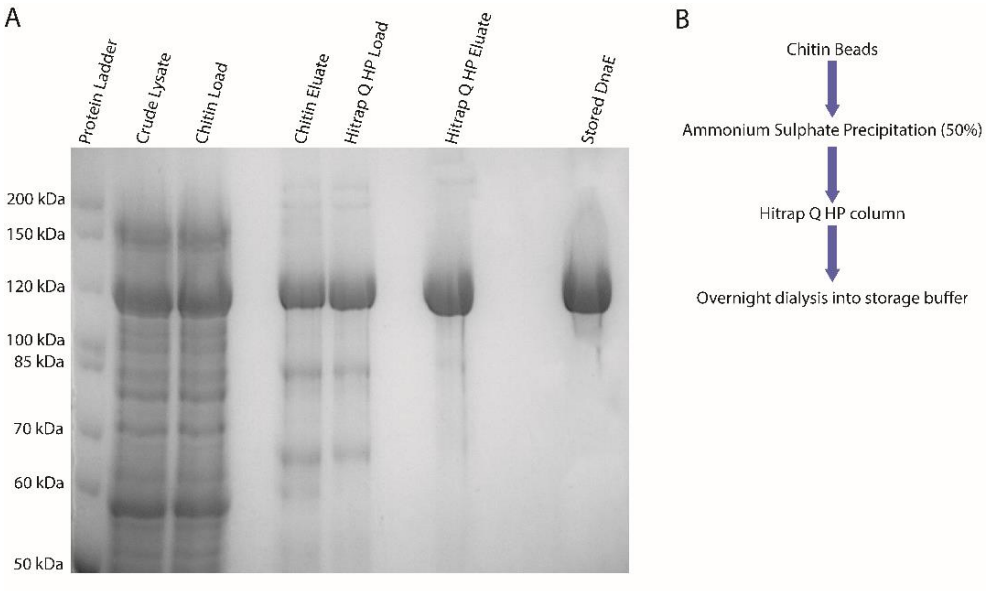


Figure 3.16 C-terminal Intein-tagged DnaE purification steps (**A**) and scheme (**B**).

3.3.1.3 DnaE polymerase Activity Test

The activity of DnaE was detected with primer extension assays using small template, as described in **Section 2.2.6.4**. Protein titration assays are shown in **Figure 3.17**.

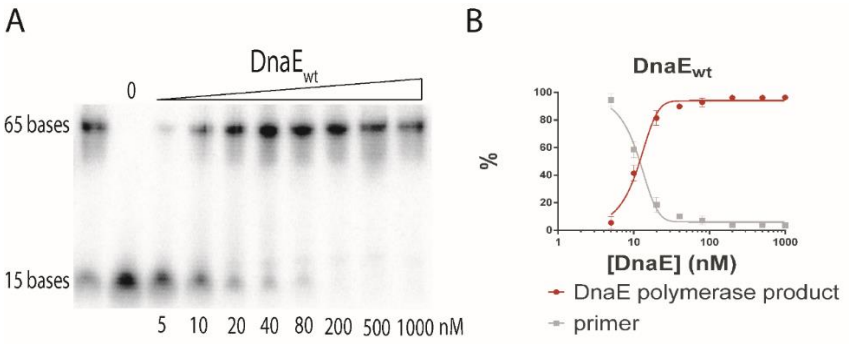


Figure 3.17 (Intein-tagged) DnaE activity assay. DNA primer extension assay using short radiolabelled deoxyribonucleotide (15 bases) annealed onto longer oligonucleotide template (110 bases) for the detection of DnaE activity. Reaction products were resolved by electrophoresis through 15% (v/v) ureagel PAG (A), data were analysed using molecular imager and associated software (Bio-Rad) and the percentage of products formed was plotted using Graphpad – Prism 6 (B). Assays were performed in triplicates and error bars indicate standard deviations.

Our data indicate that purified (Intein-tagged cleaved) DnaE polymerase is active, since it can effectively extend DNA-primed templates, producing products with 65 bases final length, as expected.

3.3.2 N-terminal Hexahistidine-tagged Maltose Binding Protein-tagged DnaE polymerase

3.3.2.1 DnaE polymerase Cloning and Mutagenesis

N-terminal Hexahistidine-tagged Maltose Binding Protein (MBP)-tagged DnaE construct was created using Ligation Independent Cloning (LIC), as described in **Section 2.2.3.1**, with the plasmid p2CT (kind gift from James Berger), generating the p2CT-*Bsu*DnaE expression plasmid (**Figure 3.18**). We developed this new approach for expressing and purifying DnaE polymerase in order to ease the purification and increase the amount of the expressed and purified protein compared to the method described in **Section 3.3.1**.

For the purposes of this project, we created a polymerase deficient DnaE mutant. Previous studies revealed that the catalytic site of DNA polymerases contains three highly conserved Aspartic acid (D) residues, essential for the two-metal ion mechanism for the nucleotidyl transfer (**Figure 3.19**) (Steitz, 1999). Three Aspartic acid residues in *Escherichia coli* have been identified by site-directed mutagenesis (D401, D403, D555) (Pritchard & McHenry, 1999). An EMBOSS-Water sequence alignment (Rice et al., 2000) of *Escherichia coli* DnaE (*Ec*DnaE) and *Bacillus subtilis* DnaE (*Bsu*DnaE) polymerases revealed the essential Aspartic acid residues (D) in DnaE (**Figure 3.20**). Two of these residues were mutated to Alanines (A), in order to create the $DnaE_{pol-}$ (DnaE D382A/D384A) mutant protein.

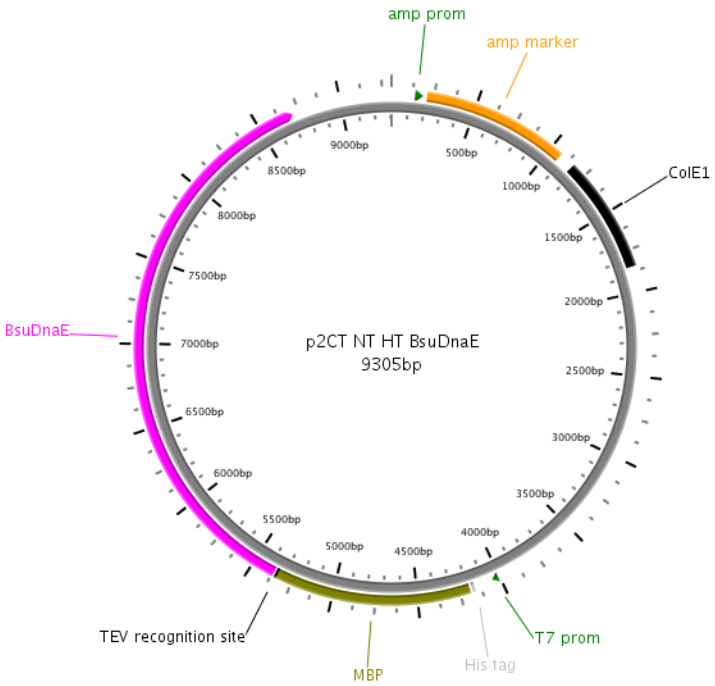


Figure 3.18 p2CT N-terminal Histidine-tagged MBP-tagged *Bsu*DnaE plasmid map.

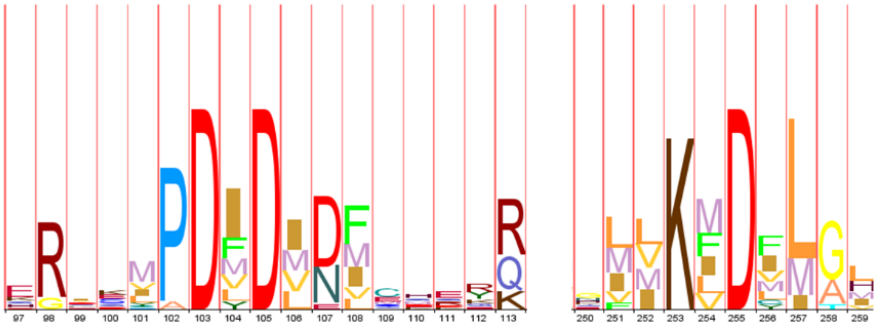


Figure 3.19 HMM logo of conserved Aspartic acid (D) residues in DNA polymerases' polymerase catalytic site. The conservation of the aspartic acid residues is essential for the nucleotidyl transfer in DNA polymerases. HMM logos were used to visualise profile HMM in a graphical form (Schuster-Böckler et al., 2004).

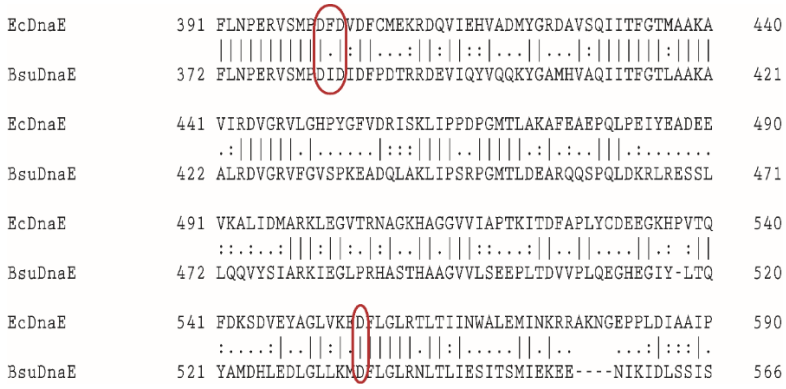


Figure 3.20 Alignment of *Ec*DnaE and *Bsu*DnaE. The essential aspartic acid residues for the polymerase activity are located at positions 401, 403 and 555 for *Escherichia coli* DnaE and 382, 384 and 535 for *Bacillus subtilis* DnaE. The alignment was created using EMBOSS-Water (Rice et al., 2000).

The p2CT-*Bsu*DnaE plasmid containing the wild type gene was stored in XL-1 Blue strain at -80ºC. Plasmids were isolated using the protocol described in **Section 2.2.2.1** and PCR was carried out according to the protocol stated in **Section 2.2.2.2** using primers shown in **Table 2.3**. Then, samples were treated with DpnI (**Section 2.2.2.4**), plasmids were extracted from gels (**Section 2.2.2.3**), phosphorylated and ligated (**Section 2.2.2.4**). The ligation product was used to transform XL-1 Blue strains (**Section 2.2.4.2**), glycerol stocks were made from single colonies (**Section 2.2.4.3**) and the mutated, purified plasmids were sequenced, to verify the mutagenesis.

3.3.2.2 DnaE polymerase Expression

Upon completion of successful subcloning and mutagenesis, a series of expression strain tests were performed, in order to optimise the expression of soluble protein, as shown in **Figure 3.21**.

Bacillus subtilis N-terminal Hexahistidine-tagged Maltose Binding Protein (MBP)-tagged DnaE polymerase was expressed in BL21 (DE3) Rosetta *Escherichia coli* strain using the p2CT plasmid. Cells were grown in 2xYT Broth with 50 μg /ml carbenicillin and 1% (w/v) sterile glucose at 37°C, 180 rpm until late stage of mid log phase (OD_{595} = 0.8) followed by incubation at 4°C for ten minutes. Subsequently, cells were induced with 1 mM IPTG and incubated further at 25°C, 180 rpm for three hours. The cell pellet was harvested by centrifugation at 3000 g, for 15 minutes at 4°C and stored at -80°C.

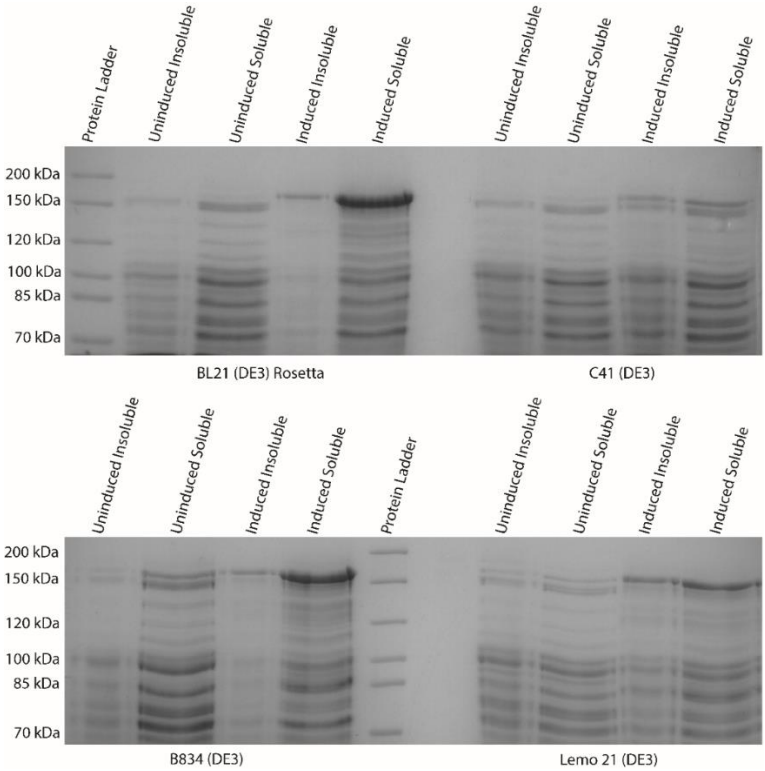


Figure 3.21 N-terminal Histidine-tagged Maltose Binding Protein (MBP)-tagged DnaE expression strain test. 10% (v/v) SDS PAGE monitoring the expression of N-terminal Hexahistidine-tagged Maltose Binding Protein (MBP)-tagged DnaE in several of our lab expression strains for T7 promoters.

3.3.2.3 DnaE polymerase Purification

The cell pellet was suspended in 30 ml/l cell growth sonication buffer [25 mM HEPES-NaOH pH 8.0, 0.5 M NaCl, 20 mM imidazole, 10% (v/v) glycerol, 1 mM PMSF and protease inhibitor cocktail mix (Fisher)] and sonicated. The lysate was clarified by centrifugation at 40000 g, 30 minutes, 4°C followed by filtering (0.22 µm diameter filters). It was then loaded on 5 ml Histrap HP column (GE Healthcare), equilibrated in 25 mM HEPES-NaOH pH 8.0, 0.5 M NaCl, 20 mM imidazole and 10% (v/v) glycerol. The column was washed extensively with the equilibration buffer

and N-terminal hexahistidine-tagged MBP-tagged DnaE polymerase was eluted with a 15 column volume gradient from 0.02 to 0.5 M (**Figure 3.22**).

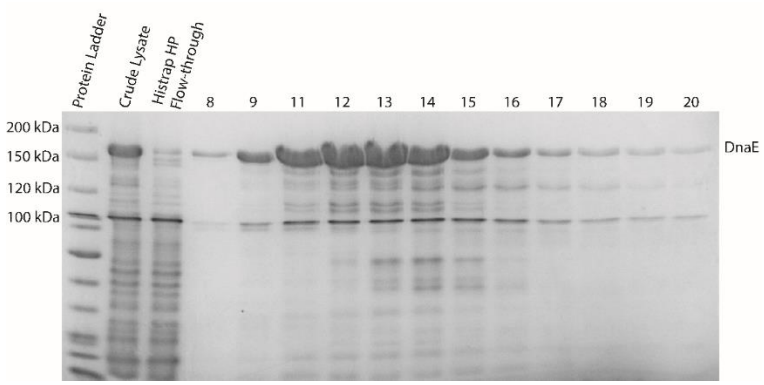


Figure 3.22 N-terminal MBP-tagged His-tagged DnaE Histrap HP column. 10% (v/v) SDS PAGE monitoring the purification of DnaE from 5 ml Histrap HP column. The size of MBP-tagged His-tagged DnaE is 167 kDa. Fractions 9 - 16 were pooled for the next purification step.

Fractions containing MBP-tagged hexahistidine-tagged DnaE polymerase were pooled and dialysed against two litres of 25 mM HEPES-NaOH pH 8.0, 2 M NaCl, 0.5 M urea and 10% (v/v) glycerol at 4°C. Thereafter, the protein concentration was quantified spectrophotometrically using NanoDrop and TEV protease was added at 1:15 (TEV:DnaE) mass ratio, followed by overnight incubation at 4°C. Then, the sample was filtered (0.22 µm diameter filters) and loaded on 5 ml Histrap HP column (GE Healthcare), equilibrated in 25 mM HEPES-NaOH pH 8.0, 2 M NaCl, 0.5 M urea and 10% (v/v) glycerol and the flow-through was collected. Solid ammonium sulphate was added to the eluate at 4°C to final concentration of 55% (w/v). Precipitated protein was collected by centrifugation at 20000 g, 15 minutes, 4°C and suspended in 25 mM HEPES-NaOH pH 8.0, 50 mM

NaCl and 10% (v/v) glycerol. Subsequently, the protein was loaded onto a 5 ml Hitrap Q HP column (GE healthcare), equilibrated in 25 mM HEPES-NaOH pH 8.0, 50 mM NaCl and 10% (v/v) glycerol, keeping the conductivity below 4 mS which is essential for column binding. DnaE polymerase was eluted performing a 15 column volume gradient from 0-1 M NaCl (**Figure 3.23**).

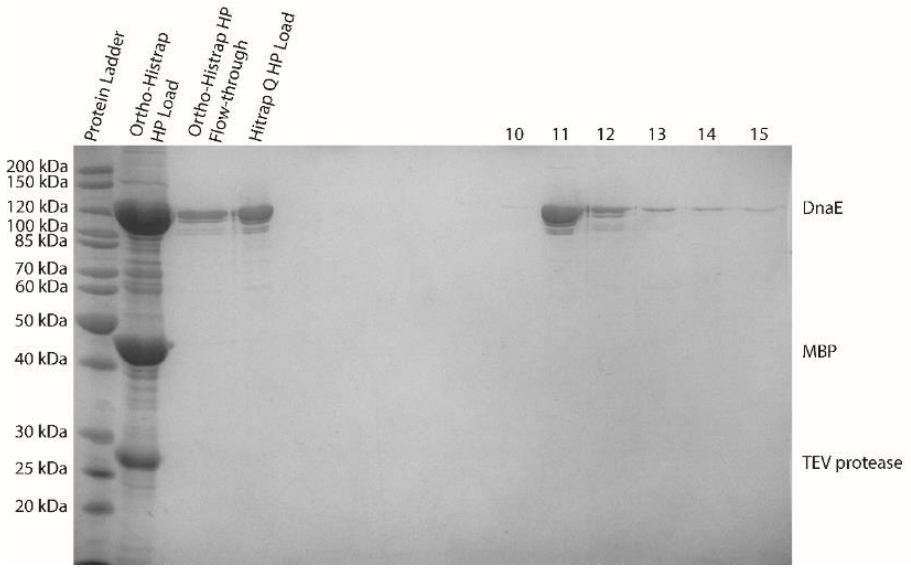


Figure 3.23 N-terminal His-tagged MBP-tagged DnaE Hitrap Q HP column. 10% (v/v) SDS PAGE monitoring the purification of DnaE from 5 ml Q HP column. The size of DnaE, Maltose Binding Protein (MBP) and TEV protease is 125 kDa, 45 kDa and 27 kDa respectively. Fractions 10-15 show the elution of DnaE performing gradient up to 1 M NaCl. Fraction 11 was dialysed into storage buffer and stored at -80°C.

Lastly, the respective peak was pooled, dialysed overnight into 20 mM HEPES pH 7.5, 300 mM NaCl, 20% (v/v) glycerol, DnaE polymerase concentration was quantified spectrophotometrically (extinction coefficient 87030 M^{-1} cm^{-1}) and stored

at -80ºC. Purification of [N-terminal Hexahistidine-tag Maltose Binding Protein (MBP)-tag cleaved] DnaE polymerase is shown in **Figure 3.24.**

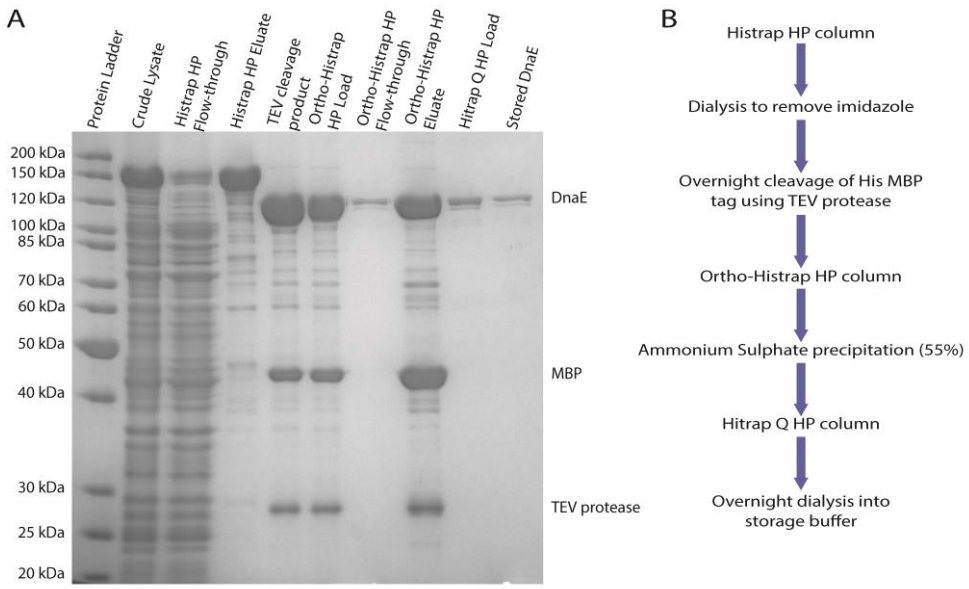


Figure 3.24 [N-terminal Hexahistidine-tag Maltose Binding Protein (MBP)-tag cleaved] DnaE purification steps (**A**) and scheme (**B**).

3.3.2.4 DnaE Polymerase Activity Test

The activities of DnaE and $DnaE_{pol-}$ (DnaE D382A/D384A) polymerases were assayed with primer extensions using small template, as described in **Section 2.2.6.4**. Protein titration assays were carried out as shown in **Figure 3.25**.

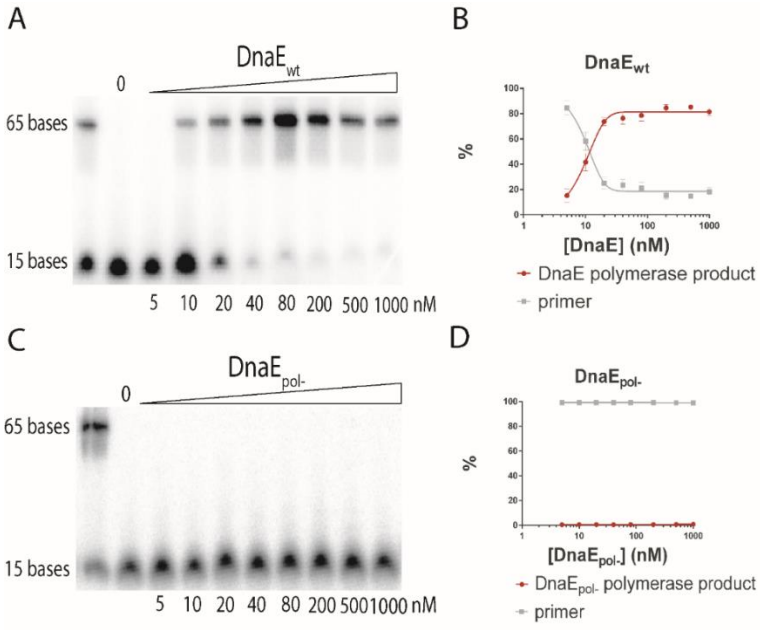


Figure 3.25 (Histidine-tag MBP-tag cleaved) DnaE/DnaE$_{pol-}$ activity assay. DNA primer extension assay using short radiolabelled deoxyribonucleotide (15 bases) annealed onto longer oligonucleotide template (110 bases) for the detection of DnaE activity. Reaction products were resolved by electrophoresis through 15% (v/v) ureagel PAG (**A, C**), data were analysed using molecular imager and associated software (Bio-Rad) and the percentage of products was plotted using Graphpad – Prism 6 (**B, D**). Assays were carried out in triplicates and error bars indicate standard deviations.

Our data indicate that purified [N-terminal Hexahistidine-tag Maltose Binding Protein (MBP)-tag cleaved] DnaE polymerase is active, since it can effectively extend DNA-primed templates, producing products with 65 bases final length. Additionally, we observed that the [N-terminal Hexahistidine-tag Maltose Binding Protein (MBP)-tag claved] DnaE$_{D382A,D384A}$ (DnaE$_{pol-}$) mutant did not exhibit any polymerase activity, as predicted.

3.4 DNA Polymerase PolC

The *polC* gene was subcloned from the pA1-Bs-PolC plasmid (kind gift from Charles McHenry) into a pET derived vector (p2BT) and the protein was expressed with N-terminal hexahistidine tag. The methodology followed for cloning, expression and purification of hexahistidine-tagged PolC is described below. Moreover, this section describes site-directed mutagenesis in order to obtain polymerase and exonuclease deficient mutants of PolC.

3.4.1 N-terminal Hexahistidine-tagged PolC

3.4.1.1 PolC Cloning and Mutagenesis

N-terminal Hexahistidine-tagged PolC construct was created using Ligation Independent Cloning (LIC), as described in **Section 2.2.3.1**, with the plasmid p2BT (kind gift from James Berger), generating the p2BT-*Bsu*PolC expression plasmid (**Figure 3.26**).

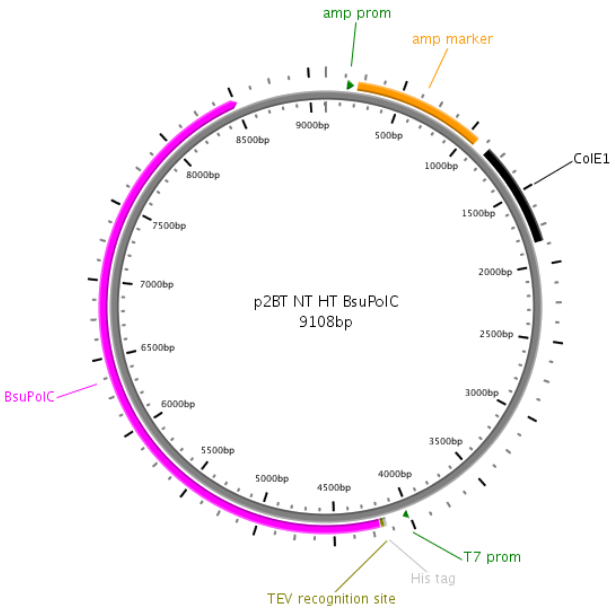


Figure 3.26 p2BT N-terminal Histidine-tagged *Bsu*PolC plasmid map.

For the purposes of this project, we created polymerase deficient and exonuclease deficient mutants of PolC. Clustal Omega (Goujon et al., 2010; McWilliam et al., 2013; Sievers et al., 2011) multiple sequence alignment of *Escherichia coli* DnaE (*Ec*DnaE) with *Bacillus subtilis* DnaE (*Bsu*DnaE) and PolC (*Bsu*PolC) polymerases identified the essential Aspartic acid (D) residues for the nucleotidyl transfer as D382, D384, D535 in DnaE polymerase, as described in **Section 3.3.2.1**, and D966, D968, D1091 in PolC (Figure **3.27**). Two of these residues were mutated to Alanines (A), in order to create the $PolC_{pol-}$ (PolC D966A/D968A) mutant protein.

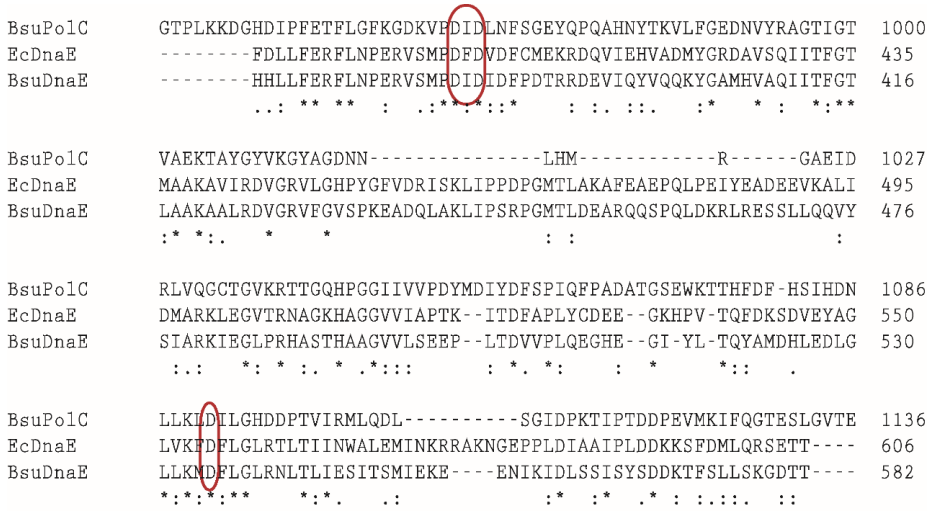


Figure 3.27 Alignment of *Ec*DnaE, *Bsu*DnaE and *Bsu*PolC. Essential aspartic acid residues for the polymerase activity are located at the positions 401, 403 and 555 for *Escherichia coli* DnaE, at positions 382, 384 and 535 in *Bacillus subtilis* DnaE and 966, 968 and 1091 in *Bacillus subtilis* PolC. The alignment was created using Clustal Omega Multiple Sequence Alignment (Goujon et al., 2010; McWilliam et al., 2013; Sievers et al., 2011).

Additionally, three acidic residues are essential for the exonuclease activity (proof-reading activity) of polymerases (**Figure 3.28**), as it has been revealed in previous studies of *Escherichia coli* PolA polymerase (*Ec*PolA) (D355, E357, D501) (Beese & Steitz, 1991) and *Escherichia coli* DnaQ (*Ec*DnaQ) (D12, E14, D167), the epsilon subunit of DNA polymerase III with 3' to 5' proof-reading activity (Fijalkowska & Schaaper, 1996). A Clustal Omega (Goujon et al., 2010; McWilliam et al., 2013; Sievers et al., 2011) multiple sequence alignment of *Escherichia coli* PolA polymerase (*Ec*PolA) with *Escherichia coli* DnaQ (*Ec*DnaQ) and *Bacillus subtilis* PolC (*Bsu*PolC) identified the equivalent conserved acidic (D, E) residues for the exonuclease activity as D425, E427, D570 in PolC (**Figure 3.29**). Two of these

residues were mutated to Alanines (A), in order to create the $PolC_{exo-}$ (PolC D425/E427A) mutant protein.

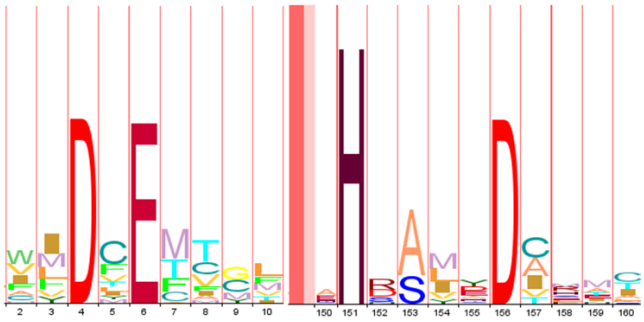


Figure 3.28 HMM logo of conserved acidic (D, E) residues in DNA polymerases' exonuclease catalytic site. The conservation of the three acid residues is essential for the exonuclease (proof-reading) activity in DNA polymerases. HMM logos were used to visualise profile HMM in a graphical form (Schuster-Böckler et al., 2004).

```
EcPolA      --IAKLEKAPVFAFDTETDSLDNISANLVGLSFAI------------------------  375
EcDnaQ      ---MSTAITRQIVLDTETTGMNQIGAHYEGHKIIEIGAVEVVNRRLTGNNFHVYLKPDRL  57
BsuPolC     AAHRLLEEETYVVFDVETTGLSAVY-----DTIIELAAVKVKGGE-IIDKFEAFANPHRP  464
                       ..:*.** .:. :       .:

EcPolA      -EPGVAAYIPVAHDY-LDAPDQISRERALELLKPLLEDEKALKVGQNLKYDRGILANY-G  432
EcDnaQ      VDPEAFGVHGIADEFLLDKPTFAEVADEF---MDYI--RGAELVIHNAAFDIGFMDYEFS  112
BsuPolC     LSATIIELTGITDDMLQDAPDVVDVIRDF---REWI--GDDILVAHNASFDMGFLNVAYK  519
             .        ::.:   * *   .    :      :       * :*  :* *::

EcPolA      IELRGI----AFDTMLESYI----LNSVAGRHDMDSLAERWLKHKTITFEEIAGKGKNQL  484
EcDnaQ      LLKRDIPKTNTFCKVTDSLAVARKMFPGKR-NSLDALCARYEIDNSKR------------  159
BsuPolC     KLLEVEK---AKNPVIDTLELGRFLYPEFKNHRLNTLCKKFDIELTQH------------  564
               .      :   : ::      :      . :::*. ::  . :

EcPolA      TFNQIALEEAGRYAAFDADVTLQLHLKM-----------WPDLQKHKGPLNV--------  525
EcDnaQ      -----TL----HGALLDAQILAEVYLAMTGGQTSMAFAMEGETQQQQGEATIQRIVR---  207
BsuPolC     -----------HRAIYDTEATAYLLLKMLKDAAEKGIQYHDELNENMGQSNAYQRSRPYH  613
                      : *  *::    : * *             : ::. *  .
```

Figure 3.29 Alignment of *Ec*PolA, *Ec*DnaQ and *Bsu*PolC. Essential acidic residues for the exonuclease activity are located at positions 355, 357 and 501 in *Escherichia coli* PolA, 12, 14 and 167 in *Escherichia coli* DnaQ and 425, 427, 570 in *Bacillus subtilis* PolC. The alignment was created using Clustal Omega Multiple Sequence Alignment (Goujon et al., 2010; McWilliam et al., 2013; Sievers et al., 2011).

The p2BT-*Bsu*PolC plasmid containing the wild type gene was stored in XL-1 Blue strain at -80ºC. Plasmids were isolated using the protocol described in **Section 2.2.2.1** and PCR was carried out according to the protocol in **Section 2.2.2.2** using primers shown in **Table 2.3**, followed by DpnI treatment (**Section 2.2.2.4**). Then plasmids were extracted from gels (**Section 2.2.2.3**), phosphorylated and ligated (**Section 2.2.2.4**). Ligation products were used to transform XL-1 Blue strains (**Section 2.2.4.2**), glycerol stocks were prepared from single colonies (**Section 2.2.4.3**) and the mutated, purified plasmids were sequenced, to verify the mutagenesis.

3.4.1.2 PolC Expression

Upon completion of successful subcloning and mutagenesis, a series of protein expression tests were performed to test strains, growth media, incubation temperature, optical density at induction, duration of induction time, temperature of induction and lysis – sonication buffers (data not shown), in order to optimise the expression of soluble PolC as shown in **Figure 3.30**.

Thus, *Bacillus subtilis* N-terminal Hexahistidine-tagged PolC was expressed in BLR (DE3) *Escherichia coli* strain using the p2BT plasmid. Cells were grown in 2xYT Broth with 50 μg /ml carbenicillin and 1% (w/v) filter sterile glucose at 37ºC, 180 rpm until late stage of mid log phase (OD_{595} = 0.9), followed by incubation at 4ºC for ten minutes. Then, cells were induced with 1 mM IPTG and incubated further at

25ºC, 180 rpm for three hours. The cell pellet was harvested by centrifugation at 3000 g, for 15 minutes at 4ºC and stored at -80ºC.

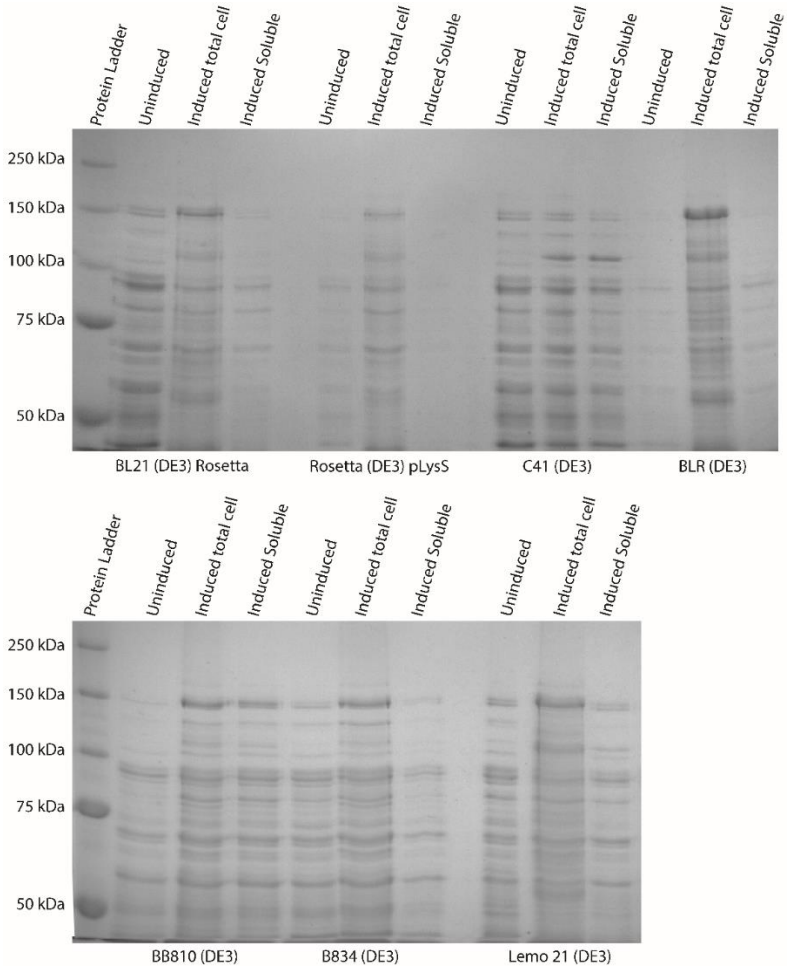


Figure 3.30 N-terminal Histidine-tagged PolC expression strain test. 10% (v/v) SDS PAGE monitoring the expression of N-terminal Hexahistidine-tagged PolC in several of our lab expression strains for T7 promoters.

3.4.1.3 PolC Purification

The cell pellet was suspended in 30 ml/l cell growth sonication buffer [25 mM HEPES-NaOH pH 7.5, 0.5 M NaCl, 20 mM imidazole, 10% (v/v) glycerol, 1 mM PMSF and protease inhibitor cocktail mix (Fisher)] and sonicated. The lysate was

clarified by centrifugation at 40000 g, 30 minutes, 4ºC, followed by filtering (0.22 µm diameter filters). It was then loaded on 5 ml Histrap HP column (GE Healthcare), equilibrated in 25 mM HEPES-NaOH pH 7.5, 0.5 M NaCl, 20 mM imidazole and 10% (v/v) glycerol. The column was washed extensively with equilibration buffer and N-terminal Histidine-tagged PolC was eluted with a 15 column volume gradient from 0.02-0.5 M imidazole (**Figure 3.31**).

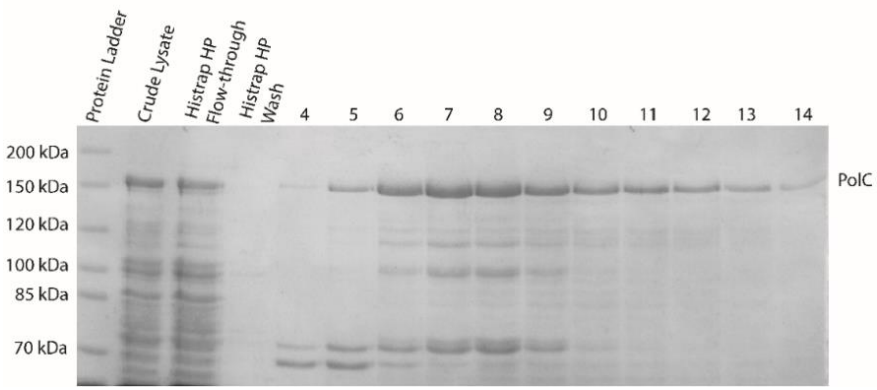


Figure 3.31 N-terminal His-tagged PolC Histrap HP column. 10% (v/v) SDS PAGE monitoring the purification of PolC from 5 ml Histrap HP column. Fractions 6 - 14 were pooled for the next purification step.

Fractions containing N-terminal Histidine-tagged PolC were pooled, the protein concentration was quantified spectrophotometrically using NanoDrop, TEV protease was added at 1:20 (TEV:PolC) mass ratio and overnight dialysis was performed against 25 mM HEPES-NaOH pH 7.5, 50 mM NaCl and 10% (v/v) glycerol at 4ºC. The dialysed sample was loaded on 5 ml Histrap HP column equilibrated in the same buffer, the flow-through was collected and loaded on a 5 ml Hitrap Q HP column (GE Healthcare), equilibrated in 25 mM HEPES-NaOH pH 7.5, 50 mM NaCl and 10% (v/v) glycerol. PolC was eluted performing a 15 column volume gradient from 0.05-1 M NaCl (**Figure 3.32**).

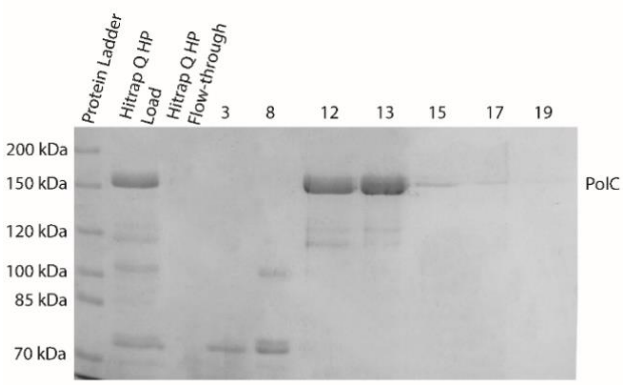


Figure 3.32 N-terminal His-tagged PolC Hitrap Q HP column. 10% (v/v) SDS PAGE monitoring the purification of PolC from 5 ml Hitrap Q HP column. Fractions 12 - 14 were pooled for the next purification step.

Lastly, fractions containing PolC were pooled and loaded on Hiload 26/60 Superdex 200 prep grade gel filtration column, equilibrated in 25 mM HEPES pH 7.5, 200 mM NaCl, 1 mM DTT and 10% (v/v) glycerol (**Figure 3.33**), PolC concentration was quantified spectrophotometrically (extinction coefficient 130835 M^{-1} cm^{-1}) and stored at -80ºC.

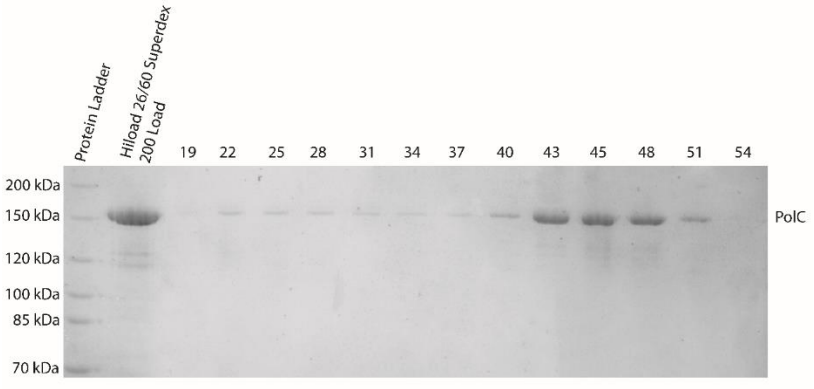


Figure 3.33 N-terminal Histidine-tagged PolC Hiload 26/60 Superdex 200 prep grade column. 10% (v/v) SDS PAGE monitoring the purification of PolC from Hiload 26/60 Superdex 200 prep grade gel filtration column. Fractions 43-51 were pooled and stored at -80ºC.

Purification of [Hexahistidine-tagged] PolC is summarised in **Figure 3.34**.

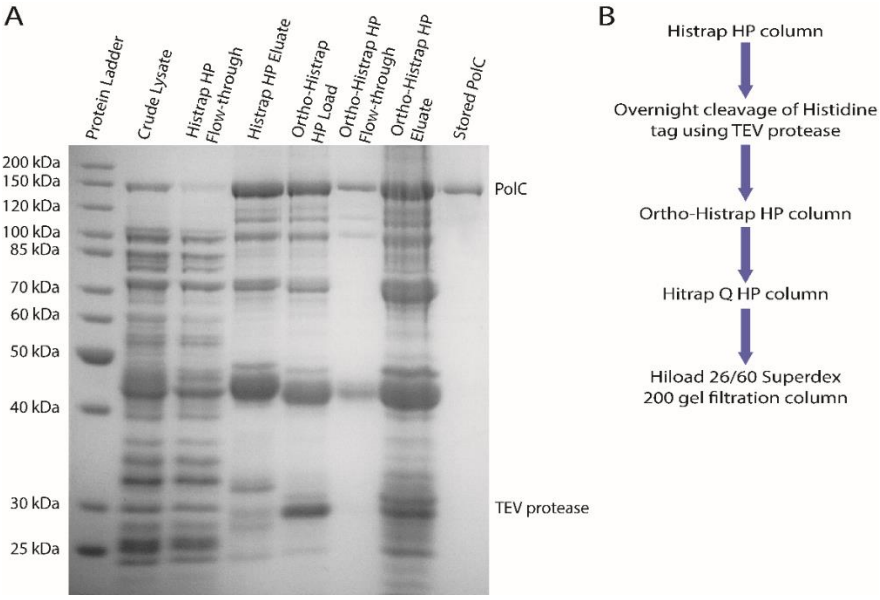


Figure 3.34 N-terminal Hexahistidine-tagged PolC purification steps (**A**) and scheme (**B**).

3.4.1.4 PolC Activity Test

The activities of PolC, $PolC_{pol-}$ (PolC D966A/D968A) and $PolC_{exo-}$ (PolC D425A/E427A) were detected with primer extension assays using small template, as described in **Section 2.2.6.4**. Protein titration assays are shown in **Figure 3.35**.

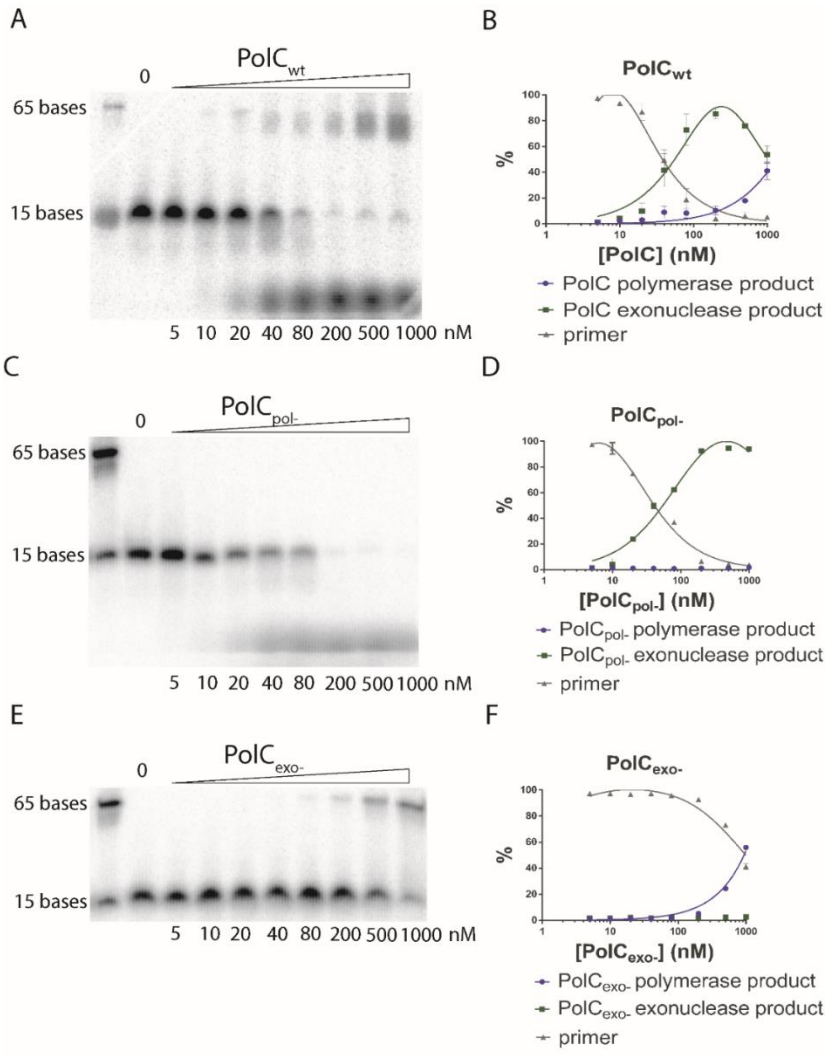


Figure 3.35 (Histidine-tag claved) PolC/PolC$_{pol-}$/PolC$_{exo-}$ activity assay. DNA primer extension assay using short radiolabelled deoxyribonucleotide (15 bases) annealed onto longer oligonucleotide template (110 bases) for the detection of PolC activity. Reaction products were resolved by electrophoresis through 15% (v/v) ureagel PAG (**A, C, E**), data were analysed using molecular imager and associated software (Bio-Rad) and the percentage of products was plotted using Graphpad – Prism 6 (**B, D, F**). Assays were performed in triplicates and error bars indicate standard deviations.

Our results indicate that the purified (N-terminal hexahistidine-tag cleaved) PolC can effectively extend DNA primers (**Figure 3.35 A, B**). Additionally, PolC exonuclease activity is also apparent resulting in degraded DNA primer and a

mixture of polymerase products with maximum length of 65 bases (**Figure 3.35 A**). The exonuclease activity is eliminated in $PolC_{exo-}$ (PolC D425A/E427A) confirming that this protein is an exonuclease deficient mutant (**Figure 3.35 E, F**). Moreover, $PolC_{pol-}$ (PolC D966A/D968A) exhibits only exonuclease activity, confirming that this protein is a polymerase deficient mutant (**Figure 3.35 C, D**).

3.5 Single-strand DNA Binding protein SSB

Bacillus subtilis native SSB (18.7 kDa) and *Bacillus subtilis* N-terminal Hexahistidine-tagged SSBΔ107-172 (11.9 kDa) were expressed and purified according to already published methods (Green et al., 2014; Green, Hatter et al., 2016).

3.5.1 Native SSB

3.5.1.1 SSB Expression

Bacillus subtilis native SSB (18.7 kDa) was expressed in Rosetta (DE3) pLysS *Escherichia coli* strain using the pET22b-SSB plasmid. Cells were grown in 2xYT Broth with 50 μg /ml carbenicillin at 37°C, 180 rpm until late stage of mid log phase (OD_{595} >2.0), followed by induction with 1 mM IPTG and further incubation at 30°C, 180 rpm overnight. The cell pellet was harvested by centrifugation at 3000 g, for 15 minutes at 4°C and stored at -80°C.

3.5.1.2 SSB Purification

The cell pellet was suspended in 30 ml/l cell growth sonication buffer [25 mM HEPES-NaOH pH 7.5, 0.5 M NaCl, 1 mM DTT, 1 mM EDTA, 10% (v/v) glycerol, 1 mM PMSF and protease inhibitor cocktail mix (Fisher)] and sonicated. The lysate

was clarified by centrifugation at 40000 g, 30 minutes, 37ºC, followed by filtering (0.22 µm diameter filters). Solid ammonium sulphate was afterwards added to the filtered protein solution at 4ºC to final concentration of 25% (w/v) and precipitated proteins were collected by centrifugation at 20000 g, 15 minutes, 4ºC, followed by suspension in 25 mM HEPES-NaOH pH 7.5, 200 mM NaCl, 1 mM DTT, 1 mM EDTA and 10% (v/v) glycerol. Then, the protein sample was filtered (0.22 µm diameter filters) and loaded on 5 ml Hitrap Q HP column (GE Healthcare), equilibrated in 25 mM HEPES-NaOH pH 7.5, 1 mM EDTA, 1 mM DTT and 10% (v/v) glycerol, keeping the conductivity below 4 mS which is essential for column binding. The column was washed extensively with the equilibration buffer and native SSB was eluted performing a 20 column volume gradient from 0-1 M NaCl (**Figure 3.36**).

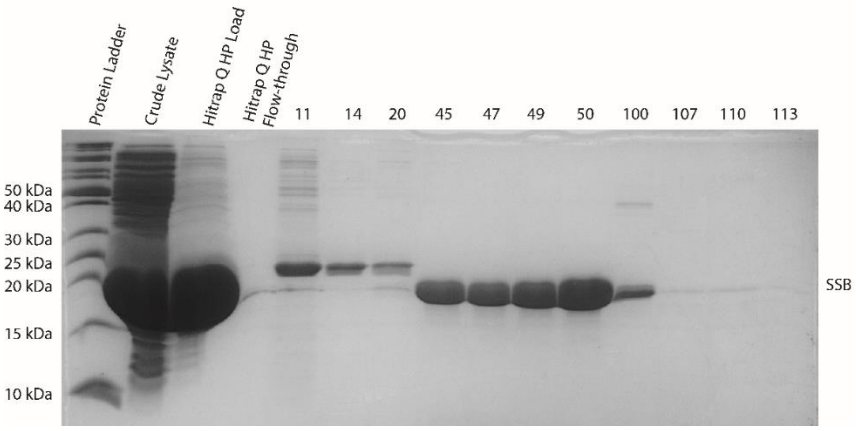


Figure 3.36 Native SSB Hitrap Q HP column. 20% (v/v) SDS PAGE monitoring the purification of SSB from 5 ml Hitrap Q HP column. Fractions 47 - 50 were pooled for the next purification step.

In the next step, fractions containing SSB were pooled and loaded on Hiload 26/60 Superdex 75 prep grade gel filtration column, equilibrated in 25 mM HEPES-NaOH pH 7.5, 200 mM NaCl, 1 mM DTT and 10% (v/v) glycerol (**Figure 3.37**), SSB concentration was quantified spectrophotometrically (extinction coefficient 11460 M^{-1} cm^{-1}) and stored at -80ºC.

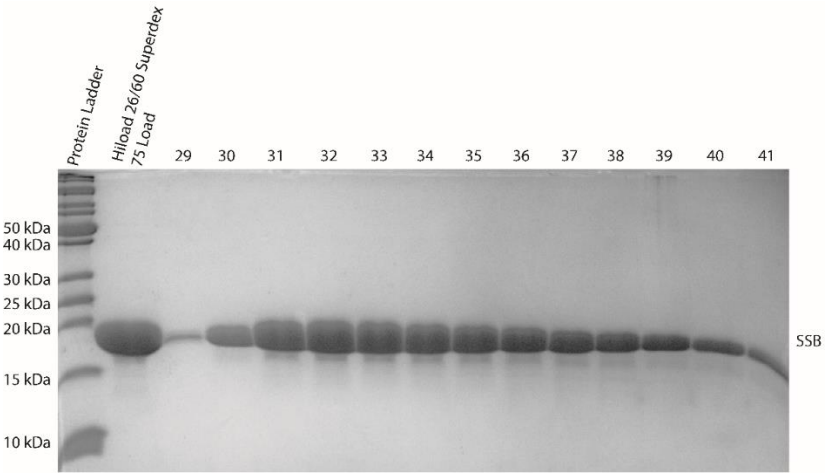


Figure 3.37 Native SSB Hiload 26/60 Superdex 75 prep grade column. 20% (v/v) SDS PAGE monitoring the purification of SSB from Hiload 26/60 Superdex 75 prep grade gel filtration column. Fractions 31-34 and 30,35-40 were pooled separately and stored at -80ºC.

Purification of native SSB is shown in **Figure 3.38**.

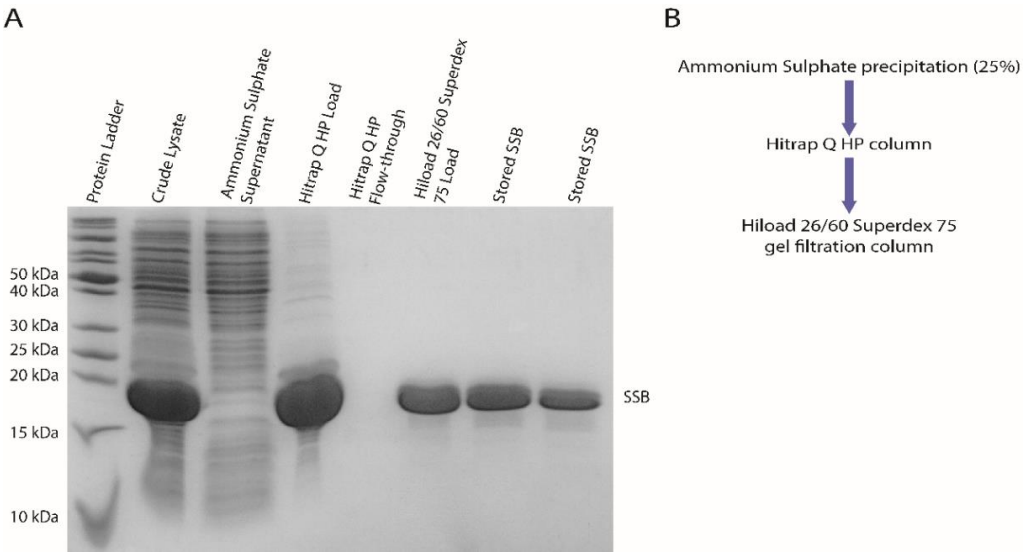


Figure 3.38 Native SSB purification steps (**A**) and scheme (**B**).

3.5.2 N-terminal Hexahistidine-tagged SSBΔ107-172

N-terminal Hexahistidine-tagged SSBΔ107-172 was expressed and purified in order to investigate the contribution of the intrinsically disordered C-terminal domain of SSB in processivity of DnaE and PolC polymerases (**Section 6.1.2**).

3.5.2.1 SSBΔ107-172 Expression

Bacillus subtilis N-terminal Hexahistidine-tagged SSBΔ107-172 (11.9 kDa), truncated SSB, lacking the intrinsically disordered C-terminal domain, was expressed in Rosetta (DE3) pLysS *Escherichia coli* strain using the pET28b-His SSBΔ107-172 plasmid. Cells were grown in 2xYT Broth with 50 μg /ml kanamycin at 37°C, 180 rpm until late stage of mid log phase (OD_{595} >2.0) followed by induction

with 1 mM IPTG and further incubation at 30°C, 180 rpm overnight. The cell pellet was harvested by centrifugation at 3000 g, for 15 minutes at 4°C and stored at -80°C.

3.5.2.2 SSBΔ107-172 Purification

The cell pellet was suspended in 30 ml/l cell growth sonication buffer [25 mM HEPES-NaOH pH 7.5, 0.5 M NaCl, 20 mM imidazole, 10% (v/v) glycerol, 1 mM PMSF and protease inhibitor cocktail mix (Fisher)] and sonicated. The lysate was clarified by centrifugation at 40000 g, 30 minutes, 37°C, followed by filtering (0.22 μm diameter filters). It was then loaded on 5 ml Histrap HP column (GE Healthcare), equilibrated in 25 mM HEPES-NaOH pH 7.5, 0.5 M NaCl, 20 mM imidazole and 10% (v/v) glycerol. The column was washed extensively with the equilibration buffer and N-terminal Hexahistidine-tagged SSBΔ107-172 was eluted with a 15 column volume gradient from 0.02-0.5 M imidazole (**Figure 3.39**).

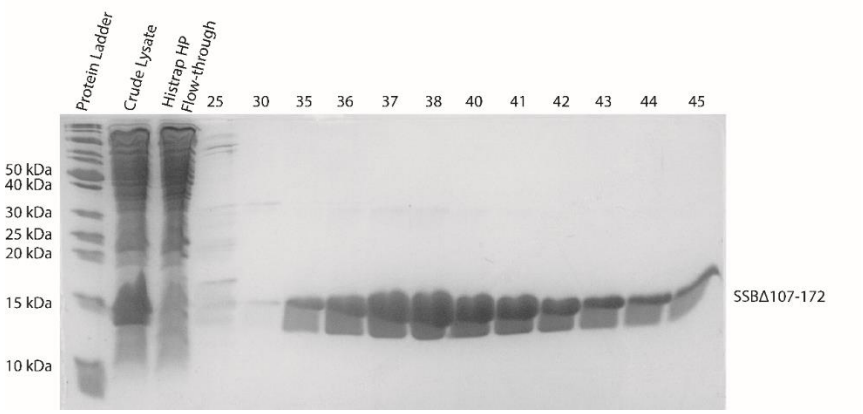


Figure 3.39 N-terminal Histidine-tagged SSBΔ107-172 Histrap HP column. 20% (v/v) SDS PAGE monitoring the purification of SSBΔ107-172 from 5 ml Histrap HP column. Fractions 37 - 40 were pooled for the next purification step.

Fractions containing N-terminal Histidine-tagged SSBΔ107-172 were pooled and loaded on Hiload 26/60 Superdex 75 prep grade gel filtration column, equilibrated in 25 mM HEPES pH 7.5, 200 mM NaCl, 1 mM DTT and 10% (v/v) glycerol (**Figure 3.40**), N-terminal Hexahistidine-tagged SSBΔ107-172 concentration was quantified spectrophotometrically (extinction coefficient 8480 M^{-1} cm^{-1}) and stored at -80ºC.

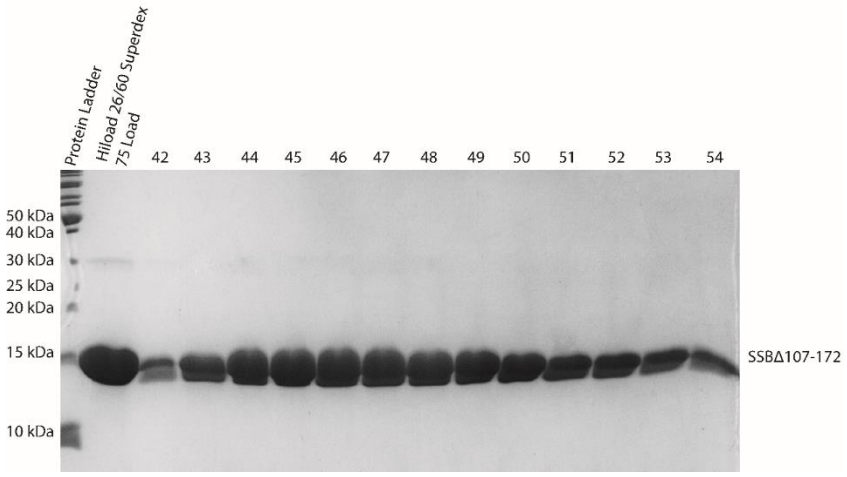


Figure 3.40 N-terminal Histidine-tagged SSBΔ107-172 Hiload 26/60 Superdex 75 prep grade column. 20% (v/v) SDS PAGE monitoring the purification of N-terminal Hexahistidine-tagged SSBΔ107-172 from Hiload 26/60 Superdex 75 prep grade gel filtration column. Fractions 45-47 and 43,44,48-51 were pooled separately and stored at -80ºC.

Purification of N-terminal Hexahistidine-tagged SSBΔ107-172, SSB lacking the intrinsically disordered C-terminal domain, is shown in **Figure 3.41**.

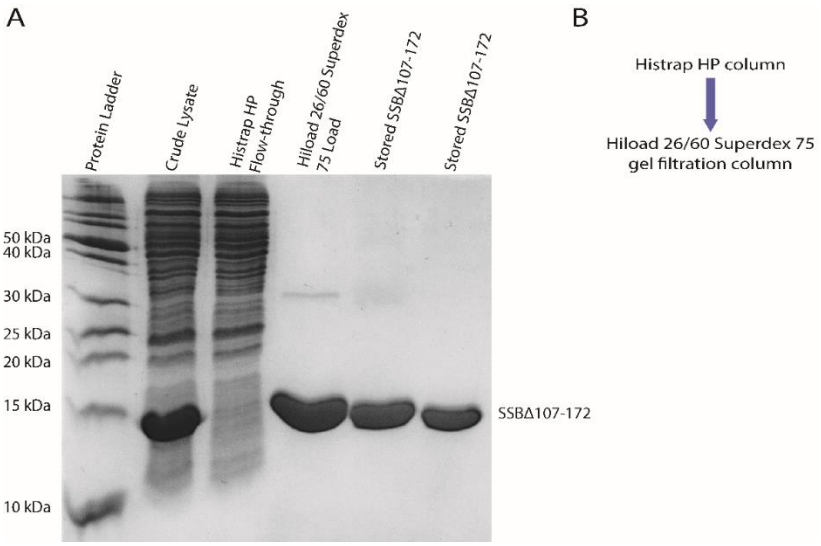


Figure 3.41 N-terminal Histidine-tagged SSBΔ107-172 purification steps (**A**) and scheme (**B**).

3.6 Processivity Clamp (DnaN) and Clamp-Loader (DnaX-tau subunit, YqeN-δ subunit, HolB-δ′ subunit)

The *Bacillus subtilis* processivity clamp (DnaN) and the components of the *Bacillus subtilis* clamp-loader (DnaX, YqeN and HolB) were kind gift form Dr José Afonso, member of the Neil Oldham Group, The University of Nottingham, UK. These proteins were purified according to already published methods and their ability to form active pentameric clamp-loader was verified (Afonso et al., 2013). Concentrations of purified proteins were quantified spectrophotometrically using the following extinction coefficients: 14440 M^{-1} cm^{-1} for DnaN (β clamp-42.1 kDa), 33390 M^{-1} cm^{-1} for DnaX (τ subunit-62.7 kDa), 20190 M^{-1} cm^{-1} for HolB (δ' subunit-37.6 kDa) and 23505 M^{-1} cm^{-1} for YqeN (δ subunit-40.5 kDa). Purified clamp and clamp-loader proteins are shown in **Figure 3.42**.

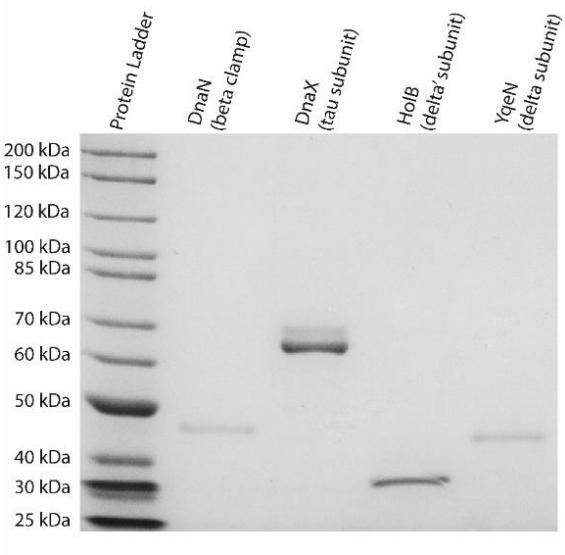


Figure 3.42 Processivity clamp and clamp-loader proteins. 12% (v/v) SDS PAGE monitoring the purified DnaN (β clamp-42.1 kDa), DnaX (τ subunit-62.7 kDa), HolB (δ' subunit-37.6 kDa) and YqeN (δ subunit-40.5 kDa).

4 Ribonucleotides and Deoxyribonucleotides at the fork

4.1 RNA primer extension

Bacillus subtilis DnaE and PolC polymerases cannot synthesise *de novo* primers in order to replicate the chromosomal DNA and rely on *de novo* synthesised RNA primers by the DnaG primase. Consequently, at the replication fork, replicative polymerases may compete for RNA primers. Thus, we wanted to explore the ability of DnaE and PolC polymerases to recognise and extend RNA primers.

The activities of DnaE and PolC were detected with RNA primer extension assays using small template, as described in **Section 2.2.6.4**. Protein titration assays are shown in **Figure 4.1**.

Our results indicate that only DnaE polymerase, not PolC polymerases, can effectively extend RNA primers, confirming previous published data (Sanders et al., 2010). We postulated that PolC does not recognise or cannot bind to RNA primed template, in order to digest the RNA primer, since there were no visible exonuclease products (degraded primer) (**Figure 4.1 C**).

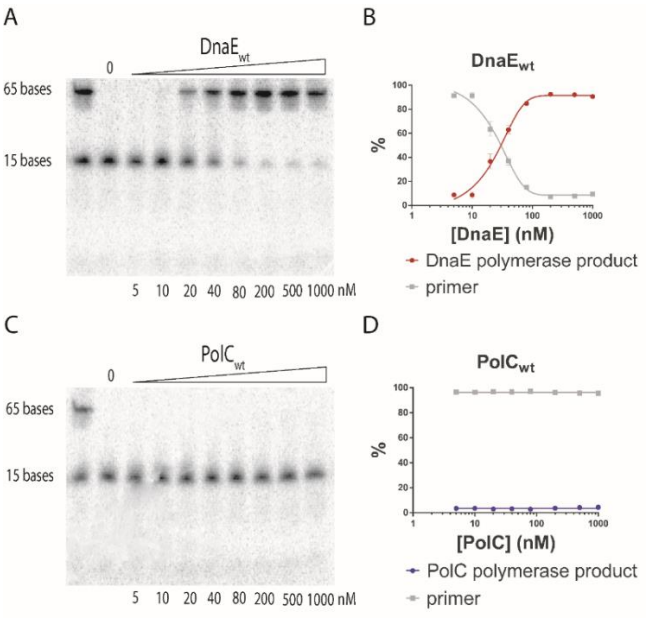


Figure 4.1 DnaE and PolC RNA primer extension assays. RNA primer extension assay using short radiolabelled ribonucleotide (15 bases) annealed onto longer oligonucleotide template (110 bases) for the detection of the polymerase activity. Reaction products were resolved by electrophoresis through 15% (v/v) ureagel PAG (**A, C**), data were analysed using molecular imager and associated software (Bio-Rad) and the percentage of products was plotted using Graphpad – Prism 6 (**B, D**). Assays were carried out in triplicates and error bars show standard deviations.

The discrimination against the RNA primer by PolC may be explained by examining its structure. The RNA-DNA hybrid adopts A conformation with 2,3 nm helical diameter (Conn et al., 1999; Hantz et al., 2001; Y. Xiong et al., 1998). By comparison the DNA-DNA duplex adopts B conformation with 1,9 nm helical diameter (McAuley-Hecht et al., 1994; Skelly et al., 1993). Thus, we speculate that the RNA-DNA hybrid does not fit within the binding channel of PolC, whereas the DNA-DNA duplex does. This could potentially explain the selectivity on the primed template.

There is no crystal structure of *Bacillus subtilis* PolC and the closest structure is that of *Geobacillus kaustophilus* PolC (*Gka*PolC) (PDB: 3F2D) (Evans et al., 2008). Two highly conserved antiparallel beta strands of the *Gka*PolC thumb play crucial role in interacting with DNA along the minor groove, through hydrogen bonds and van der Waals interactions with the phosphodiester backbones of both the primer and the template (B-type double helix). Moreover, the published crystal structures of both *Taq*DnaE (PDB: 2HPI, 2HPM) (Scott Bailey et al., 2006; Wing et al., 2008) and *Ec*DnaE (PDB: 2HQA, 2HNH) (Lamers et al., 2006), indicate that they utilise multiple positively charged residues within two α - helices of the thumb, in order to create electrostatic interactions with the negatively charged phosphodiester backbone of the primer and the template (A-type double helix). Hence, this difference in the interaction with the primed templates may provide an explanation for the selectivity of PolC for DNA primed templates.

In order to investigate further this notion, we performed a Clustal Omega (Goujon et al., 2010; McWilliam et al., 2013; Sievers et al., 2011) multiple sequence alignment of *Bacillus subtilis* PolC (*Bsu*PolC) and DnaE (*Bsu*DnaE) with *Geobacillus kaustophilus* PolC (*Gka*PolC), *Escherichia coli* DnaE (*Ec*DnaE) and *Thermus aquaticus* DnaE (*Taq*DnaE) polymerases (**Figure 4.2**). The alignment revealed that PolC also appears to possess these β-strands. By comparison, the β-strands are absent from DnaE thumb, indicating that primer-template binding by DnaE may be different.

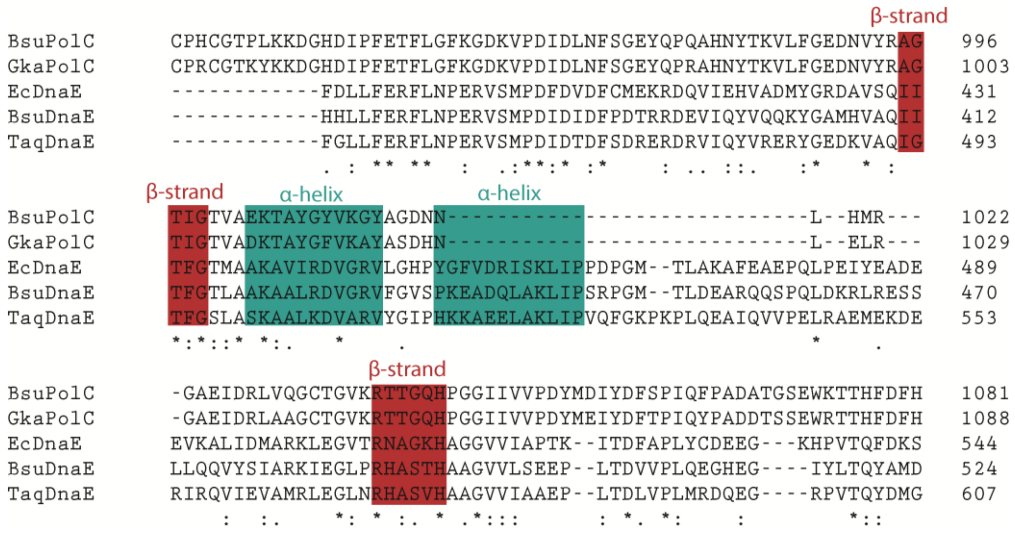


Figure 4.2 Alignment of *Bsu*PolC with *Bsu*DnaE, *Gka*PolC, *Ec*DnaE and *Taq*DnaE Thumb domains. Alignment of the Thumb domains of *Bsu*PolC, *Bsu*DnaE, *Gka*PolC, *Ec*DnaE and *Taq*DnaE polymerases indicating the different approaches of DNA binding between *Bsu*PolC and *Bsu*DnaE. The red rectangle shows the residues predicted to form beta (β) strands (A995-G999 and R1038-H1043 in *Bsu*PolC, A1002-G1006 and R1045-H1050 in *Gka*PolC) and the teal rectangle the residues predicted to form alpha (α) helices (A438-V448 and Y453-P464 in *Ec*DnaE, A419-V429 and P434-P445 in *Bsu*DnaE, S500-V510 and H515-P526 in *Taq*DnaE). The alignment was created using Clustal Omega Multiple Sequence Alignment (Goujon et al., 2010; McWilliam et al., 2013; Sievers et al., 2011).

The above data indicate that PolC may not effectively bind to RNA- primed templates because of the structure of the Thumb domain and the conformation of the RNA-DNA hybrid. On the contrary, DnaE polymerase binds and extends RNA-primed templates, because the DNA binding channel is more loose and the A conformation of the substrate is not stereochemically hindered (**Figure 4.3**). Additionally, this observation may also provide evidence that PolC requires DnaE polymerase and/or other auxiliary proteins in order to be localised at the replication fork.

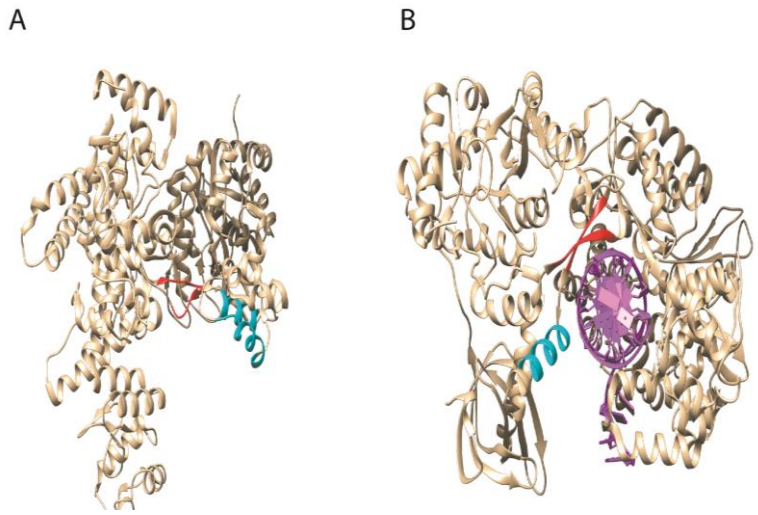


Figure 4.3 *Ec*DnaE and *Gka*PolC DNA binding. Crystal structures of *Escherichia coli* DnaE (PDB: 2HQA) and *Geobacillus kaustophilus* PolC (PDB: 3F2D) showing the β-strands (red) and α-helixes (teal) important for the DNA (purple) binding.

4.2 Impact of deoxyribonucleotides (dNTPs) on polymerase activity

In order to investigate how the deoxyribonucleotide (dNTP) concentration affects the PolC polymerase and exonuclease activities, we performed DNA primer extension assays using a small template, as described in **Section 2.2.6.4**. dNTP concentration titration assays for PolC wild type, $PolC_{pol-}$ (D966A/D968A) and $PolC_{exo-}$ (D425A/E427A) are shown in **Figure 4.4**.

Our data indicate that the concentration of dNTPs plays a crucial role in the switch between polymerase and exonuclease activities, consistent with current literature (Ganai et al., 2015). Efficient translesion synthesis (TLS) requires moderate increase in dNTP levels that transiently attenuate Polymerase III's exonuclease (proofreading) activity (Gon et al., 2011). As we are focusing on the elongation-extension activity of PolC we did not carry out further detailed titrations to establish the exact concentration of dNTPs in which the switch occurs in *Bacillus subtilis* PolC or the rate of spontaneous mutagenesis that increases proportionally with dNTP levels (Gon et al., 2011; L. N. Williams et al., 2015).

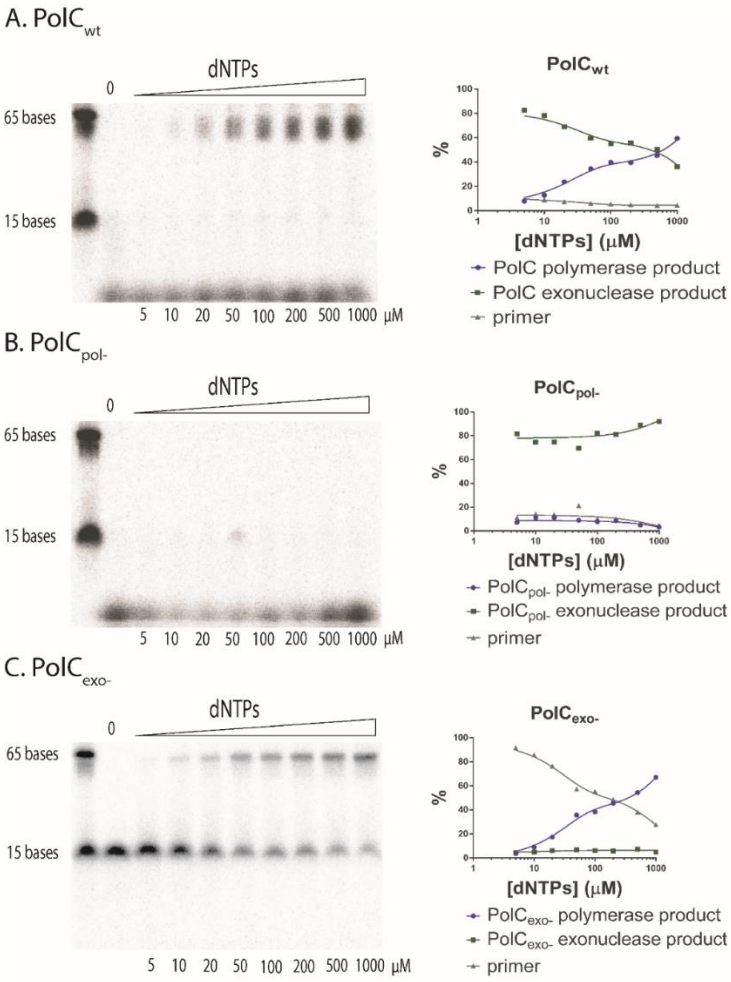


Figure 4.4 DNA primer extension assays (dNTP concentration titration). PolC wild type (**A**), PolC$_{pol-}$ (D966A/D968A) (**B**) and PolC$_{exo-}$ (D425A/E427A) (**C**) activity was detected performing dNTP titration assays in presence of 500 nM polymerase and 2 nM substrate. Samples were incubated at 37°C for 15 minutes, resolved through 15% sequencing gels, analysed using molecular imager and associated software (Bio-Rad) and the percentage of products was plotted using Graphpad – Prism 6.

4.3 Incorporation of ribonucleotides (rNTPs) during DNA replication

Bacillus subtilis in vivo incorporates ribonucleoside monophosphates (rNMPs) hence marking the nascent DNA strand in order to recruit the Mismatch Repair system (MMR) (Yao et al., 2013). Moreover, it is known that translesion synthesis (TLS) polymerases facilitate rNTP incorporation in order to overcome lesions, allowing cells to avoid the consequences of replication fork stalling and collapse (Donigan et al., 2015). More evidence of rNTP incorporation by DNA polymerases comes from a recently published crystal structure of the human DNA polymerase η with an incoming rNTP (Y. Su et al., 2016).

Thus, given that the intracellular pool of nucleoside triphosphates is dominated by rNTPs in 10-100 fold higher than dNTPs (Ferraro et al., 2010), we investigated the stringency of DnaE and PolC polymerases in rNTP incorporation. Protein titration primer extension assays were carried out using DNA and RNA primers with small template in the presence of only rNTPs (**Figure 4.5**), as described in **Section 2.2.6.4**.

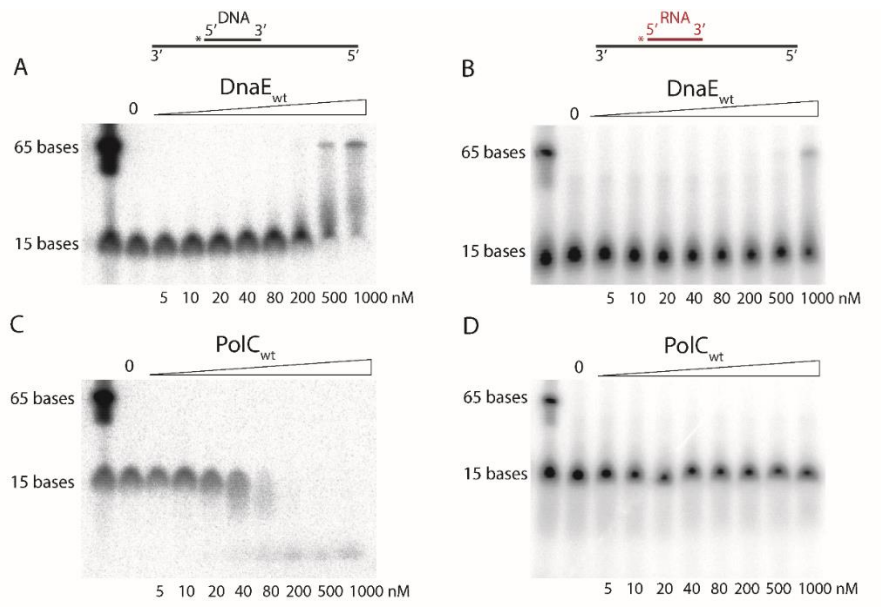


Figure 4.5 rNTPs incorporation. DNA (**A**, **C**) and RNA (**B**, **D**) primer extension assays using short radiolabelled nucleotide (15 bases) annealed onto longer oligonucleotide template (110 bases) for the detection of the polymerase activity in the presence of 200 μM rNTPs. The reaction samples were incubated at 37°C for 15 minutes, resolved by electrophoresis through 15% (v/v) ureagel PAG and data were analysed using molecular imager and associated software (Bio-Rad).

Under our experimental conditions only DnaE polymerase can efficiently extend either DNA or RNA primers using rNTPs (**Figure 4.5**). Consequently, we investigated further this difference between DnaE and PolC polymerases.

Previous studies revealed that polymerases distinguish between the ribo- and deoxyribo- sugar moieties using a "steric-gate", which is a "bulky" residue that is positioned in the active site. The hydroxyl group in the position two of the ribose would sterically clash with the "steric-gate" residue (DeLucia et al., 2006). These residues have been identified in *Geobacillus kaustophilus* PolC (*Gka*PolC) (PDB: 3F2D) as H1275 and Y1279 (Evans et al., 2008), in *Escherichia coli* DnaE (*Ec*DnaE)

(PDB: 2HQA, 2HNH) as H760 and Y764 (Lamers et al., 2006) and in *Thermus aquaticus* DnaE (*Taq*DnaE) (PDB: 2HPI, 2HPM) as H817 and Y821(Scott Bailey et al., 2006; Wing et al., 2008).

A Clustal Omega (Goujon et al., 2010; McWilliam et al., 2013; Sievers et al., 2011) multiple sequence alignment of *Bsu*PolC and *Bsu*DnaE with *Gka*PolC, *Ec*DnaE and *Taq*DnaE polymerases revealed that both *Bsu*PolC and *Bsu*DnaE contain the same "bulky" residues (H1268, Y1272 and H729, Y733 correspondingly) (**Figure 4.6**). Thus, it is apparent that the selectivity for dNTPs over rNTPs does not solely rely upon the highly conserved "steric gate" residues.

Additionally, it has been shown that mutagenesis in adjacent residues to the "steric gate" confers decreased selectivity over rNTPs (J. S. Williams et al., 2016). Indeed, we observed a significant difference between PolC and DnaE polymerases (A1267 to S728 correspondingly) that might explain the difference in rNTP incorporation (**Figure 4.6**). We speculate that S728 in DnaE polymerase might form a hydrogen bond with the 2'-OH group of the ribonucleotide, stabilising it in the active site, in contrast to the A1267 in PolC. However, this might be a difference in the protein sequence that has nothing to do with the sugar selectivity. In *Bacillus subtilis* DNA polymerase I it has been suggested that both the "steric gate" residues, as well as motions of the fingers domain play a crucial role in discrimination against ribonucleotides (Wanget al., 2012).

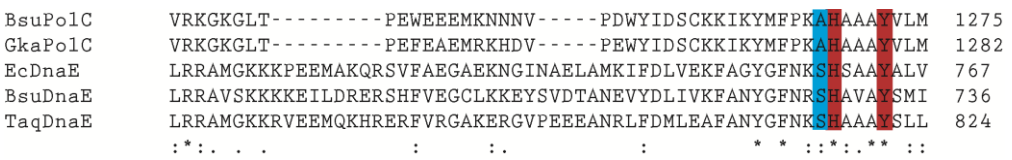


Figure 4.6 Alignment of *Bsu*PolC with *Bsu*DnaE, *Gka*PolC (PDB: 3F2D), *Ec*DnaE (PDB: 2HQA) and *Taq*DnaE (PDB: 2HPI) "steric gate". Identification of the "steric gate" amino acids in *Bsu*PolC and *Bsu*DnaE performing Clustal Omega sequence alignment. The "steric gate" residues correspond to H1268 and Y1272 in *Bsu*PolC and H729 and Y733 in *Bsu*DnaE. The alignment was created using Clustal Omega Multiple Sequence Alignment (Goujon et al., 2010; McWilliam et al., 2013; Sievers et al., 2011).

Although DnaE polymerase is able to incorporate rNTPs, the efficiency of incorporation is significantly lower than that of dNTPs (compare **Figure 4.5** with **Figure 3.17** and **Figure 3.25**). dNTP incorporation is considerably favoured over rNTP incorporation by DNA polymerases, with different selectivity (incorporation) coefficients ranging from 10^2 to 10^6 (Brown & Suo, 2011), as we also observed in our experiments.

Moreover, our data indicate that DnaE polymerase incorporates rNTPs at higher rate when using DNA primer compared to RNA primer (**Figure 4.5 A, B**). A possible explanation could be a combination of the ability of DnaE to recognise and bind to the substrate and its ability to incorporate rNTPs. DnaE is able to bind and extend RNA primed templates, as described in **Section 4.1**. However, the RNA-DNA hybrid may cause different conformational changes in the binding pocket than those caused by a DNA-DNA hybrid, generating a less stable DnaE-template complex.

Finally, a significant observation was that PolC cannot cleave the RNA primer (**Figure 4.5 D**). By comparison the exonuclease activity of PolC was able to digest the

primer producing a range of digested products as shown in **Figure 4.5 C**. The apparent inability of PolC to engage the RNA primer may be due to its inability to effectively accommodate the RNA primed template into its binding channel, as described in **Section 4.1**.

5 Functional Interaction Studies

This chapter describes preliminary interaction studies in order to investigate the formation of DnaG-DnaE and DnaE-PolC complexes. It should be noted that the investigated interactions are functional and not physical. Moreover, it presents an attempt to explore the cooperative actions of DnaE and PolC during DNA replication, aiming at the scope of the thesis that is to reconstruct *Bacillus subtilis* replisome *in vitro*.

5.1 DnaG-DnaE and DnaE-PolC Complexes

Electrophoretic Mobility Shift Assays (EMSAs) were carried out with the purified primase and polymerases, as described in **Section 2.2.6.6** in order to detect the presence of the relevant complexes in the absence of any other auxiliary proteins.

5.1.1 The DnaG-DnaE Complex

The range of oligonucleotide substrates used in EMSAs are shown in **Figure 2.3**. These include: **A.** radiolabelled RNA (15 nucleotides) annealed onto DNA (30 nucleotides), **B.** radiolabelled DNA (15 nucleotides) annealed onto DNA (30 nucleotides) and **D.** radiolabelled DNA (30 nucleotides). EMSA results are shown in **Figure 5.1**.

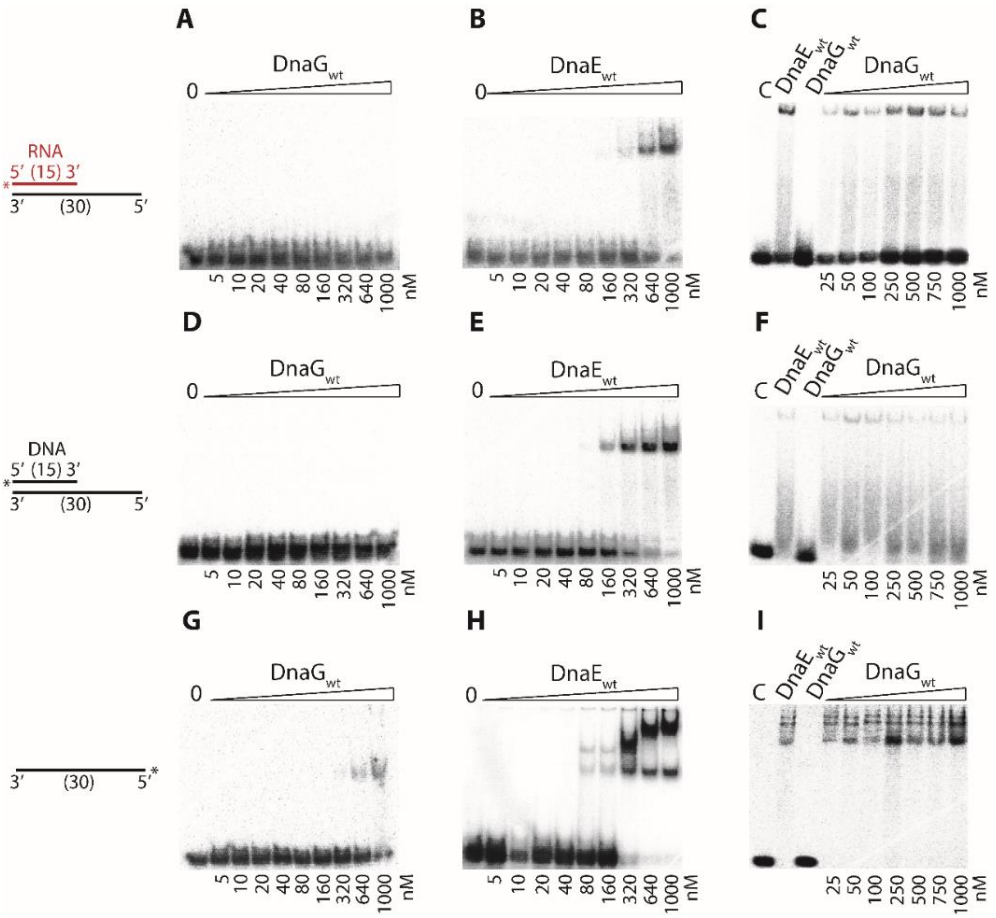


Figure 5.1 EMSAs DnaG, DnaE, DnaG-DnaG (5 mins). EMSAs showing binding affinity of DnaG (**A, D, G**) and DnaE (**B, E, H**) to different radiolabelled substrates (0.66 nM), as well as the effects of increasing concentrations of DnaG on complexes of DnaE (1 μM) with the substrates (**C, F, I**). The reaction mixture of buffer and substrate (0.66 nM) was pre-incubated at 37°C for five minutes before addition of the proteins at different concentrations, as indicated, and further incubation at 37°C for 15 minutes. For **C**, **F** and **I** assays, where both DnaE and DnaG were used, the second protein was added after the incubation of the reaction mixture with the first protein for five minutes, followed by further incubation at 37°C for additional five minutes. Samples were mixed with loading buffer and analysed through 5% (v/v) native polyacrylamide gels. Lanes labelled 0, $DnaE_{wt}$ and $DnaG_{wt}$ show control radiolabelled substrate on its own and in the presence of DnaE (1 μM) or DnaG (1 μM), respectively. Asterisks indicate the radiolabel position at the 5'-P end.

DnaE polymerase binds better and forms more stable complexes with all three substrates than primase DnaG (compare **Figure 5.1 A**-**B**, **D**-**E** and **G**-**H**). Although, it seems that DnaG recognises and binds only to the single-strand DNA oligonucleotide 5' – ACACACACACACACACACACACACCCCCTT – 3' (**Figure 5.1 G)**. The above result implies that helicase DnaC may play an important role in correct loading of primase DnaG on the template and subsequent *de novo* synthesis of RNA primers, as shown previously (Rannou et al., 2013).

By comparison, DnaE polymerase binds to all the substrates used. Interestingly, binding is marginally better in the presence of a DNA rather than an RNA primer (compare **Figure 5.1 B** with **E**). A potential explanation could be the fact that the B conformation of a DNA-DNA hybrid is more favourable for binding rather than the A conformation of an RNA-DNA hybrid, as suggested in **Section 4.1**. Additionally, in the presence of single-strand DNA, supershifted bands were observed (**Figure 5.1 H**), suggesting multiple DnaE molecules were bound onto the substrate. Indeed, all polymerases apart from their catalytic pocket also entail a C-terminal domain that confers single-strand DNA binding ability, as described in **Section 1.3**. Potentially, polymerase molecules responsible for the supershifted bands use the secondary DNA binding site in order to engage single-strand DNA.

We then investigated the DnaG-DnaE complex formation in the absence of any other proteins. Since only DnaE polymerase forms stable detectable nucleoprotein complexes, we examined the effects of primase DnaG on pre-formed DnaE-substrate complexes (**Figure 5.1 C, F, I**). Our data indicate that the primase DnaG does not form a stable complex with DnaE polymerase once the latter has

already engaged with the substrate. Hence, we speculate that once the DnaI-DnaC-DnaG-DnaE complex is formed and the RNA primer synthesised by DnaG primase has been transferred to DnaE polymerase *via* a direct protein-protein interaction (Rannou et al., 2013), DnaE polymerase is released from the primosomal complex.

5.1.2 The DnaE-PolC Complex

DNA binding of DnaE and PolC polymerases were assayed by EMSAs, using DNA substrates, shown in **Figure 2.3**: **A.** radiolabelled RNA (15 nucleotides) annealed onto DNA (30 nucleotides), **D.** radiolabelled DNA (30 nucleotides), **E.** radiolabelled RNA (15 nucleotides) annealed onto DNA (45nucleotides) and **F.** radiolabelled DNA (45 nucleotides). EMSA results are shown in **Figure 5.2**.

Our observations indicate that DnaE polymerase binds better to all four substrates than PolC. The longer 30 nucleotides 5'-overhang in RNA annealed to DNA (45 nucleotides) substrate compared to the 15 nucleotides 5'-overhang in RNA annealed to DNA (30 nucleotides) substrate results in better binding of multiple DnaE molecules per substrate (compare **Figure 5.2 A** with **D**), as indicated by an earlier supershift observed with the former substrate. Although, when comparing DNA binding to single-strand DNA substrates with different lenghts (30 and 45 nucleotides), the binding profile is similar (compare **Figure 5.2 G** with **J**). This observation indicates that the 15 nucleotide difference in length between the two substrates does not drastically affect binding of DnaE polymerase.

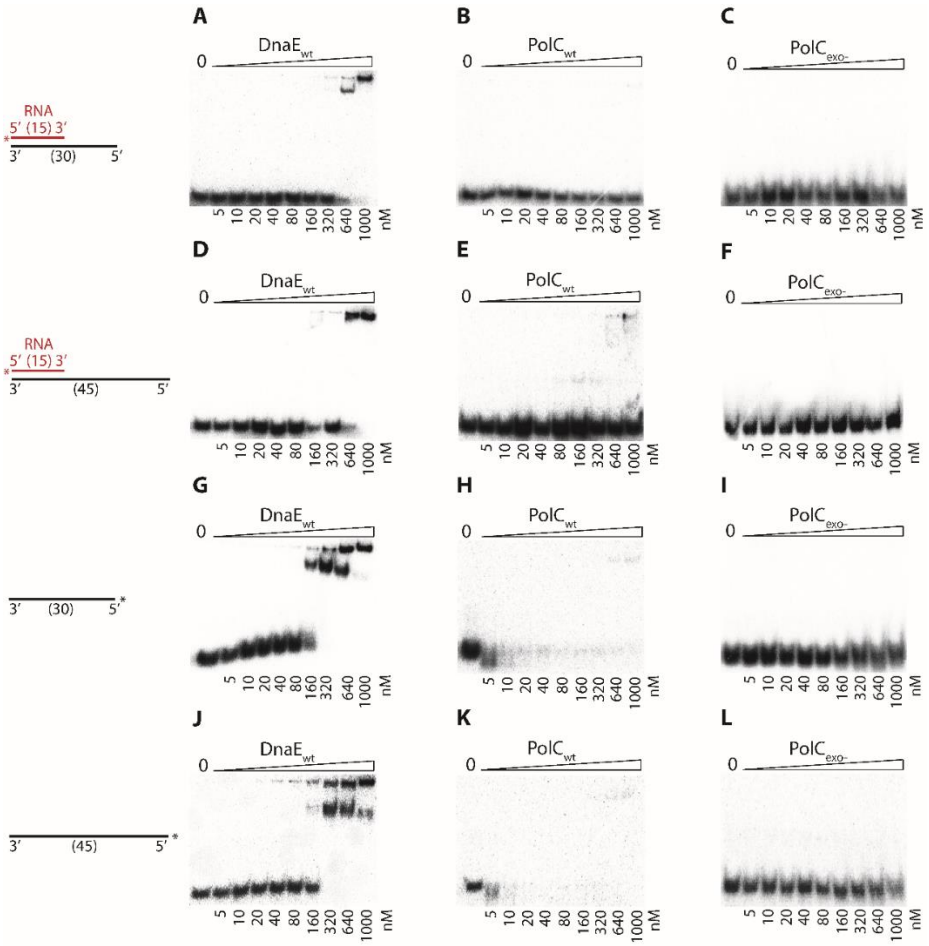


Figure 5.2 DnaE binds DNA with higher affinity than PolC (15 mins). EMSAs $DnaE_{wt}$, $PolC_{wt}$, $PolC_{exo-}$. EMSAs showing the binding affinity of DnaE (**A, D, G, J**), $PolC_{wt}$ (**B, E, H, K**) and $PolC_{exo-}$ (**C, F, I, L**) to different radiolabelled substrates. The reaction mixture of buffer and substrate (0.66 nM) was pre-incubated at 37°C for five minutes before the addition of the proteins at different concentrations, as indicated, and further incubation at 37°C for 15 minutes. Samples were mixed with loading buffer and analysed through 5% (v/v) native polyacrylamide gels. Lanes labelled 0 represent the control radiolabelled substrate on its own. Asterisks indicate the radiolabel position at the 5'-P end.

By comparison, PolC did not exhibit any detectable DNA binding, with RNA annealed onto DNA substrates (**Figure 5.2 B, E**). This observation indicates that PolC does not engage strongly with RNA-primed substates. Thus, it could be

hypothetised that PolC does not constitute part of the primosomal complex. However, PolC activity was detected in similar substrates, as described in **Section 3.4.1.4**, where polymerase and exonuclease products were observed. Consequently, the DNA specific 3'-5' exonuclease activity observed in **Figure 5.2 H, K**, verifies that PolC is active. We used PolC exonuclease deficient mutant ($PolC_{exo-}$) as a control to ensure that PolC does not exhibit any RNA exonuclease activity. We observed that the length and intensity of the bands remains the same, regardless of the protein concentration (**Figure 5.2 B, C, E, F**), confirming that PolC does not exhibit any RNA exonuclease activity. Additionally, $PolC_{exo-}$ was used to confirm the DNA specific exonuclease activity on single-strand DNA substrates by PolC (compare **Figure 5.2 H** with **I**, **K** with **L**).

We next examined the formation of DnaE-PolC complex using EMSAs with DnaE and $PolC_{exo-}$ (to avoid any exonuclease activity on the substrates) with the following constructs, as shown in **Figure 2.3**: **A.** radiolabelled RNA (15 nucleotides) annealed onto DNA (30 nucleotides) and **E.** radiolabelled RNA (15 nucleotides) annealed onto DNA (45nucleotides). EMSA results are presented in **Figure 5.3**.

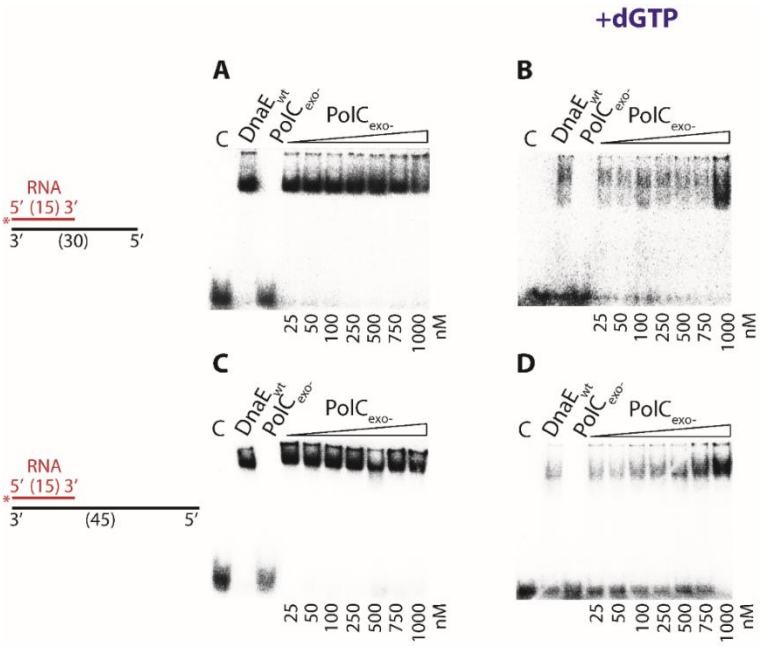


Figure 5.3 dNTPs affect the DnaE-PolC complex formation. EMSAs DnaE-PolC (+dGTP) (15 mins). EMSAs showing the effects of increasing concentrations of PolC on complexes of DnaE (1 μM) with RNA primed templates, in the absence (**A, C**) or presence (**B, D**) of dGTP (100 μM). The reaction mixture of buffer and substrate (0.66 nM) was pre-incubated at 37°C for five minutes before addition of DnaE and further incubation at 37°C for five minutes. PolC was added at different concentrations, as indicated, followed by further incubation at 37°C for 15 minutes. Samples were mixed with loading buffer and analysed through 5% (v/v) native polyacrylamide gels. Lanes labelled C, $DnaE_{wt}$ and $PolC_{exo-}$ show the control radiolabelled substrate on its own and in the presence of DnaE (1 μM) or $PolC_{exo-}$ (1 μM), respectively. Asterisks indicate the radiolabel position at the 5'-P end.

Our initial data indicated that there was no apparent DnaE-PolC complex (**Figure 5.3 A, C**). The binding profile of DnaE polymerase was unaltered irrespective of the concentration of PolC. However, in the presence of dGTP there was significant change in the observed band shifts (**Figure 5.3 B, D**). We hypothesised that DnaE polymerase misincorporates dGTPs along the template,

forming a more favourable conformation, creating a hybrid A-B DNA conformation (see **Section 4.1**). Thus the DnaE-template complex is more stable, providing a potential explanation for the observed change in band shifts. However, control assays (**Figure 5.3** lanes labelled $DnaE_{wt}$) reject our hypothesis, since in the presence of only DnaE polymerase, there was no observed change. Consequently, we hypothesised that DnaE polymerase misincorporates dGTPs along the template, generating a hybrid RNA-DNA primer annealed onto DNA. As described in **Section 4.1**, RNA-DNA hybrids adopt A conformation, whereas DNA-DNA duplexes B conformation. Thus, DnaE polymerase could potentially change the substrate conformation (from A to B) an event that might play a crucial role in the recruitment of PolC onto the substrate. Hence, the observed band shifts could also be a result of a DnaE-PolC-substrate ternary complex formation.

In order to investigate the possibility that PolC is selective over different DNA substrates, we performed EMSAs with PolC and $PolC_{exo-}$ using the following constructs, also shown in **Figure 2.3**: **G.** radiolabelled RNA (15 nucleotides), **H.** radiolabelled RNA (15 nucleotides) annealed onto DNA (30 nucleotides) creating a 3' overhang and **I.** radiolabelled DNA (30 nucleotides) annealed onto DNA (30 nucleotides) creating a 3' overhang. EMSA data are shown in **Figure 5.4**.

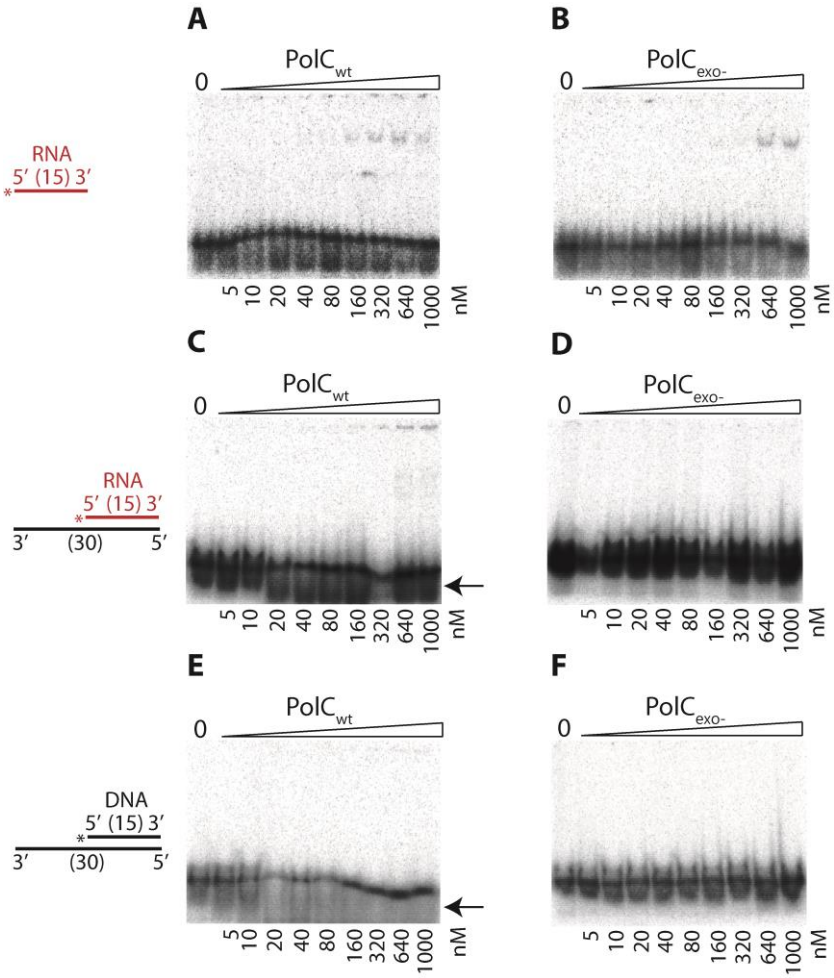


Figure 5.4 PolC does not bind to 3' overhang substrates. EMSAs PolC, PolC$_{exo-}$ (15 mins). EMSAs investigating binding of PolC$_{wt}$ (**A, C, E**) and PolC$_{exo-}$ (**B, D, F**) on different radiolabelled substrates. The reaction mixture of buffer and substrate (0.66 nM) was pre-incubated at 37°C for five minutes before addition of the proteins at different concentrations, as indicated, and further incubation at 37°C for 15 minutes. Samples were mixed with loading buffer and analysed through 5% (v/v) native polyacrylamide gels. Lanes labelled 0 show the control radiolabelled substrate on its own. The arrows indicate PolC exonuclease products. Asterisks indicate the radiolabel position at the 5'-P end.

EMSAs revealed that PolC weakly engages single-strand RNA, but does not exhibit RNA exonuclease activity, since the size and intensity of the radiolabelled substrate bands are unaffected (**Figure 5.4 A, B**). PolC also interacts with RNA- or

DNA-primed substrates with 3' overhangs, irrespective of the absence of shifted bands as assessed by evidence of exonuclease activity (**Figure 5.4 C-F**). With both RNA- and DNA-primed templates, there was clear evidence of exonuclease digestion (smaller fragments and reduction in radioactive intensity shown with arrows in **Figure 5.4 C and E**), indicating that PolC cleaves initially the non-radiolabelled template starting from its 3' overhang followed by the radiolabelled DNA primer (**Figure 5.4 E, F**). The radiolabelled RNA primer remains unaffected (**Figure 5.4 C, D**). The above observations indicate that PolC exhibits 3'-5' exonuclease activity which is apparent with single-strand or partially single-strand templates but not with fully annealed double-strand substrates.

Thus far, we did EMSAs using mainly RNA primed templates, in order to closely mimic the template handed-off to DnaE polymerase by primase DnaG. Additionally, during the 15 min incubation in our EMSAs there was clear evidence of the PolC exonuclease activity. Moreover, our data indicate that PolC may be recruited to a substrate comprised of DNA primer annealed to a longer DNA template (**Figure 5.3**).

Hence, we conducted EMSAs with DnaE, PolC and $PolC_{exo-}$ polymerases using the following constructs: **A.** radiolabelled RNA (15 nucleotides) annealed onto DNA (30 nucleotides), **B.** radiolabelled DNA (15 nucleotides) annealed onto DNA (30 nucleotides) and **D.** radiolabelled DNA (30 nucleotides), as shown in **Figure 2.3**. The derived data are shown in **Figure 5.5**.

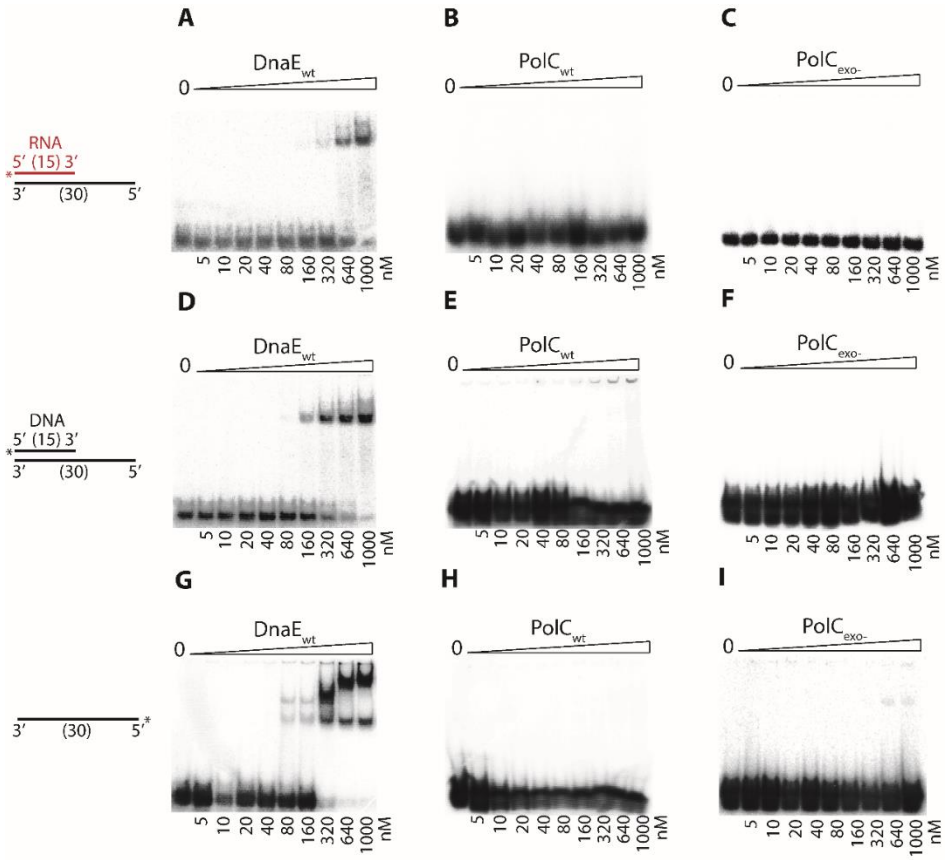


Figure 5.5 DnaE binds DNA with higher affinity than PolC (5 mins). EMSAs DnaE$_{wt}$, PolC$_{wt}$, PolC$_{exo-}$. EMSAs showing the binding of DnaE (**A, D, G**), PolC$_{wt}$ (**B, E, H**) and PolC$_{exo-}$ (**C, F, I**) on different radiolabelled substrates. The reaction mixture of buffer and substrate (0.66 nM) was pre-incubated at 37°C for five minutes before addition of the proteins at different concentrations, as indicated, and further incubation at 37°C for five minutes. Samples were mixed with loading buffer and analysed through 5% (v/v) native polyacrylamide gels. Lanes labelled 0 show the control radiolabelled substrate on its own. Asterisks indicate the radiolabel position at the 5'-P end.

DnaE polymerase binds to all the substrates used but slightly better to DNA primed rather than RNA primed templates (compare **Figure 5.5 A** with **D**). Multiple shifted bands were observed with single-strand DNA (**Figure 5.5 G**), indicating multiple DnaE molecules interacting with the substrate. These EMSA data are

similar to data shown in **Figure 5.2**, indicating that the incubation time of DnaE polymerase with the substrates does not affect its binding properties.

By comparison, PolC does not bind to RNA primed template (**Figure 5.5 B, C**). This observation was confirmed by our previous EMSAs, where the proteins were incubated with the substrates for 15 minutes (**Figure 5.2**). Thus, our data indicate that PolC is not localised at the replication fork as part of the primosomal complex (DnaI-DnaC-DnaG-DnaE) (in the absence of any auxiliary proteins).

Additionally, the PolC exonuclease activity observed before in EMSAs with 15 minutes incubation was weaker when the incubation time was reduced to 5 minutes (compare **Figure 5.2 H, K** with **Figure 5.5 E, H**). Similar data regarding the interactions of PolC with various substrates were obtained with $PolC_{exo-}$ (**Figure 5.5 C, F, I**).

Our previous EMSAs for the DnaE-PolC complex (**Figure 5.3 B, D**) suggested that the presence of dGTP may promote complex formation. In order to investigate whether the presence of dNTPs affect the DNA binding properties of PolC, we conducted EMSAs using the following constructs, as shown in **Figure 2.3**: **A.** radiolabelled RNA (15 nucleotides) annealed onto DNA (30 nucleotides), **B.** radiolabelled DNA (15 nucleotides) annealed onto DNA (30 nucleotides) and **D.** radiolabelled DNA (30 nucleotides). Data are shown in **Figure 5.6**.

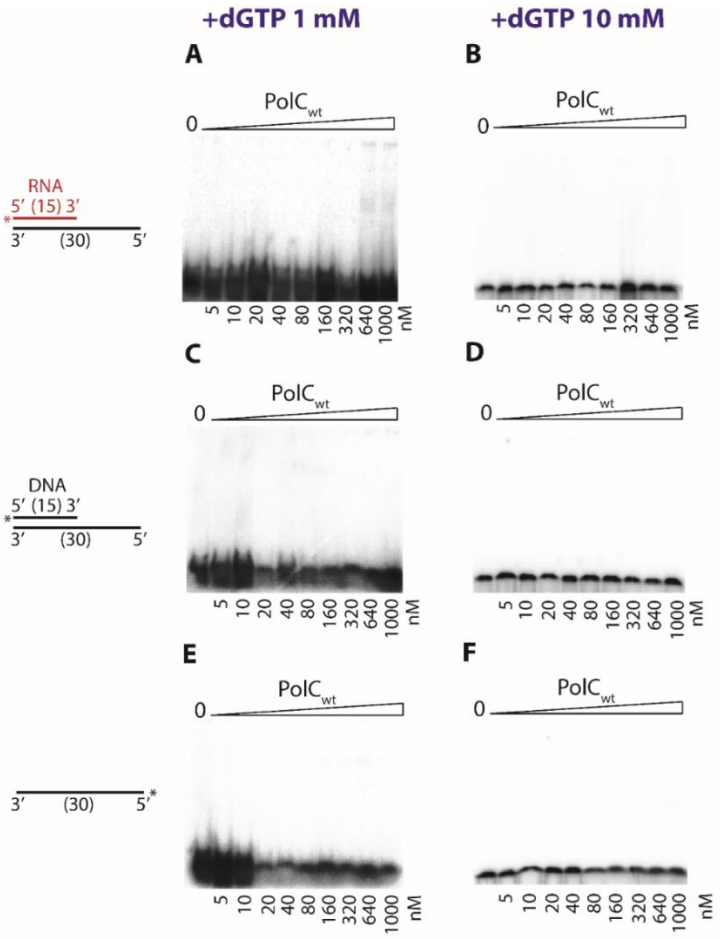


Figure 5.6 dNTPs do not affect PolC binding to DNA**.** EMSAs PolC in the presence of 1 mM and 10 mM dGTP. EMSAs showing binding of $PolC_{wt}$ to different radiolabelled substrates in the presence of 1 mM dGTP (**A, C, E**) or 10 mM dGTP (**B, D, F**). The reaction mixture of buffer and substrate (0.66 nM) was pre-incubated at 37°C for five minutes before addition of the proteins at different concentrations, as indicated, and further incubation at 37°C for five minutes. Samples were mixed with loading buffer and analysed through 5% (v/v) native polyacrylamide gels. Lanes labelled 0 show the control radiolabelled substrate on its own. Asterisks indicate the radiolabel position at the 5'-P end.

Our data indicate that binding of PolC to these substrates was unaffected by dGTP (**Figure 5.6 A-F**). However, PolC exonuclease activity was substantially lower at higher dGTP concentration (compare **Figure 5.6 C** with **D**, **E** with **F**). These data

are consistent with data obtained during our investigation of the impact of dNTPs on polymerase activity (see **Section 4.2**).

Lastly, since all the parameters that could affect the interactions between DnaE, PolC and the template were investigated (template preference, presence of dNTPs), we proceeded to try and detect the formation of a stable ternary complex by EMSAs. We examined the effects of PolC and $PolC_{exo-}$ on pre-formed DnaE-template complexes. EMSAs were performed with DnaE, PolC and $PolC_{exo-}$ polymerases using the following constructs, as shown in **Figure 2.3**: **A.** radiolabelled RNA (15 nucleotides) annealed onto DNA (30 nucleotides), **B.** radiolabelled DNA (15 nucleotides) fully annealed onto DNA (30 nucleotides) and **C.** radiolabelled DNA (15 nucleotides), where 14 nucleotides were annealed onto DNA (30 nucleotides), generating a mismatch (A:G). EMSA results are shown in **Figure 5.7**.

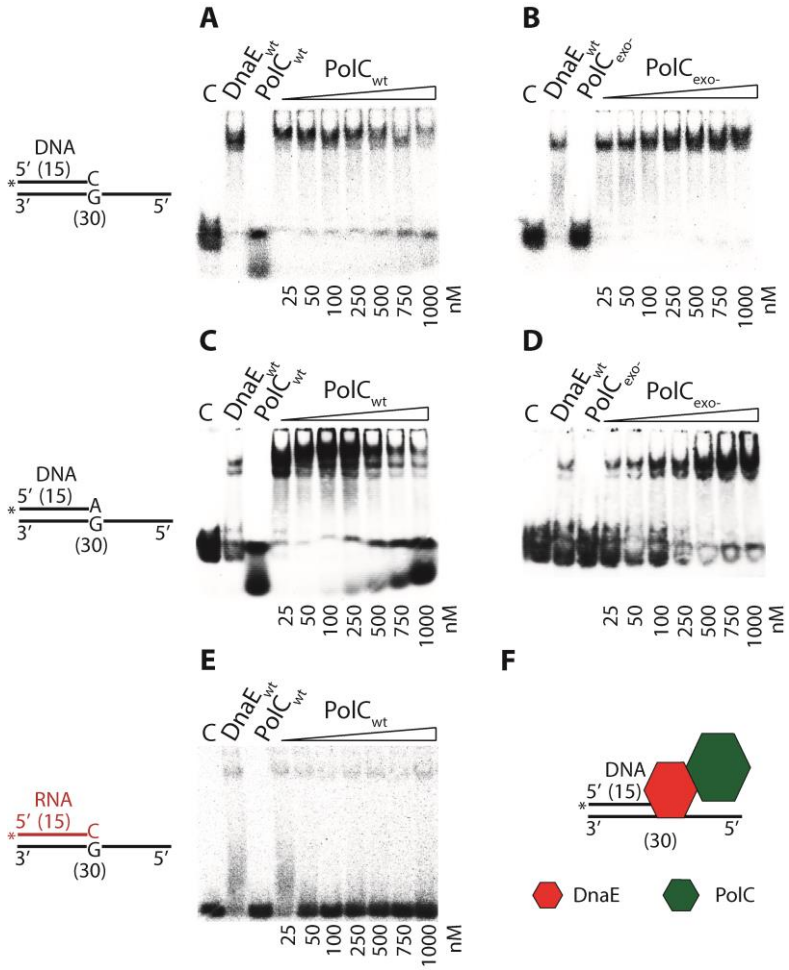


Figure 5.7 DNA-DnaE-PolC complex is template specific. EMSAs DnaE-PolC, DnaE-PolC$_{exo-}$ (5 mins). EMSAs showing the effects of increasing concentrations of PolC (**A, C, E**) or PolC$_{exo-}$ (**B, D**) on complexes of DnaE (1 μM) with the substrates. The reaction mixture of buffer and substrate (0.66 nM) was pre-incubated at 37°C for five minutes before addition of DnaE and further incubation at 37°C for five minutes. PolC or PolC$_{exo-}$ was added at different concentrations, as indicated, followed by further incubation at 37°C for five minutes. Samples were mixed with loading buffer and analysed through 5% (v/v) native polyacrylamide gels. Lanes labelled C, DnaE$_{wt}$, PolC$_{wt}$ and PolC$_{exo-}$ show the control radiolabelled substrate on its own and in the presence of DnaE (1 μM) or PolC$_{wt}$ (1 Mm) or PolC$_{exo-}$ (1 μM), respectively. Asterisks indicate the radiolabel position at the 5'-P end. **F**. Schematic diagram suggesting the DNA-DnaE-PolC ternary complex.

The DnaE-PolC complex is template specific, since stable DNA-DnaE-PolC complex was only observed with a DNA primer annealed to a DNA template (compare **Figure 5.7 A** and **C** with **E**). The stable ternary complex (DNA-DnaE-PolC) was apparent even at protein concentration DnaE:PolC ratio 4:1, but at higher PolC concentrations, the radiolabelled substrate was digested by the 3'-5' exonuclease activity of PolC (**Figure 5.7 A, C**). In the assays where $PolC_{exo-}$ was used, the ternary complex (DNA-DnaE-$PolC_{exo-}$) was observed, irrespective of the $PolC_{exo-}$ concentration, confirming previous data obtained with PolC (**Figure 5.7 B, D**). Additionally, no differences were observed between fully annealed primer and partially annealed mismatched primer, indicating that the complex is not only formed in the presence of a mismatch (i.e. during the need for PolC proof-reading activity) (compare **Figure 5.7 A** with **C, B** with **D**). The above data indicate that DnaE polymerase extends the RNA primer briefly, synthesising an RNA-DNA hybrid and then recruits PolC at the 3'-OH end directly *via* a physical protein-protein interaction. This is an important observation because if PolC were to directly engage the 3'-OH ends of RNA primers, it would potentially interfere with primer transfer from the primase DnaG to DnaE polymerase and hence impede progression of DNA replication.

5.2 Polymerase cooperation

We carried out DNA primer extension assays with small template, as described in **Section 2.2.6.4**, in order to investigate the cooperation between DnaE and PolC polymerases in the absence of any other proteins. Data are shown in **Figure 5.8** and analyses in **Figure 5.9**.

DnaE polymerase appears to extend more effectively a DNA primer than PolC polymerase (compare **Figure 5.8 A** with **B**, **Figure 5.9 A** with **B**). Moreover, it is evident that DnaE and PolC compete for the DNA primed template (**Figure 5.8 C**, **Figure 5.9 C**) and that DnaE polymerase binds to the template stronger than PolC polymerase inhibiting PolC polymerase and exonuclease activities (**Figure 5.8 D-F**, **Figure 5.9 D-F**). These observations are consistent with our data in **Section 5.1.2**.

Additionally, it seems that DnaE polymerase extends the DNA primer up to the end of the template, dissociates and then PolC binds the template (**Figure 5.8 G-H**, **Figure 5.9 G-H**). It is evident that PolC engages with the DnaE polymerase products, since in the reaction containing DnaE and $PolC_{pol-}$, the amount of the exonuclease products increases within time, whereas the amount of polymerase products decreases (**Figure 5.9 G**). Probably the length of the used template wasn't enough so as DnaE polymerase to dissociate physiologically and/or for hand-off between the two polymerases to occur.

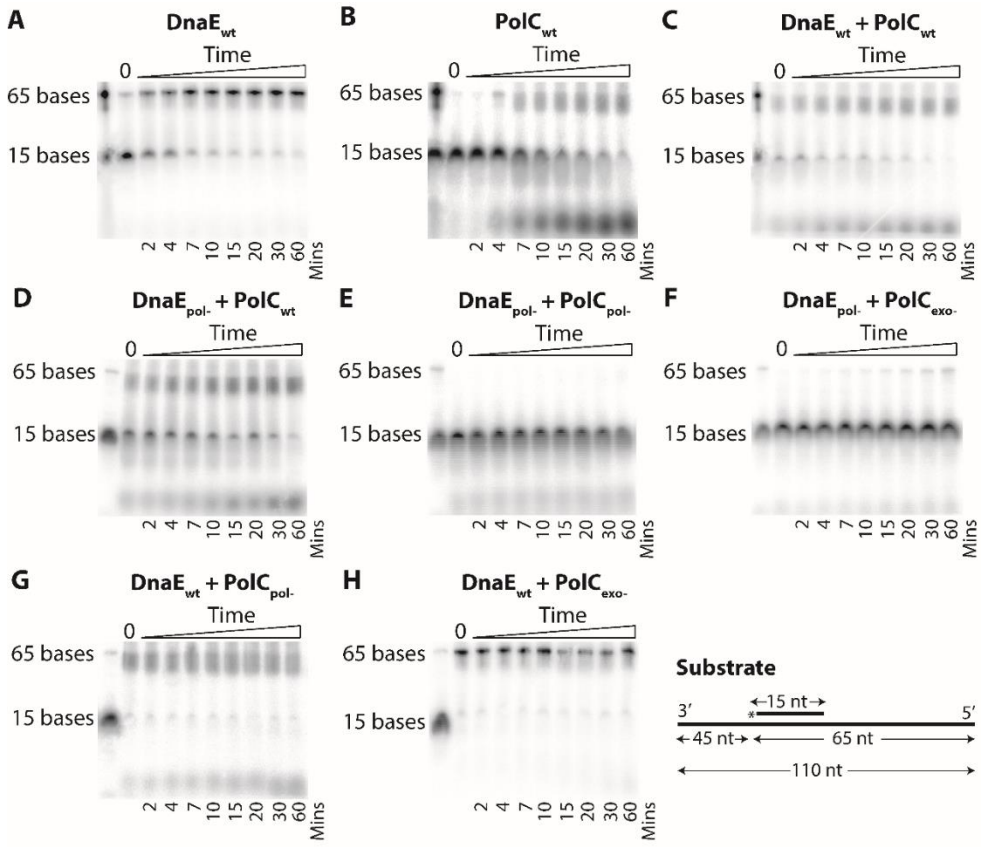


Figure 5.8 Primer hand-off between DnaE and PolC is unlikely to occur in early stages of primer extension. DNA Primer extension assays with small template (time course). The activities of DnaE and PolC polymerases as well as combinations of the wild type proteins and their mutants ($DnaE_{pol-}$, $PolC_{pol-}$ and $PolC_{exo-}$) were examined with time course assays at 37°C (2, 4, 7, 10, 15, 20, 30 and 60 minutes), in the presence of 200 μM dNTPs and 2 nM substrate, using equimolar concentrations of proteins (40 nM for **A-C** and 500 nM for **D-H**). Samples were mixed with loading buffer and resolved through 15% (v/v) ureagel denaturing PAG. A schematic diagram of the radiolabelled substrate used in these assays is shown in the lower right panel with the asterisk indicating the radiolabel position at the 5'-end. Assays were carried out in triplicates.

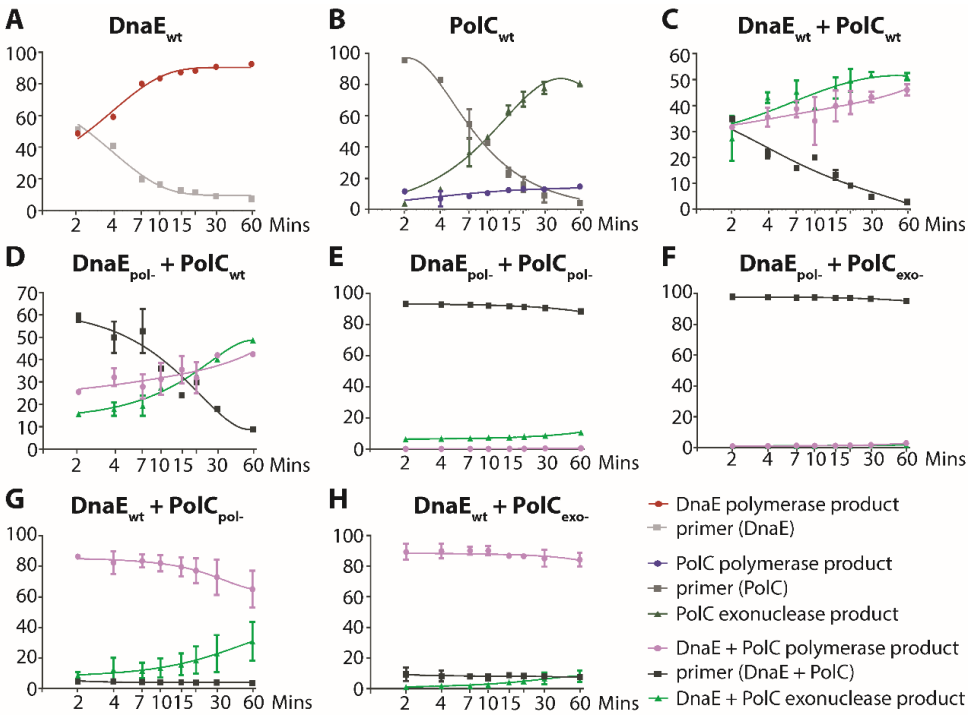


Figure 5.9 DnaE and PolC cooperate in DNA primer extension. Data analysis of the DNA primer extension assays using small template. Analyses of the assays shown in **Figure 5.8** were carried out using molecular imager and associated software (Bio-Rad) and the percentage of products formation was plotted against the incubation time at 37°C using GraphPad – Prism 6. Assays were carried out in triplicates and error bars show standard deviations.

However, it is evident that DnaE and PolC polymerases cooperate in DNA primer extension. This observation indicates that error prone polymerase DnaE may be essential in both leading and lagging strand DNA replication not only to transfer the primer to PolC, but also to potentially overcome replication fork arrest, as it has been suggested for translesion polymerases (Friedberg et al., 2001; Rattray & Strathern, 2003). Additionally, PolC exonuclease activity is higher than its own polymerase activity, when PolC acts alone. Albeit, our results indicate that

polymerase DnaE protects the newly synthesised strand from PolC exonuclease activity or that PolC activity is drastically affected by other accessory proteins.

6 Polymerase Processivity and Functional Cooperation

This chapter explores the processivities of the main replicative polymerases in *Bacillus subtilis* DnaE and PolC and how they are affected by the presence of the clamp DnaN and SSB. Additionally, it investigates the error-prone polymerase activity of DnaE and its modulation by PolC polymerase, clamp DnaN and SSB.

6.1 Collaborative functionality during DNA replication

Primer Extension Assays with single-strand M13mp18 template were carried out (described in **Section 2.2.6.5**) in order to investigate DNA synthesis by DnaE and PolC on long templates.

Initially, we wanted to ensure that DnaE polymerase was capable of binding and extending primers annealed onto single-strand M13mp18 DNA. We thus carried out simple primer extension assays with DnaE polymerase using DNA- and RNA- primed M13mp18 and the results are shown in **Figure 6.1**.

DnaE polymerase binds and extends both primers, synthesising more nascent DNA as the concentration of the polymerase increases (**Figure 6.1 A, B**). All subsequent assays were carried out at 80 nM DnaE, so that we can observe stimulatory or inhibitory effects in the presence of additional replication proteins.

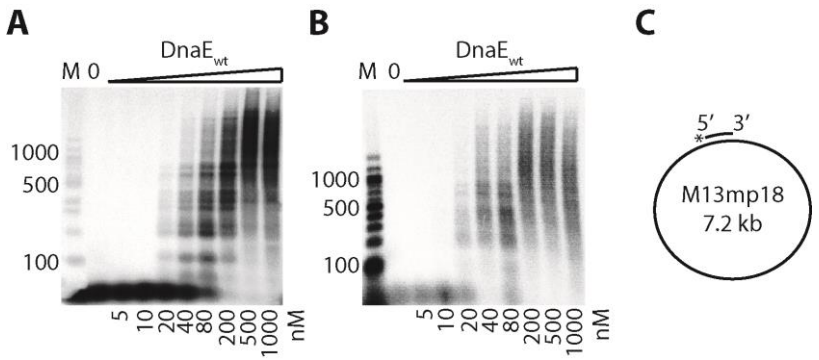


Figure 6.1 DnaE can synthesize long nascent DNA. DnaE primer extension assays on a long template. Primer extension assays at different DnaE concentrations (5, 10, 20, 40, 80, 200, 500 and 1000 nM), using long single-strand M13mp18 template (2 nM) primed with DNA (**A**) and RNA (**B**) primers. Reaction mixtures were incubated at 37°C for 32 minutes and terminated by addition of loading dye and incubation at 95°C for five minutes. Reaction products were analysed through 1.5 % (w/v) alkaline agarose gels. Lanes labelled M and 0 show molecular weight markers and a control reaction without any polymerases, respectively. C. A schematic diagram of the radiolabelled oligonucleotide (20 bases) annealed onto single-strand M13mp18 plasmid (7.2 kb). The asterisk indicates the radiolabel position at the 5'-end.

6.1.1 DnaE and PolC activity on naked DNA template

Primer extension assays were used in order to investigate the activities of DnaE and/or PolC polymerases, in the absence or presence of the clamp DnaN, using long single-strand M13mp18 as template (**Figure 6.2**).

In the absence of the clamp DnaN, DnaE polymerase synthesises DNA fragments up to ~300-500 nucleotides, whereas in the presence of clamp DnaN the amount of the nascent DNA fragments was increased but the length remained at ~300-500 nucleotides (**Figure 6.2 A**). By comparison, PolC did not exhibit any

substantial polymerase activity in the absence of clamp DnaN. In the presence of clamp DnaN, PolC synthesised nascent DNA fragments of ~100-200 nucleotides (**Figure 6.2 B**). When both polymerases were used, in the absence of the clamp DnaN very long nascent DNA fragments were synthesised (**Figure 6.2 C**). On the contrary, in the presence of clamp DnaN, the sizes of nascent DNA fragments were ~300-500 nucleotides, similar to the size of nascent DNA fragments obtained with DnaE polymerase alone (compare **Figure 6.2 A** with **Figure 6.2 C**).

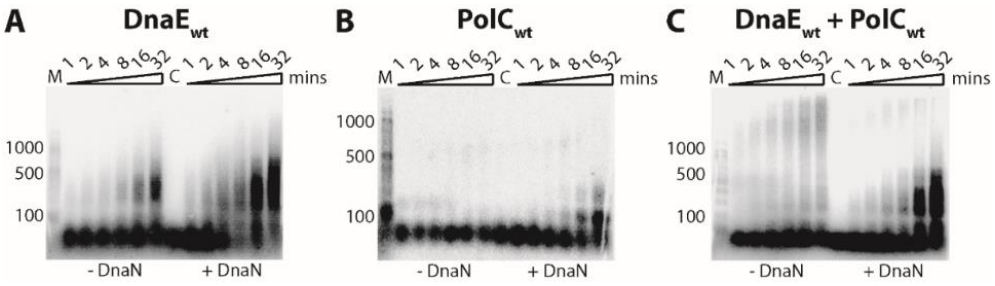


Figure 6.2 DnaE, PolC and DnaE+PolC activities on naked M13mp18 template. Time course (indicated by rectangular triangles) reactions using DNA primer (**B**) and RNA primer (**A, C**) annealed on naked single-strand M13mp18 template (2 nM) with DnaE (80 nM), PolC (80 nM) and equimolar concentrations of a mixture of both polymerases (80 nM), in the absence or presence of the clamp DnaN (80 nM) [clamp-loader: DnaX (120 nM), HolB (40 nM), YqeN (40 nM)]. Reactions were incubated at 37°C for the indicated time and terminated by addition of loading dye and incubation at 95°C for five minutes. Nascent DNA synthesis was assessed with 1.5 % (w/v) alkaline agarose gels. Lanes labelled M and C show molecular weight markers and a control reaction without polymerases, respectively.

The above data indicate that both DnaE and PolC activities are enhanced in the presence of clamp DnaN, whose interaction has been previously confirmed by yeast-two-hybrid (Rannou et al., 2013). In addition, the distributive activities of

DnaE and PolC are capable of synthesising very long nascent DNA fragments in the absence of the clamp, presumably with DnaE polymerase extending the RNA primers initially and then handing off to PolC for further extension. However, in the presence of the clamp, nascent DNA synthesis is limited to ~300-500 nucleotides, probably due to PolC inability to efficiently displace DnaE polymerase when clamped onto the RNA-primed template by the clamp DnaN.

We then carried out primer extension assays with twice as much protein concentration in order to investigate the activities of DnaE or PolC, in the absence or presence of the clamp DnaN, using M13mp18 template (**Figure 6.3 A, B**). Additionally, we investigated the cooperation of the polymerases in the presence of the clamp, using DNA-primed M13mp18 (**Figure 6.3 C**).

Under our experimental conditions, DnaE polymerase was able to fully extend the RNA primer, replicating very long stretches of the M13mp18 template, either in the absence or presence of clamp DnaN (**Figure 6.3 A**). Similar results were obtained with PolC using DNA primed M13mp18 (**Figure 6.3 B**). In both cases, it was apparent that the presence of the clamp DnaN, stimulates their activities. Thus, the observed weaker activity for PolC could be explained due to PolC inability to target the 3'-OH ends of the primers, which is consistent with our EMSA data presented in **Section 5.1.2**.

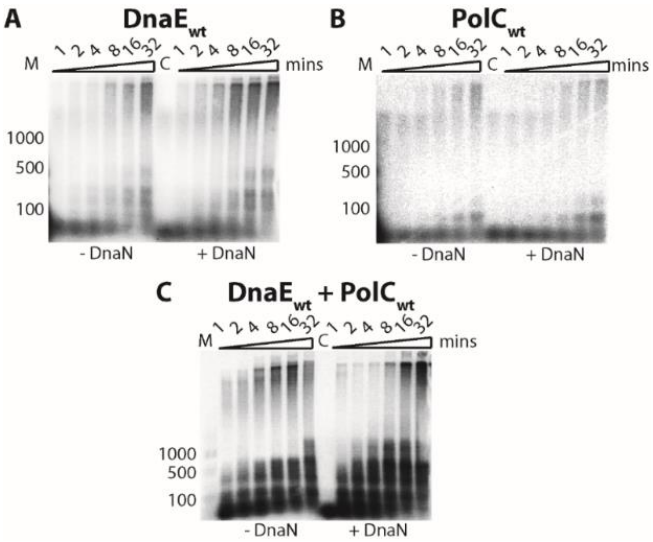


Figure 6.3 Control primer extension assays on naked M13mp18 template. Time course (indicated by rectangular triangles) primer extension assays were carried out with DNA primer (**B, C**) and RNA primer (**A**) annealed onto single-strand M13mp18 DNA (2 nM) with (**A**) DnaE (160 nM), (**B**) PolC (160 nM) and (**C**) a mixture of equimolar concentrations of DnaE and PolC (80 nM), in the absence or presence of the clamp DnaN (80 nM) [clamp-loader: DnaX (120 nM), HolB (40 nM), YqeN (40 nM)]. Reactions were incubated at 37°C for the indicated time and terminated by addition of loading dye and incubation at 95°C for five minutes. Nascent DNA synthesis was assessed with electrophoresis through 1.5 % (w/v) alkaline agarose gels. Lanes labelled M and C show molecular weight markers and control reactions without polymerases, respectively.

Interestingly, with both polymerases in equimolar concentrations (80 nM) using naked DNA primed M13mp18 template, we observed slightly different pattern than when using RNA primed template, especially in the presence of clamp DnaN (compare **Figure 6.3 C** with **Figure 6.2 C**). In both RNA and DNA primed templates, in the absence of clamp DnaN, the distributive activities of DnaE and PolC replicate collaboratively very long stretches of the template. Although, in the case of the DNA primed template, the amount of the nascent DNA fragments was

significantly higher than that with the RNA primed template. Noteworthy, in the presence of the clamp DnaN the size of nascent DNA fragments was not limited to ~300-500 nucleotides, observed when using RNA primed M13mp18 template, but instead the entire template was replicated. This observation indicates that PolC cannot efficiently displace polymerase DnaE when the latter is clamped onto RNA primers, by the clamp DnaN. After DnaE polymerase extends RNA primers, it recruits PolC and collaboratively the two polymerases replicate the template. This notion correlates with our EMSA data for the DnaE-PolC-template ternary complex formation, where the presence of DNA primed template is essential (**Section 5.1.2**).

6.1.2 DnaE and PolC activity on SSB-coated DNA template

In vivo, single-strand DNA is covered by SSBs, either binding in the SSB(35) or in SSB(70) binding modes (Green et al., 2014). These modes represent the affinity of SSB over the template as well as the distance between the SSB molecules, described in Green et al., 2014. SSB is homotetrameric with NTDs binding DNA and intrinsically disordered CTDs, that interact with a vast variety of proteins during DNA replication and DNA repair (Antony et al., 2013; Costes et al., 2010). Thus, we carried out primer extension assays using single-strand M13mp18 template (2 nM), coated with 1 μM SSB (x500 molar excess of SSB tetramer over the template) (**Figure 6.4 A**-**C**).

Polymerase DnaE is substantially stimulated, regardless of the presence of the clamp, replicating long stretches of the M13mp18 template (compare **Figure 6.2 A**

with **Figure 6.4 A**). By comparison, PolC is stimulated only in the presence of clamp DnaN, generating DNA fragments with maximum length just over 1000 nucleotides, but the bulk of nascent DNA fragments at ~200-500 nucleotides (compare **Figure 6.2 B** with **Figure 6.4 B**). In the absence of the clamp, PolC does not exhibit any polymerase activity, similar to the case with naked template. Moreover, the distributive polymerase activities of both enzymes together cooperate efficiently and replicate long stretches of the SSB-coated template, irrespective of the presence of clamp DnaN (**Figure 6.4 C**). Interestingly, the size of the bulk of nascent DNA fragments is approximately the Okazaki fragment size (~1000 nucleotides), suggesting that PolC attenuates the SSB-mediated stimulation of DnaE (compare **Figure 6.4 A** with **Figure 6.4 C**). Our data above indicate the significance of PolC during DNA lagging strand synthesis to limit the size of nascent DNA to Okazaki fragment size. This notion is corroborated by our observations with naked templates, where PolC is unable to efficiently collaborate with DnaN-clamped DnaE polymerase (**Figure 6.2 C**).

The strong stimulation of DnaE and PolC activities on SSB-coated templates may be a direct result of a functional interaction between the intrinsically disordered CTD of SSB and the polymerases or an indirect result of SSB binding onto the DNA template ahead of the polymerases, removing hairpins that could impede polymerase progression (Green et al., 2014). In order to distinguish between these two possibilities, we carried out similar primer extension assays using single-strand M13mp18 template (2 nM), coated with 1 μM SSBΔ107-172 (x500 molar excess of SSB tetramer over the template). This SSB protein is a truncated version of native

SSB retaining its ability to bind single-strand DNA but lacking the intrinsically disordered CTD, which has been predicted to interact with various effector proteins (Toseland & Webb, 2010) (**Figure 6.4 D – F**).

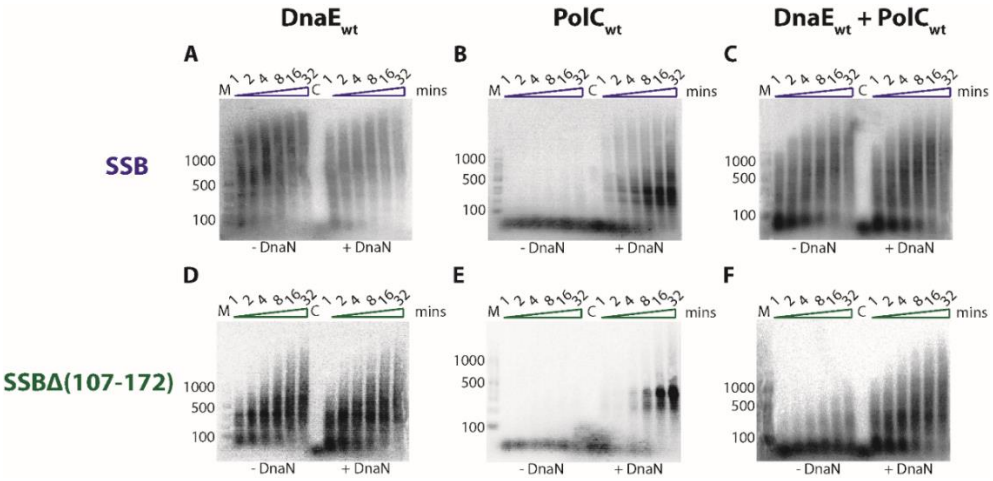


Figure 6.4 DnaE, PolC and DnaE+PolC primer extension assays on SSB and SSBΔ107-172-coated M13mp18 template. Time course assays were carried out with DNA -(**B, E**) and RNA- primed (**A, C, D, F**) SSB- (blue labelled) or SSBΔ107-172-coated (green labelled) single-strand M13mp18 (2 nM) templates, with DnaE (80 nM), PolC (80 nM) and equimolar mixtures of DnaE and PolC (80 nM), in the absence or presence of the clamp DnaN (80 nM) [clamp-loader: DnaX (120 nM), HolB (40 nM), YqeN (40 nM)]. Reactions were incubated at 37°C for the indicated time and terminated by addition of loading dye and incubation at 95°C for five minutes. Nascent DNA was analysed with electrophoresis through 1.5 % (w/v) alkaline agarose gels. Lanes labelled M and C show molecular weight markers and a control reaction without polymerases, respectively.

The activities of both polymerases are stimulated but to a lesser extent compared to data obtained using native SSB (compare **Figure 6.4 A** with **D** and **Figure 6.4 B** with **E**). The bulk of nascent DNA synthesised by DnaE polymerase

was <1000 nucleotides, but longer than DNA synthesised with naked templates (compare **Figure 6.2 A** with **Figure 6.4 D**). In the presence of native SSB, nascent DNA was much longer than 1000 nucleotides (compare **Figure 6.4 A** with **D**). Similarly, the bulk of nascent DNA fragments synthesised by PolC was ~300-500 nucleotides, longer than that synthesised with naked M13mp18 templates (~100-200 nucleotides) (compare **Figure 6.2 B** with **Figure 6.4 E**), but shorter than that synthesised with full length SSB-coated templates (compare **Figure 6.4 B** with **E**). The above data indicate that the CTD of SSB functionally interacts with both DnaE and PolC polymerases, recruiting them to the 3'-OH ends of primers and/or stimulating their activities.

Attenuation of the SSB-mediated stimulation of DnaE polymerase was more apparent in the absence of the clamp DnaN (compare **Figure 6.4 A** with **C** and **F**), suggesting that the interaction of the CTD of SSB with DnaE polymerase is essential to direct DnaE to the 3'-OH end of an RNA primer. However, in the presence of the clamp, no attenuation was observed, suggesting that the CTD of SSB functionally interacts and recruits PolC at the 3'-OH end of nascent DNA fragments synthesised by polymerase DnaE.

To summarise, SSBs affect polymerase processivity both indirectly, by binding ahead of the polymerases and removing any hairpins, and directly by functionally interacting *via* their intrinsically disordered CTDs recruiting the polymerases at the 3'-OH ends of primers. The presence of clamp DnaN and SSB favours recruitment of DnaE polymerase and not of PolC at the 3'-OH ends.

6.1.3 DnaE dominant activity and displacement from the 3′-OH end of primers

Our data above indicate that PolC cannot efficiently displace DnaE polymerase, when clamped to the 3'-OH ends of primers by clamp DnaN (**Section 6.1.1**). In order to provide further evidence, we carried out DNA primer extension assays using single-strand M13mp18 template and a mixture of $DnaE_{pol-}$ with PolC (**Figure 6.5 A, D, G**). Since $DnaE_{pol-}$ is polymerase dead, we hypothesised that only if PolC can displace $DnaE_{pol-}$, nascent DNA will be synthesised.

Under our experimental conditions, with SSB-coated templates (either with native or Δ107-172), there was no nascent DNA synthesis, regardless of the absence or presence of the clamp (**Figure 6.5 D**, **G**). This observation confirms that, in the presence of the clamp and SSB, DnaE polymerase binds first ahead of PolC to the 3'-OH ends and PolC is unable to displace it. Interestingly, on naked DNA primed template, PolC exhibited better activity than in the absence of DnaE (~100-500 nucleotides compared to ~100-200 nucleotides) (compare **Figure 6.2 B** with **Figure 6.5 A**), suggesting that when the two proteins interact DnaE polymerase functionally stimulates PolC.

Furthermore, our data thus far indicate that DnaE activity dominates over PolC, since it binds better and forms more stable complexes with primed templates, it is preferentially loaded at the 3'-OH ends in the presence of the clamp DnaN and SSB and exhibits higher activity. In order to corroborate this notion, we carried out

RNA primer extension assays using M13mp18 template and a mixture of DnaE with either $PolC_{pol-}$ or $PolC_{exo-}$ deficient mutants (**Figure 6.5 B, C, E, F, H, I**).

The size of nascent DNA fragments synthesised by the distributive activities of $DnaE_{pol-}$ and PolC was significantly shorter than the size of nascent DNA fragments synthesised by DnaE and $PolC_{pol-}$, irrespective of the absence or the presence of the clamp DnaN (compare **Figure 6.5 A** with **B**). Additionally, comparing nascent DNA synthesised by the distributive activities of DnaE and PolC with nascent DNA synthesised by DnaE and $PolC_{pol-}$, in the absence or presence of clamp DnaN, SSB and/or SSBΔ107-172, it was evident that these were similar (compare **Figure 6.4 C** with **Figure 6.5 E** and **Figure 6.4 F** with **Figure 6.5 H**). These data indicate that when the two polymerases are working together, the bulk of nascent DNA synthesis is carried out by DnaE polymerase.

However, comparing nascent DNA when using the combination of DnaE and $PolC_{exo-}$ polymerases with nascent DNA synthesised by the distributive activities of DnaE and PolC, in the absence or presence of clamp DnaN in SSB or SSBΔ107-172 coated templates, it is evident that in the former case it is significantly lower (compare **Figure 6.4 C** with **Figure 6.5 F** and **Figure 6.4 F** with **Figure 6.5 I**). A similar observation can be made comparing nascent DNA synthesised by DnaE and $PolC_{exo-}$ polymerases with nascent DNA synthesised by DnaE and $PolC_{pol-}$ polymerases (compare **Figure 6.5 C** with **B**). The above data stipulate the importance of the exonuclease (proof-reading) activity of PolC in DnaE polymerase progression, since in its absence, DnaE is more prone to errors, which slow down its progression thus reducing the size synthesised DNA fragments.

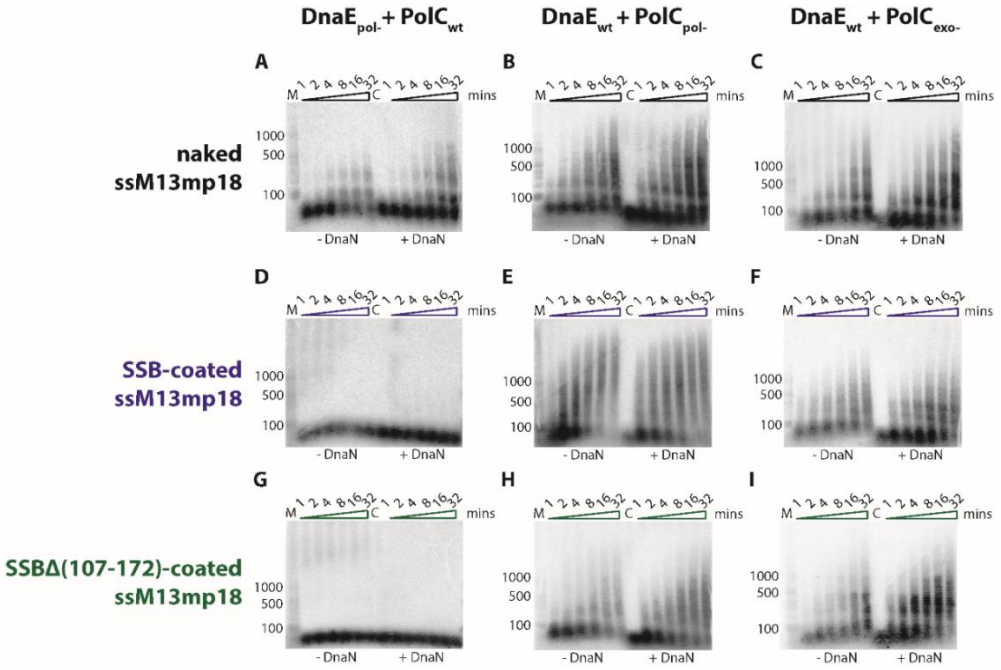


Figure 6.5 DnaN and SSB stimulate polymerase activity. DnaE dominant activity and displacement from the 3'-OH ends. Time course primer extension assays were carried out using DNA primer (**A**, **D**, **G**) and RNA primer (**B**, **C**, **E**, **F**, **H**, **I**) annealed onto naked (black labelled), SSB-coated (blue labelled) or SSBΔ107-172-coated (green labelled) single-strand M13mp18 template (2 nM) with combinations of native (DnaE, PolC) (80 nM) and mutant ($DnaE_{pol-}$, $PolC_{pol-}$ or $PolC_{exo-}$)(80 nM) polymerases, in the absence or presence of DnaN (80 nM) [clamp-loader: DnaX (120 nM), HolB (40 nM), YqeN (40 nM)]. Reactions were incubated at 37°C for the indicated time and terminated by addition of loading dye and incubation at 95°C for five minutes. Primer extension products were analysed through 1.5 % (w/v) alkaline agarose gels. Lanes labelled M and C show molecular weight markers and a control reaction without polymerases, respectively.

In **Section 4.1** we investigated the ability of DnaE and PolC polymerases to extend RNA primers, using small template, in the absence of any other proteins. Thus, we decided to carry out RNA primer extension assays using naked, SSB-coated and SSBΔ107-172-coated single-strand M13mp18 template with a combination of

equimolar concentrations of $DnaE_{pol-}$ and PolC, in order to ensure that PolC cannot efficiently extend RNA (**Figure 6.6**). Additionally, we wanted to confirm that $DnaE_{pol-}$ polymerase is also unable to extend RNA primers, in the presence of the clamp DnaN in SSB-coated templates. Our data verified the fact that PolC and $DnaE_{pol-}$ polymerases do not exhibit RNA primer extension activities, even in the presence of DnaE or PolC polymerases, clamp DnaN and SSB, respectively.

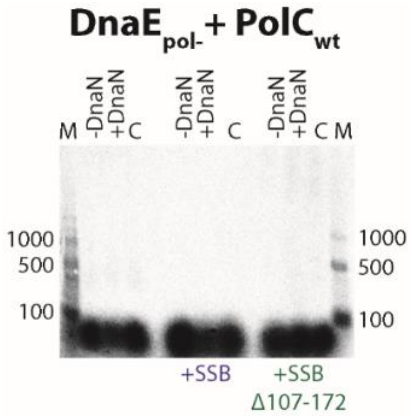


Figure 6.6 Control primer extension assays with $DnaE_{pol-}$ and PolC in RNA primed template. Final-point RNA primer extension assays were carried out using naked, SSB-coated or SSBΔ107-172-coated single-strand M13mp18 template (2 nM) with $DnaE_{pol-}$ (80 nM) and PolC (80nM) in the absence or presence of DnaN (80 nM) [clamp-loader: DnaX (120 nM), HolB (40 nM), YqeN (40 nM)]. Reactions were incubated at 37°C for 32 minutes and terminated by addition of loading dye and incubation at 95°C for five minutes. Primer extension products were analysed through 1.5 % (w/v) alkaline agarose gel. Lanes labelled M and C show molecular weight markers and control reactions without polymerases, respectively.

6.2 PolC trans-proofreading activity on DnaE

In **Section 5.1.2** it was postulated that DNA-DnaE-PolC ternary complex formation is template specific. However, this investigation was conducted solely in the presence of DnaE and PolC polymerases. Thus, we wanted to explore how clamp DnaN and/or SSBs affect complex formation. Consequently, we carried out exonuclease activity assays (see **Section 2.2.6.7**) using DNA primer annealed onto naked, SSB or SSBΔ107-172- coated single-strand M13mp18 template, in the presence or absence of clamp DnaN (clamp-loader: DnaX, HolB, YqeN), using DnaE, PolC, $PolC_{pol-}$, $PolC_{exo-}$ and combinations of DnaE with either the native PolC or one of the deficient PolC proteins (**Figure 6.7**).

In reactions containing DnaE alone and $PolC_{exo-}$, either alone or in combination with DnaE, there was no primer digestion, irrespective of the absence or presence of clamp DnaN and/or SSB/SSBΔ107-172, as expected (**Figure 6.7** lanes **2-7**, **20-25**, **38-43**). By comparison, in reactions containing PolC alone, $PolC_{pol-}$ alone, DnaE with PolC and DnaE with $PolC_{pol-}$, regardless of the absence or presence of clamp DnaN and/or SSB/SSBΔ107-172, the primer was digested, also as expected (**Figure 6.7** lanes **8-19**, **26-37**). However, the degree of degradation differed with reaction combinations. It is apparent that the presence of SSB restrains the exonuclease activity of PolC, with the CTD of SSB playing crucial role, irrespective of the absence or presence of clamp DnaN (compare **Figure 6.7** lanes **8** with **9** and **10**, **11** with **12** and **13**, **14** with **15** and **16**, **17** with **18** and **19**, **26** with **27** and **28**, **29** with **30** and **31**, **32** with **33** and **34**, **35** with **36** and **37**). Additionally, $PolC_{pol-}$ digests

the primer more efficiently than PolC, probably because in $PolC_{pol-}$ the primer finds itself more often in the exonuclease active site in the absence of a functional polymerase active site (compare **Figure 6.7** lanes **8**-**13** with **14**-**19**). Moreover, on naked template, DnaE polymerase recruits PolC, which then digests the primer more effectively than in the absence of DnaE (compare **Figure 6.7** lanes **8** with **26**). Although, that wasn't the case in the absence or presence of clamp DnaN on SSB or SSBΔ107-172 coated template, where digestion was clearly less (compare **Figure 6.7** lanes **9** with **27**, **10** with **28**, **11** with **29**, **12** with **30**, **13** with **31**). Finally, when comparing the activities of $PolC_{pol-}$ in the absence or presence of DnaE polymerase, the patterns were similar to those obtained with PolC in terms of decreased degradation in the presence of DnaE (compare **Figure 6.7** lanes **14** with **32**, **15** with **33**, **16** with **34**, **17** with **35**, **18** with **36**, **19** with **37**).

Our data from exonuclease activity assays confirm that polymerase DnaE binds strongly to primers and then recruits PolC, forming a ternary DNA-DnaE-PolC complex. Thus, PolC can effectively proof-read *in trans* the nascent DNA synthesised by DnaE polymerase.

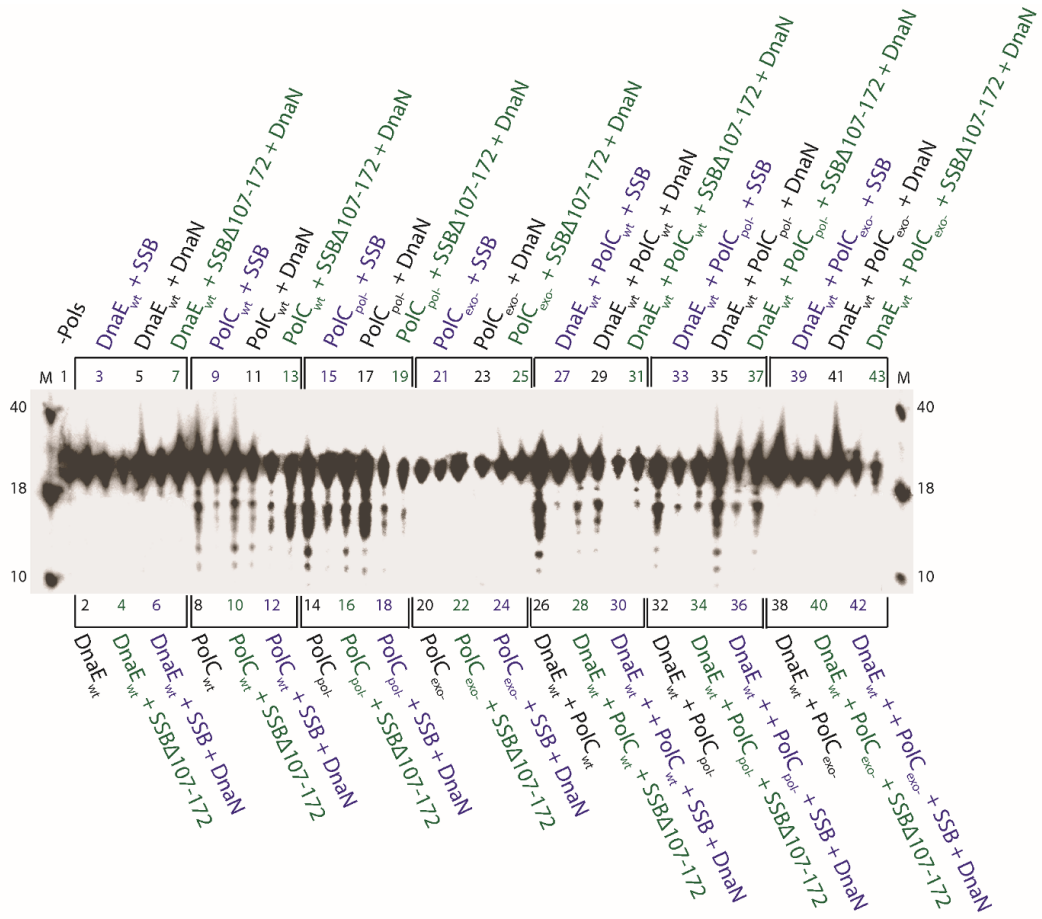


Figure 6.7 Evidence for physical recruitment of PolC by DnaE at the 3'-OH ends of nascent DNA Exonuclease Assays.. PolC exonuclease assays were carried out with DnaE (80 nM), PolC (80 nM), $PolC_{pol-}$ (80 nM) and $PolC_{exo-}$ (80 nM) and equimolar combinations of DnaE and either native PolC or one of the PolC deficient mutants, in the presence or absence of the processivity clamp DnaN (80 nM) [clamp-loader: DnaX (120 nM), HolB (40 nM), YqeN (40 nM)], using DNA primed naked (black labelled), SSB-coated (blue labelled) or SSBΔ107-172-coated (green labelled) single-strand M13mp18 template (2 nM). The reaction mixture containing everything but the polymerases was pre-incubated at 37°C for five minutes, DnaE was added followed by further incubation at 37°C for five minutes and then PolC (wt/pol-/exo-) was added and incubated at 37°C for 15 minutes, prior to termination with boiling at 95°C for five minutes. Samples were mixed with loading buffer and resolved through 15% (v/v) ureagel denaturing PAG. Lanes labelled M show molecular markers (40, 18 and 10 bases) and the lane labelled -Pols represents the control radiolabelled SSB-coated substrate with DnaN.

Thus far, we have investigated the recruitment of PolC by DnaE polymerase at the 3'-OH ends of primers in the absence of dNTPs, where DnaE is stalled. DnaE polymerase can effectively bypass T and C positions along the template, in the absence of dATP and dGTP correspondingly. The error-prone synthesis by DnaE is modulated by the presence of the replicative helicase DnaC and the primase DnaG, by increasing allosterically the stringency of the catalytic site (Rannou et al., 2013). Hence, the next step was to explore the effects of PolC polymerase, clamp DnaN and SSB in the error-prone DNA synthesis by DnaE polymerase. However, the error-prone DnaE polymerase activity was previously investigated using short DNA primed DNA templates. Thus, we explored the error-prone synthesis using RNA primed single-strand M13mp18 template.

Initially, we investigated the activity of DnaE polymerase in the absence of dATP and dGTP and to determine the appropriate concentration of DnaE, so as to visualise the error-prone synthesis. We carried out RNA primer extension assays using naked single-strand M13mp18 template (**Figure 6.8**).

Our data show that in the absence of dGTP, DnaE polymerase is more processive than in the absence of dATP, synthesising nascent DNA fragments up to 500 nucleotides, with the bulk nascent DNA ~100-300 nucleotides long (**Figure 6.8** compare lane -dATP with -dGTP). It was also apparent that DnaE error-prone synthesis was concentration dependent (**Figure 6.8** compare lane -dGTP 120 nM with 1000 nM). Although, the difference between nascent DNA when using 360 nM and 1000 nM of DnaE was negligible (~100-500 nucleotides compared to ~100-600 nucleotides).

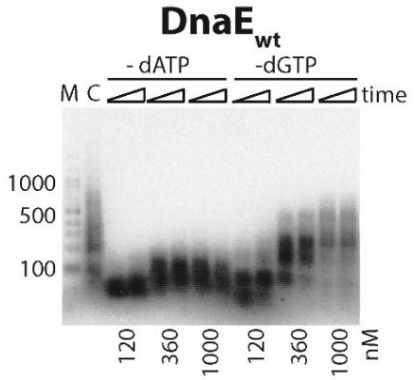


Figure 6.8 DnaE error-prone polymerase activity. DnaE activity assays carried out at 37°C omitting dATP or dGTP using radiolabelled RNA primer annealed onto single-strand M13mp18 template (2 nM). Time course assays were carried out at 30 and 60 minutes (indicated by the rectangular triangles), with three different DnaE concentrations (120, 360 and 1000 nM). Reactions were terminated by addition of loading dye and incubation at 95°C for five minutes. Primer extension products were analysed through 1.5 % (w/v) alkaline agarose gel. Lanes labelled M and C show molecular weight markers and a control reaction containing 40 nM DnaE with all dNTPs incubated at 37°C for 30 minutes, respectively.

We next investigated the effects of PolC, clamp DnaN and SSB on DnaE polymerase fidelity, with RNA primer extension assays in the absence of dGTP, using 360 nM of DnaE and adjusting the concentrations of the rest proteins, so as to keep the concentration ratios between all proteins the same as with primer extension assays in the presence of all dNTPs (**Figure 6.9**).

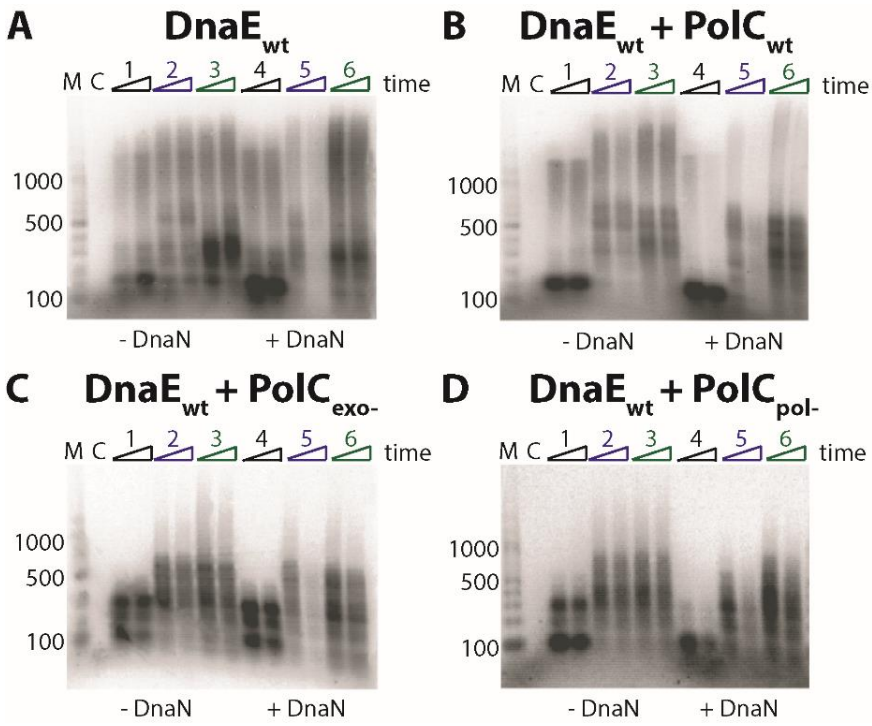


Figure 6.9 The effect of PolC on DnaE error-prone polymerase activity. Primer extension assays were carried out omitting dGTP with (**A**) DnaE (360 nM), equimolar concentrations (360 nM) of (**B**) DnaE and PolC, (**C**) DnaE and $PolC_{exo-}$, as well as (**D**) DnaE and $PolC_{pol-}$, in the presence or absence of DnaN (360 nM) [clamp-loader: DnaX (540 nm), HolB (180 nM), YqeN (180 nM)], using RNA primed naked (black labelled), SSB-coated (blue labelled) or SSBΔ107-172-coated (green labelled) single-strand M13mp18 template (2 nM). Time course reactions were carried out at 30 and 60 minutes (indicated by the rectangular triangles) and terminated by addition of loading dye and incubation at 95°C for five minutes. Primer extension products were analysed through 1.5 % (w/v) alkaline agarose gels. Lanes labelled M and C show molecular weight markers and a control reaction without polymerases, respectively.

We observed that DnaE polymerase can effectively mis-incorporate dNTPs at C residues along the naked or SSB/SSBΔ107-172 coated template, synthesising nascent DNA fragments up to ~1200-1500 nucleotides long, irrespective of the absence or presence of clamp DnaN (**Figure 6.9 A**). In the absence of clamp DnaN,

on naked M13mp18, the size of bulk nascent DNA was ~200 nucleotides., On SSB-coated M13mp18 template the size of nascent DNA was evenly distributed up to the maximum size, whereas on SSBΔ107-172 coated template, nascent DNA fragments was ~200-400 nucleotides long (**Figure 6.9 A** lanes **1**-**3**). In the presence of clamp DnaN, on naked template, the size of nascent DNA was also ~200 but there was more of it with more DNA fragments longer than 1000 compared to the absence of clamp DnaN (compare **Figure 6.9 A** lane **1** with **4**). On SSB-coated M13mp18, in the presence of clamp DnaN, the distribution of nascent DNA fragments was even, similar to that in the absence of clamp DnaN (compare **Figure 6.9 A** lane **2** with **5**). On SSBΔ107-172 coated template, in the presence of clamp DnaN, the bulk of nascent DNA fragments was ~200-400 as well as >1000 nucleotides (**Figure 6.9 A** lane **6**). The above data indicate that error-prone synthesis is substantially stimulated in the presence of SSB and to a lesser extend in the presence of clamp DnaN. Moreover, it is evident that the C-terminal domain of SSB, in the presence of clamp DnaN, restrains the error-prone DnaE-mediated DNA synthesis.

In the presence of PolC polymerase and in the absence of the clamp DnaN, a slight reduction in the maximum size of nascent DNA was observed. This was more apparent in the presence of clamp DnaN (compare **Figure 6.9** lanes **A 1-3** with **B 1-3, A 4-6** with **B 4-6**). In the DnaE+PolC reactions, with naked M13mp18 template, in the absence of clamp DnaN, the bulk of nascent DNA was ~200 nucleotides with some longer fragments up to ~1200 nucleotides, whereas in the presence of clamp DnaN, the size of nascent DNA was limited to ~100-200 nucleotides (**Figure 6.9 B** lane **1** with **4**). Comparing the size of nascent DNA in the absence and presence of

clamp DnaN, on SSB/SSBΔ107-172 coated templates, it is apparent that the presence of the clamp significantly reduces error-prone synthesis in reactions with DnaE and PolC (compare **Figure 6.9 B** lanes **2-3** with **5-6**). However, on SSB or SSBΔ107-172 coated templates, irrespective of the absence or presence of clamp DnaN, error-prone synthesis is stimulated (compare **Figure 6.9 B** lane **1** with **2** and **3**, lane **4** with **5** and **6**). These data indicate that DnaE error-prone synthesis is reduced in the presence of PolC polymerase and clamp DnaN, whereas SSB enhances error-prone synthesis, but the enhancement is limited in the presence of PolC.

Interestingly, inactivating either the exonuclease-proofreading or the polymerase activities of PolC had a drastic effect on error-prone synthesis by DnaE polymerase. In DnaE+PolC$_{exo-}$ reactions, irrespective of the absence or presence of clamp DnaN, nascent DNA is up to ~700 nucleotides (**Figure 6.9 C**). Similar length of nascent DNA was obtained due to the distributive activities of DnaE and PolC$_{pol-}$ (**Figure 6.9 D**). However, comparing DnaE and PolC$_{exo-}$ (~100-400 nucleotides) with DnaE and PolC$_{pol-}$ (~100 nucleotides), when using naked template in the presence of clamp DnaN, the exonuclease activity of PolC seems to be important for the DnaE activity (compare **Figure 6.9 C** lane **4** with **D** lane 4). Moreover, in both cases (combination with PolC$_{exo-}$ or PolC$_{pol-}$), regardless of the absence or presence of clamp DnaN, SSB stimulates error-prone synthesis (compare **Figure 6.9 C** lanes **1** with **2** and **3**, **4** with **5** and **6**, **D** lanes **1** with **2** and **3**, **4** with **5** and **6**). Although, nascent DNA was considerably shorter than that synthesised with DnaE alone or with combination of DnaE and PolC (compare **Figure 6.9 A** and **B** with **C** and **D**).

To summarise, DnaE error-prone synthesis is substantially stimulated in the presence of SSB. The CTD of SSB in the presence of clamp DnaN somewhat restrains this stimulation. PolC reduces error-prone synthesis of clamped (by DnaN) DnaE and minimises the SSB stimulation. Moreover, it is evident that both the polymerase and the exonuclease activities of PolC are important for DnaE activity. The exonuclease domain provides proof-reading *in trans*. Finally, in all cases, synthesis of long nascent DNA in the presence of PolC, provides evidence for the recruitment of PolC. Our data indicate that PolC is not an integral part of the primosome. We hypothesise that the replicative helicase DnaC and the primase DnaG modulate the stringency of DnaE polymerase initially but when PolC polymerase is recruited it provides proof-reading activity for DnaE *in trans*.

7 Conclusory Remarks and Revised Model

7.1 Concluding Remarks

In this study we reconstructed *Bacillus subtilis* replisome *in vitro* and we investigated the activities of DnaE and PolC polymerases. Our data indicate that DnaE effectively extends RNA and DNA primers whereas PolC extends only DNA-primed templates. These data correlate with the published literature (Sanders et al., 2010). Interestingly, only DnaE can incorporate rNTPs during the replication process. Although, it has been previously published that translesion synthesis polymerases facilitate rNTP incorporation so as to overcome lesions (Donigan et al., 2015), this is the first time that rNTP incorporation has been shown for *Bacillus subtilis*. Moreover, Y. Su et al have recently published a crystal structure of human DNA polymerase with an incoming rNTP (Y. Su et al., 2016). Thus, we hypothesize that DnaE plays more important role than only extending the RNA primers only by a few nucleotides.

Addiotionally, it has been shown that the dNTP concentration affects the switch between the polymerase and exonuclease activities of PolC, data that are consistent with the current literature (Ganai et al., 2015). PolC engages single-strand RNA without exhibiting RNA exonuclease activity. However, PolC does not engage with RNA-primed templates. These observations have not been mentioned before in the literature.

We also investigated the DNA binding properties of DnaG, DnaE and PolC This hadn't been covered by the literature thus far. Our data indicate that DnaE forms more stable complexes with the substrates used than DnaG and PolC. The binding of DnaE to the template was stronger in the presence od DNA than RNA primer. Our findings also include that DnaG does not form a complex with DnaE, once the latter is already loaded onto the substrate, which correlates with the literature that suggests the sequential order of the primosomal complex formation (Rannou et al., 2013). Finally, we have shown that the DNA-DnaE-PolC ternary complex is template specific, something that is the first time suggested.

We then explored the processivity of DnaE and PolC polymerases in the presence of clamp DnaN and SSBs. Our data indicate that DnaE activity is predominantly stimulated by SSBs and to a lesser extent by the clamp DnaN, whereas PolC activity is stimulated by the presence of SSBs, clamp DnaN and DnaE. PolC attenuates the SSB-mediated stimulation of DnaE, restricting the size of the nascent DNA to Okazaki fragment size. SSBs interact and recruit both polymerases at the primer sites through their CTD and remove hairpins that could impede the polymerase progression (Green et al., 2014). Lastly, we have shown that when DnaE and PolC polymerases are working together, the bulk of the nascent DNA synthesis is accomplished by DnaE. PolC provides proof-reading activity *in trans*, where SSB CTD plays important role in restraining PolC exonuclease activity. While SSB stimulates the error-prone synthesis by DnaE, in the presence of PolC and DnaN the error-prone synthesis is reduced.

7.2 Research Outputs

- DnaE and PolC polymerases can effectively extend DNA primers (**Sections 3.3.1.3, 3.3.2.4** and **3.4.1.4**)
- Only DnaE polymerase can extend RNA primers (**Section 4.1**)
- PolC engages single-strand RNA but does not exhibit RNA exonuclease activity (**Sections 4.1**, **4.3** and **5.1.2**)
- The dNTP concentration plays crucial role in the switch between the polymerase and exonuclease activity sites in PolC (**Section 4.2**) and does not affect DNA binding of PolC (**Section 5.1.2**)
- Only DnaE polymerase (not PolC) can extend DNA or RNA primers using rNTPs, although with a lower rate than that of dNTPs (**Section 4.3**)
- DnaE polymerase binds better to DNA and forms more stable complexes than DnaG primase (**Section 5.1.1**) and PolC polymerase (**Section 5.1.2**)
- Helicase DnaC is essential for recruitment and loading of primase DnaG onto the DNA template (**Section 5.1.1**)
- Primase DnaG does not form a stable complex with DnaE polymerase once the latter is loaded on the DNA substrate (**Section 5.1.1**)
- PolC polymerase does not engage with RNA primed templates and is thus excluded from the primosomal complex (**Section 5.1.2**)
- DnaE binding to the template is better in the presence of DNA than RNA primer (**Section 5.1.2**)

- DNA-DnaE-PolC ternary complex is template specific (DNA primed template) and formed both with mismatch and match 3'-OH ends (**Sections 5.1.2** and **6.1.1**)
- DnaE and PolC polymerases cooperate effectively to replicate long stretches of DNA (**Sections 5.2, 6.1.1** and **6.1.2**)
- DnaE activity is mainly stimulated by SSBs (**Section 6.1.2**) and to a lesser extent by clamp DnaN (**Section 6.1.1**)
- PolC activity is stimulated by clamp DnaN (**Section 6.1.1**), SSBs (**Section 6.1.2**) and DnaE polymerase (**Section 6.1.3**)
- PolC attenuates the SSB-mediated stimulation of DnaE polymerase, limiting the size of nascent DNA to Okazaki fragment size (**Section 6.1.2**)
- SSB modulates the polymerase activity by interacting and recruiting the polymerases at the primers through its CTD and by removing hairpins ahead of the polymerase to aid its progression (**Section 6.1.2**)
- In the presence of clamp DnaN and SSB, DnaE polymerase binds first ahead of PolC to primers and PolC polymerase is unable to displace it (**Sections 5.2, 6.1.1** and **6.1.3**)
- When DnaE and PolC polymerases are working together, the bulk of nascent DNA synthesis is accomplished by DnaE (**Section 6.1.3**) with PolC providing proof-reading *in trans* (**Section 6.2**)
- SSB restrains the PolC exonuclease activity, with the SSB CTD playing an important role (**Section 6.2**)

- DnaE polymerase misincorporates dNTPs along templates and SSB stimulates error-prone synthesis (**Section 6.2**)
- Error-prone synthesis is reduced in the presence of PolC polymerase and clamp DnaN while SSB-mediated stimulation is minimised (**Section 6.2**)
- PolC polymerase and exonuclease activities are important for DnaE processivity (**Sections 6.1.3** and **6.2**)

7.3 *Bacillus subtilis* DNA replication fork Revised Model

The current model for *Bacillus subtilis* DNA replication suggests that DnaE polymerase is essential but only a minor polymerase, with PolC acting as major processive replicative polymerase in both leading and the lagging strands (**Section 1.4**). Our combined data indicate that DnaE is a multi-functional polymerase with major roles in lagging strand DNA replication and DNA repair.

The replicative helicase DnaC unwinds the DNA and recruits the primase DnaG that synthesises *de novo* short RNA primers. DnaE polymerase is recruited at the 3'-OH ends of RNA primers aided by the SSB CTD and a physical interaction with DnaG to synthesise the bulk of nascent DNA. DnaE recruits PolC polymerase *via* a direct protein-protein interaction, inferred by DNA binding and exonuclease assays, in order to provide proof-reading *in trans* during lagging strand synthesis. The fidelity of DnaE is further improved by its interactions with helicase DnaC and primase DnaG that modulate allosterically the catalytic site and increase its stringency. We speculate that when PolC is recruited, the DnaE/PolC complex is released from the primosomal complex to continue lagging strand synthesis and the vital proof-reading activity is provided *in trans* by the PolC exonuclease domain, with SSB and clamp DnaN playing additional contributing roles. The proposed revised model for the *Bacillus subtilis* replisome is illustrated in **Figure 7.1**.

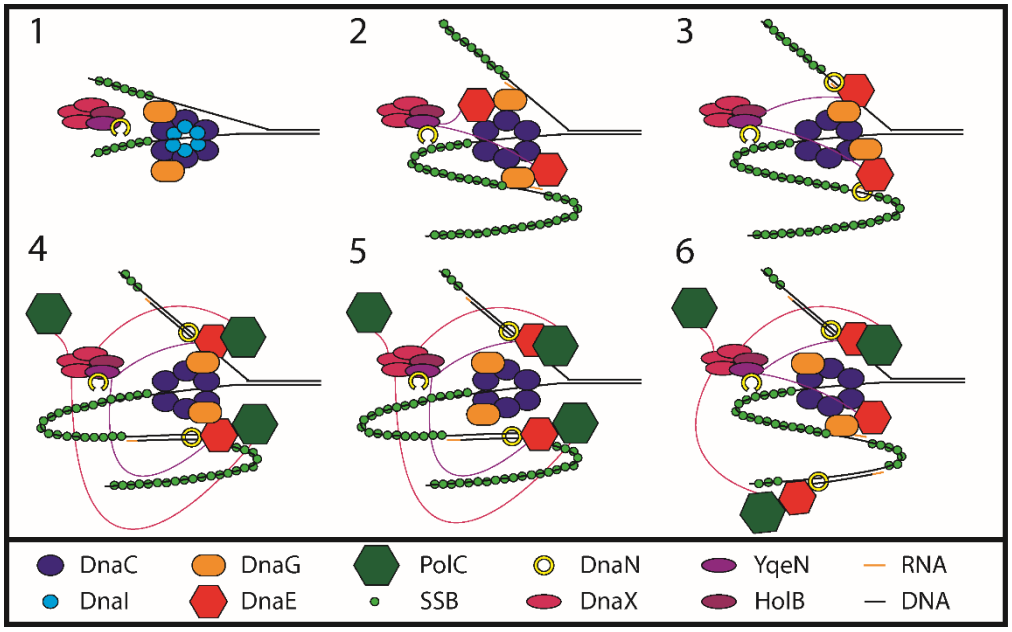


Figure 7.1 A revised speculative model for the *Bacillus subtilis* replisome. **1.** The replicative helicase DnaC is loaded by the helicase-loader DnaI onto the lagging strand of DNA. DnaC recruits the primase DnaG, DnaI is released and DnaC translocates 5'-3', excluding the leading strand template from the hexameric ring interior. **2.** DnaE is recruited at the replisome *via* a direct protein-protein interaction with DnaG, the SSB CTD and the δ subunit (YqeN) of the clamp-loader complex. Primase DnaG synthesises *de novo* short RNA primers. **3.** The clamp-loader complex (YqeN subunit) loads the processivity clamp DnaN onto the primed template. DnaG transfers RNA primers to DnaE *via* a direct hand-off. **4.** DnaE extends RNA primers incorporating dNTPs, increasing the size of the lagging strand loop. PolC is recruited by the τ subunit (DnaX) of the clamp-loader complex, SSB CTD and *via* a physical protein-protein interaction with DnaE. **5.** The DnaE-PolC complex dissociates from the primosomal complex, promoting the release of lagging strand, so as **6.** a new priming cycle to begin in the lagging strand of DNA.

Bibliography

Afonso, J. P., Chintakayala, K., Suwannachart, C., Sedelnikova, S., Giles, K., Hoyes, J. B., … Oldham, N. J. (2013). Insights into the structure and assembly of the Bacillus subtilis clamp-loader complex and its interaction with the replicative helicase. *Nucleic Acids Research*, *41*(9), 5115–5126. http://doi.org/10.1093/nar/gkt173

Antony, E., Weiland, E., Yuan, Q., Manhart, C. M., Nguyen, B., Kozlov, A. G., … Lohman, T. M. (2013). Multiple C-terminal tails within a single E. coli SSB homotetramer coordinate DNA replication and repair. *Journal of Molecular Biology*, *425*(23), 4802–4819. http://doi.org/10.1016/j.jmb.2013.08.021

Argiriadi, M. A., Goedken, E. R., Bruck, I., O'Donnell, M., & Kuriyan, J. (2006). Crystal structure of a DNA polymerase sliding clamp from a Gram-positive bacterium. *BMC Structural Biology*, *6*, 2. http://doi.org/10.1186/1472-6807-6-2

Arias-Palomo, E., O'Shea, V. L., Hood, I. V., & Berger, J. M. (2013). The Bacterial DnaC Helicase Loader Is a DnaB Ring Breaker. *Cell*, *153*(2), 438–448. http://doi.org/10.1016/j.cell.2013.03.006

Bailey, S., Eliason, W. K., & Steitz, T. a. (2007). Structure of hexameric DnaB helicase and its complex with a domain of DnaG primase. *Science (New York, N.Y.)*, *318*(5849), 459–63. http://doi.org/10.1126/science.1147353

Bailey, S., Eliason, W. K., Steitz, T. A., Lamers, M. H., Bailey, S., Eliason, W., … Mchenry, C. (2007). Structure of Hexameric DnaB Helicase and Its Complex with a Domain of DnaG Primase. *Science*, *318*(5849), 459–463. http://doi.org/10.1126/science.1147353

Bailey, S., Wing, R. A., & Steitz, T. A. (2006). The Structure of T. aquaticus DNA Polymerase III Is Distinct from Eukaryotic Replicative DNA Polymerases. *Cell*, *126*(5), 893–904. http://doi.org/10.1016/j.cell.2006.07.027

Baranovskiy, A. G., Babayeva, N. D., Zhang, Y., Gu, J., Suwa, Y., Pavlov, Y. I., & Tahirov, T. H. (2016). Mechanism of Concerted RNA-DNA Primer Synthesis

by the Human Primosome. *Journal of Biological Chemistry*, *291*(19), 10006–10020. http://doi.org/10.1074/jbc.M116.717405

Battistuzzi, F. U., Feijao, A., & Hedges, S. B. (2004). A genomic timescale of prokaryote evolution: insights into the origin of methanogenesis, phototrophy, and the colonization of land. *BMC Evolutionary Biology*, *4*, 44. http://doi.org/10.1186/1471-2148-4-44

Beese, L. S., & Steitz, T. A. (1991). Structural basis for the 3'-5' exonuclease activity of Escherichia coli DNA polymerase I: a two metal ion mechanism. *The EMBO Journal*, *10*(1), 25–33. Retrieved from http://www.pubmedcentral.nih.gov/articlerender.fcgi?artid=452607

BIO-RAD. (n.d.). A Guide To Polyacrylamide Gel Electrophoresis and Detection. Retrieved June 12, 2016, from http://www.bio-rad.com/webroot/web/pdf/lsr/literature/Bulletin_6040.pdf

Bird, L. E., Pan, H., Soultanas, P., & Wigley, D. B. (2000). Mapping protein-protein interactions within a stable complex of DNA primase and DnaB helicase from Bacillus stearothermophilus. *Biochemistry*, *39*(1), 171–182. Retrieved from hhttps://www.ncbi.nlm.nih.gov/pmc/articles/PMC3188359/?tool=pmcentrez

Blaesing, F., Weigel, C., Welzeck, M., & Messer, W. (2000). Analysis of the DNA-binding domain of Escherichia coli DnaA protein. *Molecular Microbiology*, *36*(3), 557–69. Retrieved from http://www.ncbi.nlm.nih.gov/pubmed/10844646

Block, H., Maertens, B., Spriestersbach, A., Brinker, N., Kubicek, J., Fabis, R., … Schäfer, F. (2009). Chapter 27 Immobilized-Metal Affinity Chromatography (IMAC): A Review. In *Methods in Enzymology* (Vol. 463, pp. 439–473). http://doi.org/10.1016/S0076-6879(09)63027-5

Briggs, G. S., Smits, W. K., & Soultanas, P. (2012). Chromosomal replication initiation machinery of low-G+C-content Firmicutes. *Journal of Bacteriology*, *194*(19), 5162–5170. http://doi.org/10.1128/JB.00865-12

Brown, J. A., & Suo, Z. (2011). Unlocking the Sugar "Steric Gate" of DNA Polymerases. *Biochemistry*, *50*(7), 1135–1142. http://doi.org/10.1021/bi101915z

Bruck, I., Georgescu, R. E., & O'Donnell, M. (2005). Conserved interactions in the

Staphylococcus aureus DNA PolC chromosome replication machine. *The Journal of Biological Chemistry*, *280*(18), 18152–18162. http://doi.org/10.1074/jbc.M413595200

Bruck, I., & O'Donnell, M. (2000). The DNA replication machine of a gram-positive organism. *The Journal of Biological Chemistry*, *275*(37), 28971–83. http://doi.org/10.1074/jbc.M003565200

Carneiro, M. J. V. M., Zhang, W., Ioannou, C., Scott, D. J., Allen, S., Roberts, C. J., & Soultanas, P. (2006). The DNA-remodelling activity of DnaD is the sum of oligomerization and DNA-binding activities on separate domains. *Molecular Microbiology*, *60*(4), 917–924. http://doi.org/10.1111/j.1365-2958.2006.05152.x

Coloma, J., Johnson, R. E., Prakash, L., Prakash, S., & Aggarwal, A. K. (2016). Human DNA polymerase α in binary complex with a DNA:DNA template-primer. *Scientific Reports*, *6*, 23784. http://doi.org/10.1038/srep23784

Conn, G. L., Brown, T., & Leonard, G. A. (1999). The crystal structure of the RNA/DNA hybrid r(GAAGAGAAGC). d(GCTTCTCTTC) shows significant differences to that found in solution. *Nucleic Acids Research*, *27*(2), 555–61. http://doi.org/10.1093/NAR/27.2.555

Costa, A., Hood, I. V, & Berger, J. M. (2013). Mechanisms for initiating cellular DNA replication. *Annual Review of Biochemistry*, *82*, 25–54. http://doi.org/10.1146/annurev-biochem-052610-094414

Costes, A., Lecointe, F., McGovern, S., Quevillon-Cheruel, S., & Polard, P. (2010). The C-terminal domain of the bacterial SSB protein acts as a DNA maintenance hub at active chromosome replication forks. *PLoS Genetics*, *6*(12), e1001238. http://doi.org/10.1371/journal.pgen.1001238

Davey, M. J., & O'Donnell, M. (2003). Replicative helicase loaders: ring breakers and ring makers. *Current Biology*, *13*(15), R594–R596. http://doi.org/10.1016/S0960-9822(03)00523-2

DeLucia, A. M., Chaudhuri, S., Potapova, O., Grindley, N. D. F., & Joyce, C. M. (2006). The properties of steric gate mutants reveal different constraints within the active sites of Y-family and A-family DNA polymerases. *The Journal of*

Biological Chemistry, *281*(37), 27286–17291. http://doi.org/10.1074/jbc.M604393200

Dervyn, E., Suski, C., Daniel, R., Bruand, C., Chapuis, J., Errington, J., … Ehrlich, S. D. (2001). Two essential DNA polymerases at the bacterial replication fork. *Science (New York, N.Y.)*, *294*(5547), 1716–1719. http://doi.org/10.1126/science.1066351

Doherty, A. J., Serpell, L. C., & Ponting, C. P. (1996). The helix-hairpin-helix DNA-binding motif: a structural basis for non-sequence-specific recognition of DNA. *Nucleic Acids Research*, *24*(13), 2488–2497. Retrieved from http://www.pubmedcentral.nih.gov/articlerender.fcgi?artid=145986&tool=pmcentrez&rendertype=abstract

Donigan, K. A., Cerritelli, S. M., McDonald, J. P., Vaisman, A., Crouch, R. J., & Woodgate, R. (2015). Unlocking the steric gate of DNA polymerase η leads to increased genomic instability in Saccharomyces cerevisiae. *DNA Repair*, *35*, 1–12. http://doi.org/10.1016/j.dnarep.2015.07.002

Downey, C. D., & McHenry, C. S. (2010). Chaperoning of a replicative polymerase onto a newly assembled DNA-bound sliding clamp by the clamp loader. *Molecular Cell*, *37*(4), 481–91. http://doi.org/10.1016/j.molcel.2010.01.013

Duong-Ly, K. C., & Gabelli, S. B. (2014). Salting out of proteins using ammonium sulfate precipitation. *Methods in Enzymology*, *541*, 85–94. http://doi.org/10.1016/B978-0-12-420119-4.00007-0

Evans, R. J., Davies, D. R., Bullard, J. M., Christensen, J., Green, L. S., Guiles, J. W., … Jarvis, T. C. (2008). Structure of PolC reveals unique DNA binding and fidelity determinants. *Proceedings of the National Academy of Sciences of the United States of America*, *105*(52), 20695–20700. http://doi.org/10.1073/pnas.0809989106

Farooqui, A. A. (1980). Purification of enzymes by heparin-sepharose affinity chromatography. *Journal of Chromatography A*, *184*(3), 335–345. http://doi.org/10.1016/S0021-9673(00)89004-4

Felczak, M. M., & Kaguni, J. M. (2004). The box VII motif of Escherichia coli DnaA

protein is required for DnaA oligomerization at the E. coli replication origin. *The Journal of Biological Chemistry*, *279*(49), 51156–62. http://doi.org/10.1074/jbc.M409695200

Ferraro, P., Franzolin, E., Pontarin, G., Reichard, P., & Bianchi, V. (2010). Quantitation of cellular deoxynucleoside triphosphates. *Nucleic Acids Research*, *38*(6), e85. http://doi.org/10.1093/nar/gkp1141

Fijalkowska, I. J., & Schaaper, R. M. (1996). Mutants in the Exo I motif of Escherichia coli dnaQ: defective proofreading and inviability due to error catastrophe. *Proceedings of the National Academy of Sciences of the United States of America*, *93*(7), 2856–61. Retrieved from http://www.pubmedcentral.nih.gov/articlerender.fcgi?artid=39723

Frick, D. N., & Richardson, C. C. (2001). DNA primases. *Annual Review of Biochemistry*, *70*, 39–80. http://doi.org/10.1146/annurev.biochem.70.1.39

Friedberg, E. C., Fischhaber, P. L., & Kisker, C. (2001). Error-Prone DNA Polymerases. *Cell*, *107*(1), 9–12. http://doi.org/10.1016/S0092-8674(01)00509-8

Ganai, R. A., Bylund, G. O., & Johansson, E. (2015). Switching between polymerase and exonuclease sites in DNA polymerase ε. *Nucleic Acids Research*, *43*(2), 932–942. http://doi.org/10.1093/nar/gku1353

Gille, H., & Messer, W. (1991). Localized DNA melting and structural pertubations in the origin of replication, oriC, of Escherichia coli in vitro and in vivo. *The EMBO Journal*, *10*(6), 1579–84. Retrieved from http://www.pubmedcentral.nih.gov/articlerender.fcgi?artid=452823&tool=pmcentrez&rendertype=abstract

Glover, B. P., & McHenry, C. S. (1998). The chi psi subunits of DNA polymerase III holoenzyme bind to single-stranded DNA-binding protein (SSB) and facilitate replication of an SSB-coated template. *The Journal of Biological Chemistry*, *273*(36), 23476–84. Retrieved from http://www.ncbi.nlm.nih.gov/pubmed/9722585

Gon, S., Napolitano, R., Rocha, W., Coulon, S., & Fuchs, R. P. (2011). Increase in dNTP pool size during the DNA damage response plays a key role in

spontaneous and induced-mutagenesis in Escherichia coli. *Proceedings of the National Academy of Sciences of the United States of America*, *108*(48), 19311–19316. http://doi.org/10.1073/pnas.1113664108

Goujon, M., McWilliam, H., Li, W., Valentin, F., Squizzato, S., Paern, J., & Lopez, R. (2010). A new bioinformatics analysis tools framework at EMBL-EBI. *Nucleic Acids Research*, *38*(Web Server), W695–W699. http://doi.org/10.1093/nar/gkq313

Green, M., Gilhooly, N. S., Abedeen, S., Scott, D. J., Dillingham, M. S., & Soultanas, P. (2014). Engineering a reagentless biosensor for single-stranded DNA to measure real-time helicase activity in Bacillus. *Biosensors & Bioelectronics*, *61C*, 579–586. http://doi.org/10.1016/j.bios.2014.06.011

Green, M., Hatter, L., Brookes, E., Soultanas, P., & Scott, D. J. (2016). Defining the Intrinsically Disordered C-Terminal Domain of SSB Reveals DNA-Mediated Compaction. *Journal of Molecular Biology*, *428*(2), 357–364. http://doi.org/10.1016/j.jmb.2015.12.007

Hamdan, S., Carr, P. D., Brown, S. E., Ollis, D. L., & Dixon, N. E. (2002). Structural Basis for Proofreading during Replication of the Escherichia coli Chromosome. *Structure*, *10*(4), 535–546. http://doi.org/http://dx.doi.org/10.1016/S0969-2126(02)00738-4

Hantz, E., Larue, V., Ladam, P., Le Moyec, L., Gouyette, C., & Huynh Dinh, T. (2001). Solution conformation of an RNA--DNA hybrid duplex containing a pyrimidine RNA strand and a purine DNA strand. *International Journal of Biological Macromolecules*, *28*(4), 273–84. Retrieved from http://www.ncbi.nlm.nih.gov/pubmed/11311717

Harwood, A. J. (2000). Native Polyacrylamide Gel Electrophoresis. In *Nucleic Acid Protocols Handbook, The* (pp. 73–75). New Jersey: Humana Press. http://doi.org/10.1385/1-59259-038-1:73

Hedglin, M., Kumar, R., & Benkovic, S. J. (2013). Replication clamps and clamp loaders. *Cold Spring Harbor Perspectives in Biology*, *5*(4), a010165. http://doi.org/10.1101/cshperspect.a010165

Hübscher, U., Maga, G., & Spadari, S. (2003). EUKARYOTIC DNA POLYMERASES. *Annual Review of Biochemistry*, *71*, 133–163. http://doi.org/10.1146/annurev.biochem.71.090501.150041

Ioannou, C., Schaeffer, P. M., Dixon, N. E., & Soultanas, P. (2006). Helicase binding to DnaI exposes a cryptic DNA-binding site during helicase loading in Bacillus subtilis. *Nucleic Acids Research*, *34*(18), 5247–5258. http://doi.org/10.1093/nar/gkl690

Ito, J., & Braithwaite, D. K. (1991). Compilation and alignment of DNA polymerase sequences. *Nucleic Acids Research*, *19*(15), 4045–4057. Retrieved from http://www.ncbi.nlm.nih.gov/pubmed/1870963

Jeruzalmi, D., O'Donnell, M., & Kuriyan, J. (2001). Crystal structure of the processivity clamp loader gamma (gamma) complex of E. coli DNA polymerase III. *Cell*, *106*(4), 429–41. Retrieved from http://www.ncbi.nlm.nih.gov/pubmed/11525729

Johansson, E., & MacNeill, S. A. (2010). The eukaryotic replicative DNA polymerases take shape. *Trends in Biochemical Sciences*, *35*(6), 339–347. http://doi.org/10.1016/j.tibs.2010.01.004

Johnson, A., & O'Donnell, M. (2003). Ordered ATP hydrolysis in the gamma complex clamp loader AAA+ machine. *The Journal of Biological Chemistry*, *278*(16), 14406–13. http://doi.org/10.1074/jbc.M212708200

Johnson, R. E., Klassen, R., Prakash, L., Prakash, S., Acharya, N., Klassen, R., … Zhang, Z. (2015). A Major Role of DNA Polymerase δ in Replication of Both the Leading and Lagging DNA Strands. *Molecular Cell*, *59*(2), 163–175. http://doi.org/10.1016/j.molcel.2015.05.038

Kaguni, J. M. (2006). DnaA: controlling the initiation of bacterial DNA replication and more. *Annual Review of Microbiology*, *60*, 351–75. http://doi.org/10.1146/annurev.micro.60.080805.142111

Kaguni, J. M. (2011). Replication initiation at the Escherichia coli chromosomal origin. *Current Opinion in Chemical Biology*, *15*(5), 606–613. http://doi.org/10.1016/j.cbpa.2011.07.016

Kato, M., Ito, T., Wagner, G., & Ellenberger, T. (2004). A molecular handoff between bacteriophage T7 DNA primase and T7 DNA polymerase initiates DNA synthesis. *The Journal of Biological Chemistry*, *279*(29), 30554–30562. http://doi.org/10.1074/jbc.M403485200

Kelman, Z., & O'Donnell, M. (1995). DNA polymerase III holoenzyme: structure and function of a chromosomal replicating machine. *Annual Review of Biochemistry*, *64*, 171–200. http://doi.org/10.1146/annurev.bi.64.070195.001131

Kelman, Z., Yuzhakov, A., Andjelkovic, J., & O'Donnell, M. (1998). Devoted to the lagging strand-the subunit of DNA polymerase III holoenzyme contacts SSB to promote processive elongation and sliding clamp assembly. *The EMBO Journal*, *17*(8), 2436–49. http://doi.org/10.1093/emboj/17.8.2436

Kim, D. R., & McHenry, C. S. (1996). Identification of the beta-binding domain of the alpha subunit of Escherichia coli polymerase III holoenzyme. *The Journal of Biological Chemistry*, *271*(34), 20699–20704. Retrieved from http://www.ncbi.nlm.nih.gov/pubmed/8702820

Kong, X. P., Onrust, R., O'Donnell, M., & Kuriyan, J. (1992). Three-dimensional structure of the beta subunit of E. coli DNA polymerase III holoenzyme: a sliding DNA clamp. *Cell*, *69*(3), 425–37. Retrieved from http://www.ncbi.nlm.nih.gov/pubmed/1349852

Koonin, E. V. (1992). DnaC protein contains a modified ATP-binding motif and belongs to a novel family of ATPases including also DnaA. *Nucleic Acids Research*, *20*(8), 1997. Retrieved from http://www.pubmedcentral.nih.gov/articlerender.fcgi?artid=312323&tool=pmcentrez&rendertype=abstract

Laemmli, U. K. (1970). Cleavage of Structural Proteins during the Assembly of the Head of Bacteriophage T4. *Nature*, *227*(5259), 680–685. http://doi.org/10.1038/227680a0

Lamers, M. H., Georgescu, R. E., Lee, S.-G., O'Donnell, M., & Kuriyan, J. (2006). Crystal Structure of the Catalytic α Subunit of E. coli Replicative DNA Polymerase III. *Cell*, *126*(5), 881–892. http://doi.org/10.1016/j.cell.2006.07.028

Lathe, G. H., & Ruthven, C. R. (1956). The separation of substances and estimation of their relative molecular sizes by the use of colums of starch in water. *The Biochemical Journal*, *62*(4), 665–74. Retrieved from http://www.ncbi.nlm.nih.gov/pubmed/13315231

LeBowitz, J. H., & McMacken, R. (1986). The Escherichia coli dnaB replication protein is a DNA helicase. *The Journal of Biological Chemistry*, *261*(10), 4738–48. Retrieved from http://www.ncbi.nlm.nih.gov/pubmed/3007474

Lee, P. Y., Costumbrado, J., Hsu, C.-Y., & Kim, Y. H. (2012). Agarose gel electrophoresis for the separation of DNA fragments. *Journal of Visualized Experiments : JoVE*, (62). http://doi.org/10.3791/3923

Liu, B., Eliason, W. K., & Steitz, T. A. (2013). Structure of a helicase-helicase loader complex reveals insights into the mechanism of bacterial primosome assembly. *Nature Communications*, *4*, 2495. http://doi.org/10.1038/ncomms3495

Loscha, K. V, Jaudzems, K., Ioannou, C., Su, X.-C., Hill, F. R., Otting, G., … Liepinsh, E. (2009). A novel zinc-binding fold in the helicase interaction domain of the Bacillus subtilis DnaI helicase loader. *Nucleic Acids Research*, *37*(7), 2395–2404. http://doi.org/10.1093/nar/gkp092

Lujan, S. A., Williams, J. S., & Kunkel, T. A. (2016). DNA Polymerases Divide the Labor of Genome Replication. *Trends in Cell Biology*, *26*(9), 640–654. http://doi.org/10.1016/j.tcb.2016.04.012

Madadlou, A., O'Sullivan, S., & Sheehan, D. (2011). Fast protein liquid chromatography. *Methods in Molecular Biology (Clifton, N.J.)*, *681*, 439–47. http://doi.org/10.1007/978-1-60761-913-0_25

Makowska-Grzyska, M., & Kaguni, J. M. (2010). Primase directs the release of DnaC from DnaB. *Molecular Cell*, *37*(1), 90–101. http://doi.org/10.1016/j.molcel.2009.12.031

Marceau, A. H., Bahng, S., Massoni, S. C., George, N. P., Sandler, S. J., Marians, K. J., & Keck, J. L. (2011). Structure of the SSB-DNA polymerase III interface and its role in DNA replication. *The EMBO Journal*, *30*(20), 4236–4247. http://doi.org/10.1038/emboj.2011.305

Marston, F. Y., Grainger, W. H., Smits, W. K., Hopcroft, N. H., Green, M., Hounslow, A. M., … Soultanas, P. (2010). When simple sequence comparison fails: the cryptic case of the shared domains of the bacterial replication initiation proteins DnaB and DnaD. *Nucleic Acids Research*, *38*(20), 6930–6942. http://doi.org/10.1093/nar/gkq465

McAuley-Hecht, K. E., Leonard, G. A., Gibson, N. J., Thomson, J. B., Watson, W. P., Hunter, W. N., & Brown, T. (1994). Crystal Structure of a DNA Duplex Containing 8-Hydroxydeoxyguanine-Adenine Base Pairs. *Biochemistry*, *33*(34), 10266–10270. http://doi.org/10.1021/bi00200a006

McHenry, C. S. (2011a). Bacterial replicases and related polymerases. *Current Opinion in Chemical Biology*, *15*(5), 587–594. http://doi.org/10.1016/j.cbpa.2011.07.018

McHenry, C. S. (2011b). Breaking the rules: bacteria that use several DNA polymerase IIIs. *EMBO Reports*, *12*(5), 408–414. http://doi.org/10.1038/embor.2011.51

McHenry, C. S. (2011c). DNA replicases from a bacterial perspective. *Annual Review of Biochemistry*, *80*, 403–436. http://doi.org/10.1146/annurev-biochem-061208-091655

McInerney, P., Johnson, A., Katz, F., & O'Donnell, M. (2007). Characterization of a triple DNA polymerase replisome. *Molecular Cell*, *27*(4), 527–538. http://doi.org/10.1016/j.molcel.2007.06.019

McWilliam, H., Li, W., Uludag, M., Squizzato, S., Park, Y. M., Buso, N., … Lopez, R. (2013). Analysis Tool Web Services from the EMBL-EBI. *Nucleic Acids Research*, *41*(Web Server issue), W597-600. http://doi.org/10.1093/nar/gkt376

Mitchell, S. F., & Lorsch, J. R. (2015). Protein Affinity Purification using Intein/Chitin Binding Protein Tags. *Methods in Enzymology*, *559*, 111–25. http://doi.org/10.1016/bs.mie.2014.11.002

Mori, S., & Barth, H. G. (1999). *Size Exclusion Chromatography*. Berlin, Heidelberg: Springer Berlin Heidelberg. http://doi.org/10.1007/978-3-662-03910-6

Mott, M. L., Erzberger, J. P., Coons, M. M., & Berger, J. M. (2008). Structural

Synergy and Molecular Crosstalk between Bacterial Helicase Loaders and Replication Initiators. *Cell*, *135*(4), 623–634. http://doi.org/10.1016/j.cell.2008.09.058

Mueller, G. A., Kirby, T. W., DeRose, E. F., Li, D., Schaaper, R. M., & London, R. E. (2005). Nuclear magnetic resonance solution structure of the Escherichia coli DNA polymerase III theta subunit. *Journal of Bacteriology*, *187*(20), 7081–9. http://doi.org/10.1128/JB.187.20.7081-7089.2005

National Diagnostics. (n.d.). SequaGel UreaGel System. Retrieved June 13, 2016, from https://www.nationaldiagnostics.com/sites/default/files/ec833_protocol_0.pdf

Nelson, S. W., Kumar, R., & Benkovic, S. J. (2008). RNA primer handoff in bacteriophage T4 DNA replication: the role of single-stranded DNA-binding protein and polymerase accessory proteins. *The Journal of Biological Chemistry*, *283*(33), 22838–22846. http://doi.org/10.1074/jbc.M802762200

New England Biolabs Tm Calculator. (n.d.). Retrieved from http://tmcalculator.neb.com/#!/

Núñez-Ramírez, R., Velten, M., Rivas, G., Polard, P., Carazo, J. M., & Donate, L. E. (2007). Loading a Ring: Structure of the Bacillus subtilis DnaB Protein, a Co-loader of the Replicative Helicase. *Journal of Molecular Biology*, *367*(3), 764–769. http://doi.org/10.1016/j.jmb.2006.12.075

O'Donnell, M., Langston, L., & Stillman, B. (2013). Principles and concepts of DNA replication in bacteria, archaea, and eukarya. *Cold Spring Harbor Perspectives in Biology*, *5*(7), 1–13. http://doi.org/10.1101/cshperspect.a010108

Ogasawara, N., & Yoshikawa, H. (1992). Genes and their organization in the replication origin region of the bacterial chromosome. *Molecular Microbiology*, *6*(5), 629–34. Retrieved from http://www.ncbi.nlm.nih.gov/pubmed/1552862

Ozaki, S., & Katayama, T. (2009). DnaA structure, function, and dynamics in the initiation at the chromosomal origin. *Plasmid*, *62*(2), 71–82. http://doi.org/10.1016/j.plasmid.2009.06.003

Ozaki, S., & Katayama, T. (2012). Highly organized DnaA-oriC complexes recruit

the single-stranded DNA for replication initiation. *Nucleic Acids Research*, *40*(4), 1648–65. http://doi.org/10.1093/nar/gkr832

Ozaki, S., Kawakami, H., Nakamura, K., Fujikawa, N., Kagawa, W., Park, S.-Y., … Katayama, T. (2008). A common mechanism for the ATP-DnaA-dependent formation of open complexes at the replication origin. *The Journal of Biological Chemistry*, *283*(13), 8351–62. http://doi.org/10.1074/jbc.M708684200

Pellegrini, L. (2012). The Pol α-primase complex. *Sub-Cellular Biochemistry*, *62*, 157–169. http://doi.org/10.1007/978-94-007-4572-8_9

Perera, R. L., Torella, R., Klinge, S., Kilkenny, M. L., Maman, J. D., & Pellegrini, L. (2013). Mechanism for priming DNA synthesis by yeast DNA polymerase α. *eLife*, *2*, e00482. http://doi.org/10.7554/eLife.00482

Pritchard, A. E., & McHenry, C. S. (1999). Identification of the acidic residues in the active site of DNA polymerase III. *Journal of Molecular Biology*, *285*(3), 1067–80. http://doi.org/10.1006/jmbi.1998.2352

Rannou, O., Le Chatelier, E., Larson, M. a, Nouri, H., Dalmais, B., Laughton, C., … Soultanas, P. (2013). Functional interplay of DnaE polymerase, DnaG primase and DnaC helicase within a ternary complex, and primase to polymerase hand-off during lagging strand DNA replication in Bacillus subtilis. *Nucleic Acids Research*, *41*(10), 5303–5320. http://doi.org/10.1093/nar/gkt207

Rattray, A. J., & Strathern, J. N. (2003). Error-prone DNA polymerases: when making a mistake is the only way to get ahead. *Annual Review of Genetics*, *37*, 31–66. http://doi.org/10.1146/annurev.genet.37.042203.132748

Rice, P., Longden, I., & Bleasby, A. (2000). EMBOSS: The European Molecular Biology Open Software Suite. *Trends in Genetics*, *16*(6), 276–277. http://doi.org/10.1016/S0168-9525(00)02024-2

Robinson, A., & van Oijen, A. M. (2013). Bacterial replication, transcription and translation: mechanistic insights from single-molecule biochemical studies. *Nature Reviews. Microbiology*, *11*(5), 303–315. http://doi.org/10.1038/nrmicro2994

Rokop, M. E., Auchtung, J. M., & Grossman, A. D. (2004). Control of DNA

replication initiation by recruitment of an essential initiation protein to the membrane of Bacillus subtilis. *Molecular Microbiology*, *52*(6), 1757–1767. http://doi.org/10.1111/j.1365-2958.2004.04091.x

Sanders, G. M., Dallmann, H. G., & McHenry, C. S. (2010). Reconstitution of the B. subtilis Replisome with 13 Proteins Including Two Distinct Replicases. *Molecular Cell*, *37*(2), 273–281. http://doi.org/10.1016/j.molcel.2009.12.025

Schaeffer, P. M., Headlam, M. J., & Dixon, N. E. (2005). Protein--protein interactions in the eubacterial replisome. *IUBMB Life*, *57*(1), 5–12. http://doi.org/10.1080/15216540500058956

Schneider, S., Zhang, W., Soultanas, P., & Paoli, M. (2008). Structure of the N-terminal oligomerization domain of DnaD reveals a unique tetramerization motif and provides insights into scaffold formation. *Journal of Molecular Biology*, *376*(5), 1237–50. http://doi.org/10.1016/j.jmb.2007.12.045

Schuster-Böckler, B., Schultz, J., & Rahmann, S. (2004). HMM Logos for visualization of protein families. *BMC Bioinformatics*, *5*(1), 7. http://doi.org/10.1186/1471-2105-5-7

Sievers, F., Wilm, A., Dineen, D., Gibson, T. J., Karplus, K., Li, W., … Higgins, D. G. (2011). Fast, scalable generation of high-quality protein multiple sequence alignments using Clustal Omega. *Molecular Systems Biology*, *7*(1), 539. http://doi.org/10.1038/msb.2011.75

Skelly, J. V, Edwards, K. J., Jenkins, T. C., & Neidle, S. (1993). Crystal structure of an oligonucleotide duplex containing G.G base pairs: influence of mispairing on DNA backbone conformation. *Proceedings of the National Academy of Sciences of the United States of America*, *90*(3), 804–8. Retrieved from http://www.ncbi.nlm.nih.gov/pubmed/8430089

Smits, W. K., Goranov, A. I., & Grossman, A. D. (2010). Ordered association of helicase loader proteins with the Bacillus subtilis origin of replication in vivo. *Molecular Microbiology*, *75*(2), 452–461. http://doi.org/10.1111/j.1365-2958.2009.06999.x

Smits, W. K., Merrikh, H., Bonilla, C. Y., & Grossman, A. D. (2011). Primosomal

proteins DnaD and DnaB are recruited to chromosomal regions bound by DnaA in Bacillus subtilis. *Journal of Bacteriology*, *193*(3), 640–648. http://doi.org/10.1128/JB.01253-10

Soultanas, P. (2012). Loading mechanisms of ring helicases at replication origins. *Molecular Microbiology*, *84*(1), 6–16. http://doi.org/10.1111/j.1365-2958.2012.08012.x

Southern, E. M. (2002). Denaturing Gel Electrophoresis of DNA in Alkaline Agarose Gels. In *Encyclopedia of Life Sciences*. Chichester: John Wiley & Sons, Ltd. http://doi.org/10.1038/npg.els.0003758

Stano, N. M., Chen, J., & McHenry, C. S. (2006). A coproofreading Zn(2+)-dependent exonuclease within a bacterial replicase. *Nature Structural & Molecular Biology*, *13*(5), 458–459. http://doi.org/10.1038/nsmb1078

Steitz, T. A. (1999). DNA Polymerases: Structural Diversity and Common Mechanisms. *Journal of Biological Chemistry*, *274*(25), 17395–17398. http://doi.org/10.1074/jbc.274.25.17395

Stukenberg, P. T., Studwell-Vaughan, P. S., & O'Donnell, M. (1991). Mechanism of the sliding beta-clamp of DNA polymerase III holoenzyme. *The Journal of Biological Chemistry*, *266*(17), 11328–34. Retrieved from http://www.ncbi.nlm.nih.gov/pubmed/2040637

Su, X.-C., Jergic, S., Keniry, M. A., Dixon, N. E., & Otting, G. (2007). Solution structure of Domains IVa and V of the tau subunit of Escherichia coli DNA polymerase III and interaction with the alpha subunit. *Nucleic Acids Research*, *35*(9), 2825–2832. http://doi.org/10.1093/nar/gkm080

Su, X.-C., Schaeffer, P. M., Loscha, K. V, Gan, P. H. P., Dixon, N. E., & Otting, G. (2006). Monomeric solution structure of the helicase-binding domain of Escherichia coli DnaG primase. *The FEBS Journal*, *273*(21), 4997–5009. http://doi.org/10.1111/j.1742-4658.2006.05495.x

Su, Y., Egli, M., & Guengerich, F. P. (2016). Mechanism of Ribonucleotide Incorporation by Human DNA Polymerase η. *Journal of Biological Chemistry*, *291*(8), 3747–3756. http://doi.org/10.1074/jbc.M115.706226

Summer, H., Grämer, R., & Dröge, P. (2009). Denaturing urea polyacrylamide gel electrophoresis (Urea PAGE). *Journal of Visualized Experiments: JoVE*, (32). http://doi.org/10.3791/1485

Theobald, D. L., Mitton-Fry, R. M., & Wuttke, D. S. (2003). Nucleic acid recognition by OB-fold proteins. *Annual Review of Biophysics and Biomolecular Structure*, *32*, 115–133. http://doi.org/10.1146/annurev.biophys.32.110601.142506

Thirlway, J., & Soultanas, P. (2006). In the Bacillus stearothermophilus DnaB-DnaG complex, the activities of the two proteins are modulated by distinct but overlapping networks of residues. *Journal of Bacteriology*, *188*(4), 1534–9. http://doi.org/10.1128/JB.188.4.1534-1539.2006

Timinskas, K., Balvočiūtė, M., Timinskas, A., & Venclovas, Č. (2014). Comprehensive analysis of DNA polymerase III α subunits and their homologs in bacterial genomes. *Nucleic Acids Research*, *42*(3), 1393–1413. http://doi.org/10.1093/nar/gkt900

Toseland, C. P., & Webb, M. R. (2010). Fluorescence tools to measure helicase activity in real time. *Methods*, *51*(3), 259–268. http://doi.org/10.1016/j.ymeth.2010.02.012

Tougu, K., & Marians, K. J. (1996). The extreme C terminus of primase is required for interaction with DnaB at the replication fork. *The Journal of Biological Chemistry*, *271*(35), 21391–7. Retrieved from http://www.ncbi.nlm.nih.gov/pubmed/8702920

Tougu, K., Peng, H., & Marians, K. J. (1994). Identification of a domain of Escherichia coli primase required for functional interaction with the DnaB helicase at the replication fork. *The Journal of Biological Chemistry*, *269*(6), 4675–82. Retrieved from http://www.ncbi.nlm.nih.gov/pubmed/8308039

Tsai, K.-L., Lo, Y.-H., Sun, Y.-J., & Hsiao, C.-D. (2009). Molecular interplay between the replicative helicase DnaC and its loader protein DnaI from Geobacillus kaustophilus. *Journal of Molecular Biology*, *393*(5), 1056–69. http://doi.org/10.1016/j.jmb.2009.09.002

Velten, M., McGovern, S., Marsin, S., Ehrlich, S. D., Noirot, P., & Polard, P. (2003).

A Two-Protein Strategy for the Functional Loading of a Cellular Replicative DNA Helicase. *Molecular Cell*, *11*(4), 1009–1020. http://doi.org/http://dx.doi.org/10.1016/S1097-2765(03)00130-8

Wang, W., Wu, E. Y., Hellinga, H. W., & Beese, L. S. (2012). Structural Factors That Determine Selectivity of a High Fidelity DNA Polymerase for Deoxy-, Dideoxy-, and Ribonucleotides. *Journal of Biological Chemistry*, *287*(34), 28215–28226. http://doi.org/10.1074/jbc.M112.366609

Wieczorek, A., & McHenry, C. S. (2006). The NH2-terminal php domain of the alpha subunit of the Escherichia coli replicase binds the epsilon proofreading subunit. *The Journal of Biological Chemistry*, *281*(18), 12561–12567. http://doi.org/10.1074/jbc.M513844200

Williams, A., Frasca, V., Williams, A., & Frasca, V. (1999). Ion-Exchange Chromatography. In *Current Protocols in Protein Science* (p. 8.2.1-8.2.30). Hoboken, NJ, USA: John Wiley & Sons, Inc. http://doi.org/10.1002/0471140864.ps0802s15

Williams, J. S., Lujan, S. A., & Kunkel, T. A. (2016). Processing ribonucleotides incorporated during eukaryotic DNA replication. *Nature Reviews. Molecular Cell Biology*, *17*(6), 350–363. http://doi.org/10.1038/nrm.2016.37

Williams, L. N., Marjavaara, L., Knowels, G. M., Schultz, E. M., Fox, E. J., Chabes, A., & Herr, A. J. (2015). dNTP pool levels modulate mutator phenotypes of error-prone DNA polymerase ε variants. *Proceedings of the National Academy of Sciences of the United States of America*, *112*(19), E2457-2466. http://doi.org/10.1073/pnas.1422948112

Wing, R. A., Bailey, S., & Steitz, T. A. (2008). Insights into the replisome from the structure of a ternary complex of the DNA polymerase III alpha-subunit. *Journal of Molecular Biology*, *382*(4), 859–869. http://doi.org/10.1016/j.jmb.2008.07.058

Wingfield, P. T. (Ed.). (2016). Protein Precipitation Using Ammonium Sulfate. In *Current Protocols in Protein Science* (p. A.3F.1-A.3F.9). Hoboken, NJ, USA: John Wiley & Sons, Inc. http://doi.org/10.1002/0471140864.psa03fs84

Xiong, S., Zhang, L., & He, Q.-Y. (2008). Fractionation of proteins by heparin chromatography. *Methods in Molecular Biology (Clifton, N.J.)*, *424*, 213–21. http://doi.org/10.1007/978-1-60327-064-9_18

Xiong, Y., Sundaralingam, M., Stein, H., Hausen, P., Oda, Y., Iwai, S., … Gao, X. (1998). Crystal structure and conformation of a DNA-RNA hybrid duplex with a polypurine RNA strand: d(TTCTTBr5CTTC)-r(GAAGAAGAA). *Structure (London, England: 1993)*, *6*(12), 1493–501. http://doi.org/10.1016/S0969-2126(98)00148-8

Yao, N. Y., Schroeder, J. W., Yurieva, O., Simmons, L. A., & O'Donnell, M. E. (2013). Cost of rNTP/dNTP pool imbalance at the replication fork. *Proceedings of the National Academy of Sciences of the United States of America*, *110*(32), 12942–12947. http://doi.org/10.1073/pnas.1309506110

Yuzhakov, A., Kelman, Z., & O'Donnell, M. (1999). Trading Places on DNA—A Three-Point Switch Underlies Primer Handoff from Primase to the Replicative DNA Polymerase. *Cell*, *96*(1), 153–163. http://doi.org/10.1016/S0092-8674(00)80968-X

Zanders, E. D. (Ed.). (2005). *Chemical Genomics* (Vol. 310). Totowa, NJ: Humana Press. http://doi.org/10.1007/978-1-59259-948-6

Zhang, W., Allen, S., Roberts, C. J., & Soultanas, P. (2006). The Bacillus subtilis Primosomal Protein DnaD Untwists Supercoiled DNA. *Journal Of Bacteriology*, *188*(15), 5487–5493. http://doi.org/10.1128/JB.00339-06

Zhang, W., Carneiro, M. J. V. M., Turner, I. J., Allen, S., Roberts, C. J., & Soultanas, P. (2005). The Bacillus subtilis DnaD and DnaB proteins exhibit different DNA remodelling activities. *Journal of Molecular Biology*, *351*(1), 66–75. http://doi.org/10.1016/j.jmb.2005.05.065